

BACHELOR'S DEGREE PROJECT 2026

Project Report

AI AUGMENTED ADDITIVE MANUFACTURING

Prepared By:

Ahmed AbdelFattah Awad

Ahmed Shawky Basiouny

Eslam Ahmed Badr

Habiba Basiouny Basiouny

Mayar Tarek Ahmed

Mo'men Alaa Elsayed

Yomna Mahmoud Ahmed

Yousef Ahmed Samir

July 2026



BACHELOR'S DEGREE PROJECT 2026

Project Report

AI AUGMENTED ADDITIVE MANUFACTURING

Prepared By:

Ahmed AbdelFattah Awad
Ahmed Shawky Basiouny
Eslam Ahmed Badr
Habiba Basiouny Basiouny
Mayar Tarek Ahmed
Mo'men Alaa Elsayed
Yomna Mahmoud Ahmed
Yousef Ahmed Samir

Under The Supervision Of:

Prof. Dr. Ahmed Bahaadin Khairy

July 2026

ACKNOWLEDGEMENT

The culmination of this graduation project represents the synergy of collective effort, mentorship, and personal support. We are profoundly grateful to those who walked this path with us.

Special recognition is due to **Prof. Dr. Ahmed Bahaadin Khairy**. His mentorship was the cornerstone of this research; his high standards and insightful critiques pushed us to exceed our own expectations. We consider it a distinct honor to have been guided by an educator of his caliber.

We also owe a debt of gratitude to our technical advisors and consultants. Their practical advice and technical feedback provided us with the clarity needed to navigate the more complex phases of this project.

A sincere thank you goes to our friends, whose companionship turned the most stressful days into manageable ones. Whether providing a needed distraction or a much-appreciated word of encouragement, your presence made all the difference.

ABSTRACT

Additive Manufacturing (AM), particularly Fused Deposition Modeling (FDM), has become a cornerstone of modern engineering due to its ability to produce customized spare parts on demand. Despite its advantages, challenges such as dimensional inaccuracies, thermal distortions, and print failures remain significant barriers to industrial adoption. This project aims to overcome these limitations by integrating Artificial Intelligence (AI), Design of Experiments (DOE), and real-time computer vision monitoring into the 3D printing workflow.

The methodology combines reverse engineering for geometry capture, AI-driven generative design for structural optimization, and DOE-based statistical analysis to identify optimal printing parameters. Experimental trials were conducted to evaluate the effects of nozzle temperature, bed temperature, print speed, and layer height, with ANOVA applied to quantify factor interactions. A real-time monitoring system was developed using OctoPrint, Python automation, and AI-powered defect detection models to identify issues such as layer shifting, under-extrusion, and warping. Automated corrective actions reduced failure rates by 30–50 % and improved dimensional accuracy to ± 0.1 mm.

The outcomes demonstrate that AI-augmented additive manufacturing can deliver enhanced reliability, reduced material waste, and improved repeatability, establishing a framework for defect-free intelligent 3D printing systems applicable to industrial contexts.

TABLE OF CONTENTS

ACKNOWLEDGEMENT II

ABSTRACT III

TABLE OF CONTENTS IV

LIST OF SYMPOLS XI

LIST OF TERMS XII

LIST OF FIGURES XIV

LIST OF TABLES XVI

CHAPTER 1 INTRODUCTION 1

1.1 BACKGROUND AND MOTIVATION 1

1.2 PROBLEM STATEMENT 1

1.3 PROJECT OBJECTIVES 1

1.4 SCOPE AND LIMITATIONS 2

1.5 METHODOLOGICAL OVERVIEW 2

1.6 CONTRIBUTIONS 3

1.7 REPORT OUTLINE 3

CHAPTER 2 REVIEW OF LITERATURE 4

2.1 INTRODUCTION 4

2.2 Additive Manufacturing 5

2.2.1 Definition of Additive Manufacturing 5

2.2.2 Development of Additive Manufacturing 5

2.2.3 Working Principle of Additive Manufacturing 6

2.2.4 Main Characteristics of Additive Manufacturing 6

2.2.5 Additive Manufacturing Technologies 7

2.2.6 Materials Used in Additive Manufacturing 13

2.2.7 Industrial Applications of Additive Manufacturing 14

2.2.8 Advantages and Challenges of Additive Manufacturing 14

2.3 Artificial Intelligence 15

2.3.1 Evolution of Artificial Intelligence 16

2.3.2 Machine Learning 16
2.3.3 Deep Learning 17
2.3.4 Computer Vision 18
2.3.5 Artificial Intelligence in Manufacturing 19
2.4 Augmentation of Artificial Intelligence in Additive Manufacturing 19
2.4.1 Artificial Intelligence Across the Additive Manufacturing Lifecycle 20
2.4.2 AI-Assisted Design for Additive Manufacturing 20
2.4.3 Process Parameter Optimization 21
2.4.4 In-Situ Process Monitoring 22
2.4.5 Defect Detection and Quality Prediction 23
2.4.6 Closed-Loop Intelligent Additive Manufacturing 23
2.4.7 Benefits and Current Challenges 24
2.5 Recent Developments, Research Challenges, and Future Directions of AI-Augmented Additive Manufacturing 25
2.5.1 Digital Twin Technology in Additive Manufacturing 25
2.5.2 Current Research Challenges 25
2.5.3 Future Research Directions 26
2.6 Perspective on AI Applications in the Proposed System Based on the Literature Review 27
2.6.1 AI-Augmented Material Selection 27
2.6.2 AI-Based Generative Design 27
2.6.3 AI-Assisted Real-Time Process Monitoring 28
2.6.4 Integrated AI Workflow 28
2.6.5 Overall Perspective 28
CHAPTER 3 CASE STUDY: REVERSE ENGINEERING OF A TENNIS RACKET 29
3.1 INTRODUCTION 29
3.2 THEORETICAL BACKGROUND 29
3.2.1 Principles of Reverse Engineering 30
3.2.2 Photogrammetry in Industrial Applications 30
3.3 METHODOLOGY 31

3.3.1 Data Acquisition via Photogrammetry 31
3.3.2 3D CAD Reconstruction 32
3.3.3 Dimensional Compliance with ITF Standards 33
3.4 MANUFACTURING CONSTRAINTS AND SCALING STRATEGY 33
3.4.1 Assembly Strategy 33
3.4.2 Scale-Down Calculation 35
3.5 MATERIAL SELECTION AND CHARACTERIZATION 35
3.5.1 Handle Region: Thermoplastic Polyurethane (TPU 95A) 35
3.5.2 Frame and Head Region: Polyethylene Terephthalate Glycol (PETG) 37
3.6 STRUCTURAL ANALYSIS AND FINITE ELEMENT ANALYSIS 38
3.6.1 Loading Conditions 39
3.6.2 Stress Analysis Results 40
3.6.3 Modal Analysis and Frequency Response 42
3.7 GENERATIVE DESIGN VIA AUTODESK FUSION 360 43
3.7.1 Generative Design Outcomes and Observed Limitations 43
3.7.2 Infill Optimization Strategy 45
3.8 PERFORMANCE PREDICTIONS AND COMPARATIVE ANALYSIS 45
3.8.1 Vibration Transmission Reduction 45
3.8.2 Weight Reduction 46
3.8.3 Sweet Spot Enhancement 46
3.8.4 Sweet Spot Enhancement 46
CHAPTER 4 Discussion 48
4.1.1 INTRODUCTION 48
4.1.2 ADDITIVE MANUFACTURING TECHNOLOGIES AND MATERIALS USED 48
4.1.3 AI AUGMENTATION IN THE MATERIAL SELECTION SYSTEM 50
4.1.4 Dataset Collection and Preparation 50
4.1.5 Data Normalization Using AI-Based Preprocessing 52
4.1.6 Intelligent Similarity Analysis 53
4.1.7 Weighted Decision-Making 54

4.1.8 Technology-Based Intelligent Filtering..... 54
4.1.9 Ranking and Recommendation Generation..... 54
4.1.10 Human-Machine Interaction Through GUI..... 55
4.1.11 Why This System is Considered AI-Augmented..... 55
4.1.12 GUI AND SOURCE CODE..... 56
The Graphical User Interface (GUI)..... 56
..... 56
4.1.13 The Source Code..... 56
4.1.14 ADVANTAGES OF THE AI-AUGMENTED MATERIAL SELECTION SYSTEM..... 61
4.1.15 LIMITATIONS OF THE AI-AUGMENTED MATERIAL SELECTION SYSTEM..... 62
4.1.16 RECOMMENDATIONS..... 64
4.2 GENERATIVE DESIGN IN AI-AUGMENTED ADDITIVE MANUFACTURING..... 65
4.2.1INTRODUCTION..... 65
4.2.2Why Generative Design Matters..... 65
- Generative Design and Engineering Control..... 66
- Relation to the AI-Augmented AM Project..... 67
- Scope of This Report..... 68
4.2.3PROGRAMMATIC GENERATION AS THE FIRST PRACTICAL METHOD..... 68
4.2.4 Initial Implementation Workflow..... 69
4.2.4 Supported Design Families in the Programmatic Stage..... 69
4.2.5 Prompt Classification and Parameter Extraction..... 70
4.2.6 Geometry Generation Through Code..... 71
4.2.7 What We Actually Built in the Clean V1 System..... 71
4.2.8 Advantages of the Programming-Based Method..... 72
4.2.9 Limitations of the Programming-Based Method..... 73
4.2.9 Why a Code-Aware AI Model Is Needed..... 73
4.2.9 Transition: From Coding Errors to Trained Design Intelligence..... 74
4.3 PART II: GENERATIVE DESIGN THROUGH A TRAINED 3D MODEL..... 76
4.3.1 Training Data and 3D Learning Requirements..... 76

4.3.2 Prompt-to-Parameter Training Strategy 77
4.3.3 Trained 3D Model Direction 77
4.3.4 Comparison Between Programmatic and Trained 3D Generation 78
4.3.5 THE RECOMMENDED HYBRID ARCHITECTURE 79
4.3.6 VALIDATION, EXPORT, AND PREVIEW 79
4.3.7 LIMITATIONS AND FUTURE DEVELOPMENT 80
4.4 REAL-TIME MONITORING SYSTEM 81
4.4.1 INTRODUCTION 81
Problem Statement 81
Project Objectives 81
Project Scope 81
Materials and Equipment 82
4.4.2 REAL TIME MONITORING 82
4.4.3Real-Time Data Acquisition 83
4.4.4 Advantages of Real-Time Monitoring 84
4.4.5Disadvantages of Real-Time Monitoring 84
4.5METHODOLOGY 84
4.5.1Research Approach 84
4.5.2 Permutation and Combination Analysis 85
4.5.4 Selection of the Calibration Artifact 85
4.5.9 Experimental Design and Quality Metrics 87
4.5.10 Data Collection Protocol 88
4.6 SYSTEM IMPLEMENTATION 89
4.6.10 System Architecture Overview 89
4.6.11 OctoPrint Server Setup 89
4.6.12 Preparing the Calibration Artifact and Slicing via Cura 90
4.6.13 Plugin Integration and System Calibration 92
4.6.14 Connecting and Configuring Obico for AI Failure Detection 93
4.7 PYTHON SCRIPT INTEGRATION 94

4.7.10 Script Overview 94
4.7.11 System Architecture Components 94
4.7.12 Complete Python Script 94
4.7.13 Installation and Execution 97
4.8 RESULTS AND ANALYSIS 98
4.8.10 Optimum State Validation 98
4.8.11 Surface Quality Analysis 98
4.8.12 Dimensional Accuracy 98
4.8.13 First Layer Adhesion Results 99
4.8.14 Analysis of Parameter Interactions 99
4.8.15 Data Logging and Reporting Performance 99
4.5. STATISTICAL ANALYSIS AND RELIABILITY ASSESSMENT OF THE AI-BASED MONITORING SYSTEM 100
5.1 INTRODUCTION 100
5.2 EXPERIMENTAL DATA COLLECTION AND PREPROCESSING 101
5.3 STATISTICAL CHARACTERIZATION OF THERMAL BEHAVIOR 101
5.4 SAMPLE SIZE AND SAMPLING INTERVAL OPTIMIZATION 102
5.4.1 Importance of Sampling Design in Monitoring Systems 103
5.4.2 Statistical Basis of Sample Size Estimation 103
5.4.3 Confidence Interval–Based Sample Size Estimation 104
5.4.4 Hypothesis-Based Sample Size Validation 104
5.4.5 Final Sample Size Selection 105
5.4.6 Sampling Interval Optimization 106
5.4.7 Adaptive Interpretation of Sampling Behavior 107
5.5 THERMAL STABILITY AND PERFORMANCE EVALUATION 110
5.5.1 Mean Absolute Error (MAE) Analysis 110
5.5.2 Overshoot Analysis 110
5.5.3 Settling Time Analysis 111
5.5.4 Integrated Stability Assessment 112

5.6 RELIABILITY AND REPEATABILITY ANALYSIS 114
5.6.1 Multi-Run Experimental Evaluation 114
5.6.2 Performance-Based Classification (Pass/Fail Analysis) 115
5.6.3 File-Level Reliability Analysis 115
5.6.4 Overall System Reliability 116
5.6.5 Interpretation of Reliability Results 117
5.6.6 Consistency and Repeatability Analysis 117
5.7 INTEGRATED SYSTEM PERFORMANCE EVALUATION 119
CHAPTER 5 CONCLUSION AND RECOMMENDATIONS 122
5.1 CONCLUSION 122
5.2 RECOMMENDATIONS 123
5.3 PILOT CLOUD DEPLOYMENT AND LIVE BOT INTEGRATION 123
5.4 LONG-TERM INDUSTRIAL ROADMAP AND FUTURE WORK 128
GLOSSARY 130
CORE ADDITIVE MANUFACTURING TERMS 130
MATERIALS AND MATERIAL PROPERTIES 130
GEOMETRY, FILES, AND MODELING 131
REVERSE ENGINEERING AND PHOTOGRAMMETRY 132
GENERATIVE DESIGN AND AI CONCEPTS 132
MONITORING, CONTROL, AND CLOSED-LOOP SYSTEMS 133
EXPERIMENTAL METRICS AND STATISTICAL TERMS 134
PROCESS PARAMETERS AND PRINTING SETTINGS 134
MULTI-MATERIAL AND MANUFACTURING CONCEPTS 135
REFERENCES 137
ملخص المشروع 141

LIST OF SYMPOLS

Symbol	Description
µm	Micrometer (surface roughness unit)
σ	Standard Deviation
µ	Mean value
T	Nozzle Temperature (°C)
Tb	Bed Temperature (°C)
v	Print Speed (mm/s)
h	Layer Height (mm)
R	Roughness (µm)
SPH	Spindle Hours (used in DOE examples)
N	Sample Size
Δ	Difference between factor levels
F	F-statistic (ANOVA)
p	Probability value (statistical significance)
α	Significance level (e.g., 0.05)
β	Regression coefficient
Y	Response variable (predicted outcome)
E	Experimental error
df	Degrees of freedom (ANOVA)

LIST OF TERMS

Term	Description
AM	Additive Manufacturing
FDM	Fused Deposition Modeling
SLA	Stereolithography
SLS	Selective Laser Sintering
SLM	Selective Laser Melting
EBM	Electron Beam Melting
DLP	Digital Light Processing
DOE	Design of Experiments
ANOVA	Analysis of Variance
CAD	Computer-Aided Design
STL	Standard Tessellation Language (3D file format)
G-code	Machine instruction language for 3D printers
FEA	Finite Element Analysis
AI	Artificial Intelligence
CNN	Convolutional Neural Network
YOLO	“You Only Look Once” – real-time object detection algorithm
AI Vision System	Computer vision model for defect detection
Generative Design	AI-driven design process for optimized geometries
Reverse Engineering	Reconstruction of CAD models from physical products
Photogrammetry	Technique of creating 3D models from photographs
OctoPrint	Open-source platform for remote monitoring and control of 3D printers
Raspberry Pi	Low-cost single-board computer used for printer control
Jetson Nano	NVIDIA embedded computer for AI inference
Python	Programming language used for automation and control scripts
OpenCV	Computer vision library for image processing
TensorFlow	Machine learning framework for AI model training
PyTorch	Deep learning framework for research and model development
TensorRT	NVIDIA library for optimized inference on GPUs
Labellmg	Dataset labeling tool for image annotation
Roboflow	Cloud-based dataset preparation and augmentation tool
CVAT	Computer Vision Annotation Tool

PLA	Polylactic Acid – biodegradable thermoplastic
PETG	Polyethylene Terephthalate Glycol – durable polymer
TPU	Thermoplastic Polyurethane – flexible printing material
CF-PETG	Carbon Fiber Reinforced PETG – composite filament

LIST OF FIGURES

Figure 2.1 Additive Manufacturing workflow 5
Figure 2.2 Additive Manufacturing workflow 7
Figure 2.3 The seven categories of additive manufacturing 8
Figure 2.4 Principle of Fused Deposition Modeling 9
Figure 2.5 Common FDM defects 9
Figure 2.6 Principle of Stereolithography (SLA) 10
Figure 2.7 Principle of Selective Laser Sintering (SLS) 11
Figure 2.8 Principle of Selective Laser Melting (SLM/DLMS) 11
Figure 2.9 Classification of AM materials 14
Figure 2.10 3D-printed car parts 14
Figure 2.11 AI and Its Subfields 15
Figure 2.12 Different machine learning algorithms 17
Figure 2.13 Architecture of an artificial neural network 18
Figure 2.14 AI applications across the AM product lifecycle 20
Figure 2.15 AI-assisted Design for Additive Manufacturing (DfAM) workflow 21
Figure 2.16 The relationship between process parameters and printing quality 22
Figure 2.17 Real-time monitoring in additive manufacturing 22
Figure 2.18 Block diagram of AI-enabled closed-loop 3D printing 24
Figure 2.19 Digital Twin for additive manufacturing 25
Figure 3.1 The Original Tennis Racket as Primary Data Source for 3D Acquisition 32
Figure 3.2 Annotated Engineering Drawing of the Reconstructed Tennis Racket (All Dimensions in mm) 33
Figure 3.3 Rendered 3D CAD Model of the Full-Scale Tennis Racket 33
Figure 3.4 Rendered Handle and Head Components After Segmentation for FDM Printing 34
Figure 3.5 Two-Part CAD Assembly Drawing Showing Joint Geometry (Design 2) 34
Figure 3.6 Rendered 3D Model of the TPU 95A Handle Components 36
Figure 3.7 Rendered 3D Model of the PETG Frame and Head Region 37
Figure 3.8 Von Mises Stress Distribution from FEA — Sweet Spot Impact Loading 39
Figure 3.9 Modal Analysis — Frequency Amplitude Mode 1 40
Figure 3.10 Modal Analysis — Frequency Amplitude Mode 2 41
Figure 3.11 Modal Analysis — Frequency Amplitude Mode 3 41
Figure 3.12 Modal Analysis — Frequency Amplitude Mode 4 42
Figure 3.13 First Generative Design Iteration Showing Shell-Like Head Structure 44
Figure 3.14 Second Generative Design Iteration Showing Asymmetric Open-Web Frame 44
Figure 4.1 strength- density diagram 51

Figure 4.2 3d printing material comparison 52
Figure 4.3 FDM material charts properties 53
Figure 4.4 AI augmented material selection system GUI 56
Figure 5.1 Camshaft design 74
Figure 5.2 Twisted vase deign 75
Figure 5.3 tennis racket design 75
Figure 5.4 Chair design 75
Figure 5.5 Piston design 75
Figure 5.6 Crankshaft design 75
Figure 5.7 Mug Designs 75
Figure 6.1 FDM Printer System Setup with Monitoring Equipment 83
Figure 6.2 Calibration Cube 3D Model Used for Parameter Validation 87
Figure 6.3 OctoPrint Login Interface 90
Figure 6.4 Bed Visualizer 3D Topographic Heatmap 92
Figure 6.5 Obico Web Interface for AI-Powered Print Monitoring 93
Figure 6.6 Calibration Cubes Printed at Different Parameter Configurations 98
Figure 7.1 Sample size selection 106
Figure 7.2 Results 111
Figure 7.3 Temperature VS Time 112
Figure 7.4 PASS/FAIL Analysis 115
Figure 7.5 Reliability for each printing 116
Figure 7.6 Overall Reliability 117
Figure 8.1 The live user interface and welcome layout of the @ALXFFFBot Conversational HMI on the cloud server. 124
Figure 8.2 The AI Material Selector interface. 125
Figure 8.3 System snippet showing a successful background execution of the PrusaSlicer CLI engine and G-code generation triggered by user input. 126
Figure 8.4 User prompt preview demonstrating text-to-3D generation utilizing the geometry engine via the bot interface. 127
Figure 8.5 The Cost Calculator interface 128

LIST OF TABLES

Table 2.1 Comparison between AM technologies 12
Table 3.1 Scale-down calculations for the miniature prototype..... 35
Table 3.2 Mechanical properties of TPU 95A compared to common FDM thermoplastics..... 37
Table 3.3 Mechanical properties of PETG used in the FEA simulation..... 38
Table 3.4 Summary of FEA stress analysis results and safety factors. 42
Table 3.5 Predicted performance improvements of the re-engineered design versus the baseline. 47
Table 4.1 Materials Used with Their Properties and Applications..... 49
Table 5.1 Design families used in the controlled demonstration 67
Table 5.2 Examples of natural language parameter extraction across design families..... 71
Table 5.3 Software architecture layers and their responsibilities..... 72
Table 5.4 Programmatic Generation Vs Trained 3d Models 78
Table 6.6.1 Full Factorial Experimental Design Matrix Showing All Parameter Combinations..... 85
Table 6.6.2 Calibration Cube Physical Specifications..... 86
Table 6.6.3 Comparison of Calibration Artifact Candidates..... 87
Table 6.4 Surface Roughness by Nozzle Temperature..... 98
Table 7.1 Observed Results 105
Table 7.2 Overall System Performance Indicators..... 120

CHAPTER 1
INTRODUCTION

1.1 BACKGROUND AND MOTIVATION

Additive Manufacturing (AM) — the layer-by-layer fabrication of three-dimensional objects from digital models — enables unprecedented design freedom, material efficiency, and the production of complex geometries that are difficult or impossible with conventional subtractive methods. At the same time, AM workflows face persistent challenges: inconsistent process control, limited real-time quality assurance, and the growing complexity of selecting appropriate materials for specific applications. These limitations motivate the integration of Artificial Intelligence (AI) into AM to provide intelligence, adaptability, and automated optimization across the design-to-print pipeline.

1.2 PROBLEM STATEMENT

Current AM practice often separates design, material selection, process monitoring, and validation into distinct, manually driven steps. This separation leads to inefficiencies, longer development cycles, higher scrap rates, and suboptimal part performance. The project addresses the need for a unified, AI-augmented framework that:

- Automates and improves material selection for diverse AM technologies;
- Generates manufacturable designs from high-level requests while preserving engineering constraints; and
- Monitors and controls the printing process in real time to reduce defects and improve repeatability.

1.3 PROJECT OBJECTIVES

The primary objectives of the graduation project are to design, implement, and validate an AI-augmented additive manufacturing pipeline that integrates three core capabilities:

- Generative design that converts natural-language or parametric requests into validated 3D models suitable for AM;
- AI-assisted material selection that matches user requirements to candidate materials across AM technologies using a data-driven weighted scoring approach; and

- Real-time monitoring and control for FDM printing that uses AI to detect and reduce process faults and to optimize printing parameters, implementing a **Closed-Loop System**.

Secondary objectives include demonstrating reverse engineering and re-engineering of a case-study object (a tennis racket), performing structural validation (FEA), and providing statistical reliability assessment of the monitoring system.

1.4 SCOPE AND LIMITATIONS

This work focuses on a demonstrator pipeline suitable for a graduation project rather than an industrial production system. Key scope decisions include:

- Case study: reverse engineering and re-engineering of a commercially available tennis racket, including photogrammetric acquisition, CAD reconstruction, multi-material AM (PETG + TPU 95A), and structural evaluation.
- Generative design demo families: six controlled families (spur gear, piston, tennis racket, phone stand, crankshaft, twisted vase) to illustrate programmatic, model-based, and hybrid generation approaches.
- Monitoring experiments: FDM printing with PLA on a single Cartesian printer, using OctoPrint and a webcam for visual monitoring and data logging.
- Limitations include the constrained set of design families, single-printer experimental validation, and the demonstrator scale of trained 3D models (no attempt to build a universal 3D foundation model).

1.5 METHODOLOGICAL OVERVIEW

The project adopts a modular methodology combining experimental, computational, and data-driven techniques:

1. Reverse engineering: capture geometry via photogrammetry, reconstruct CAD models, and validate against standards.
2. Generative design: implement programmatic generators for parameterized families; explore trained 3D model approaches; integrate prompt understanding, parameter extraction, and mesh validation.
3. Material selection: build a normalized, weighted distance algorithm to match user requirements to material property databases across AM technologies.
4. Real-time monitoring: instrument an FDM printer with OctoPrint and a vision pipeline, collect thermal and visual data, apply AI for failure detection, and log results for statistical analysis.

5. Validation and analysis: perform FEA on re-engineered parts and conduct statistical and reliability assessments of monitoring performance.

1.6 CONTRIBUTIONS

This thesis presents a cohesive AI-augmented AM demonstrator that:
integrates generative design, AI material selection, and real-time monitoring into a single workflow; demonstrates a full reverse-engineering and re-engineering cycle for a sports equipment case study; and provides experimental evidence and statistical evaluation of an AI-based monitoring system for FDM printing.

1.7 REPORT OUTLINE

Chapter II: Review Of Literature

-Surveys AI in AM, reverse engineering methods, generative design, material selection strategies, process monitoring, and FEA foundations that justify the chosen methodology.

Chapter III: Case study: Reverse Engineering of a Tennis Racket

-Documents photogrammetric acquisition, CAD reconstruction, ITF-compliance checks, multi-material re-engineering, and structural validation for the tennis racket case study.

Chapter IV: AI-Augmented Material Selection System

-Describes the data-driven material matching algorithm, property normalization, weighted distance scoring, and the system's application across AM technologies.

Chapter V: Generative Design in AI-Augmented Additive Manufacturing

-Presents programmatic and model-based generation approaches, the hybrid architecture (prompt → family → parameter extraction → generation → validation), and the six demo families used in the demonstrator.

Chapter VI: Real-Time Monitoring System

-Explains the monitoring architecture (OctoPrint, Obico platform, camera setup, data logging), experimental design for parameter optimization, and the implementation of AI-based failure detection.

Chapter VII: Statistical Analysis and Reliability Assessment of the AI-Based Monitoring System

-Provides statistical characterization of thermal and visual data, sample-size and sampling optimization, thermal stability analysis, and reliability metrics for the monitoring system..

Chapter VIII: Conclusions and Recommendations

– Summarizes the key findings and suggests future directions for expanding the proposed framework.

CHAPTER 2
REVIEW OF LITERATURE

2.1 INTRODUCTION

Additive manufacturing (AM), commonly known as three-dimensional (3D) printing, has become one of the most important manufacturing technologies in recent decades. Unlike conventional manufacturing methods that remove material from a workpiece or shape it using molds, additive manufacturing creates parts by depositing material layer by layer according to a digital three-dimensional model. This manufacturing approach provides greater design freedom, reduces material waste, and allows the production of complex geometries that are difficult or impossible to manufacture using traditional techniques. These advantages have encouraged many industries, including aerospace, automotive, biomedical engineering, healthcare, construction, and consumer products, to adopt additive manufacturing for both prototyping and final production.

Although additive manufacturing has achieved remarkable progress, several technical challenges still limit its wider industrial use. The quality of printed parts depends on a large number of process parameters such as printing temperature, layer thickness, printing speed, nozzle movement, material properties, and environmental conditions. Small changes in these parameters may produce printing defects such as warping, poor layer bonding, porosity, dimensional errors, and surface roughness. These defects reduce the mechanical performance of printed components and increase manufacturing costs because failed parts usually cannot be repaired after printing is completed.

Artificial intelligence (AI) has recently emerged as an effective solution for many of these challenges. AI systems can process large amounts of manufacturing data, identify patterns that are difficult for humans to detect, and make intelligent decisions during the printing process. Machine learning, deep learning, and computer vision have been successfully applied to monitor printing quality, predict failures, optimize process parameters, detect defects, and improve overall manufacturing efficiency. The combination of AI and additive manufacturing is changing traditional 3D printing into a more intelligent and adaptive manufacturing process capable of improving quality while reducing waste and production time.

This chapter reviews the current literature related to additive manufacturing, artificial intelligence, and the integration of both technologies. The review begins with the fundamentals of additive manufacturing, followed by the basic concepts of artificial intelligence. Finally, the chapter discusses how AI techniques are integrated with additive manufacturing to improve process monitoring, parameter optimization, defect detection, quality control, and intelligent decision-making.

2.2 Additive Manufacturing

2.2.1 Definition of Additive Manufacturing

Additive manufacturing is a manufacturing process that builds physical objects directly from a digital three-dimensional computer-aided design (CAD) model by depositing material layer upon layer. Unlike subtractive manufacturing, where material is removed from a solid block using machining operations, additive manufacturing adds material only where it is required. As a result, material waste is significantly reduced, manufacturing flexibility is increased, and complex internal and external geometries become possible without requiring specialized tooling or molds.

The manufacturing process usually starts by creating a three-dimensional CAD model. The model is converted into a standard tessellation language (STL) file and then sliced into hundreds or thousands of thin layers using slicing software. These sliced layers are converted into machine instructions that guide the printer during fabrication. The printer deposits or solidifies material layer by layer until the complete object is produced. This digital workflow makes additive manufacturing highly suitable for rapid design modifications and customized production.

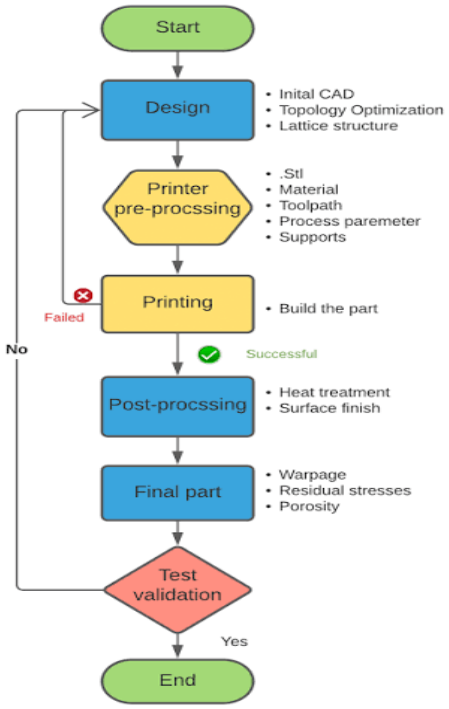


Figure 2.1 Additive Manufacturing workflow

2.2.2 Development of Additive Manufacturing

The development of additive manufacturing began during the early 1980s with the introduction of stereolithography (SLA), one of the earliest commercial 3D printing technologies. Since then, continuous improvements in materials, machine design, software, and process control have expanded the capabilities of additive manufacturing. Initially, the technology was mainly used for rapid

prototyping because it allowed engineers to quickly evaluate product designs before mass production. As printing accuracy, material quality, and mechanical properties improved, additive manufacturing gradually became suitable for producing functional engineering components instead of prototypes only.

Modern additive manufacturing now supports a wide range of engineering materials including thermoplastics, metals, ceramics, composites, and biological materials. These developments have enabled applications in aerospace structures, customized medical implants, automotive components, lightweight structures, energy systems, wearable devices, construction, and tissue engineering. Continuous improvements in hardware and software have also increased printing speed, dimensional accuracy, and process reliability.

2.2.3 Working Principle of Additive Manufacturing

Although different additive manufacturing technologies use different materials and energy sources, they generally follow the same basic manufacturing sequence. First, a digital CAD model is prepared using computer-aided design software. The model is then converted into a printable format and sliced into thin horizontal layers. During printing, each layer is fabricated according to the sliced geometry. After one layer is completed, the printer deposits or solidifies the next layer directly on top of the previous one until the final object is finished. Depending on the printing technology, the deposited material may be melted, cured using light, sintered by a laser, or bonded using adhesives.

This layer-by-layer manufacturing approach offers several important advantages. Internal channels, lattice structures, lightweight designs, and highly complex geometries can be produced without the limitations associated with traditional machining or molding processes. At the same time, manufacturing time for prototypes is significantly reduced because expensive tooling is not required. These characteristics have made additive manufacturing one of the key technologies supporting Industry 4.0 and digital manufacturing.

2.2.4 Main Characteristics of Additive Manufacturing

One of the main characteristics of additive manufacturing is its ability to produce highly customized products directly from digital models without changing production equipment. Each printed component can have different dimensions or internal structures while using the same machine. This capability is especially important in biomedical engineering, where patient-specific implants and prosthetic devices are required.

Another important characteristic is efficient material utilization. Because material is deposited only where needed, waste is much lower than in traditional subtractive manufacturing processes. This feature reduces manufacturing costs for expensive materials such as titanium alloys and contributes to more sustainable production. In addition, additive manufacturing allows engineers to combine topology optimization, lattice structures, and lightweight designs to reduce part weight while maintaining mechanical strength.

Despite these advantages, additive manufacturing still faces several limitations, including relatively slow production speed, high equipment cost for industrial systems, limited availability of certified materials, surface finish issues, dimensional accuracy challenges, and process variability. These limitations motivate researchers to integrate artificial intelligence into additive manufacturing systems to improve process control and product quality, which will be discussed in the following sections.

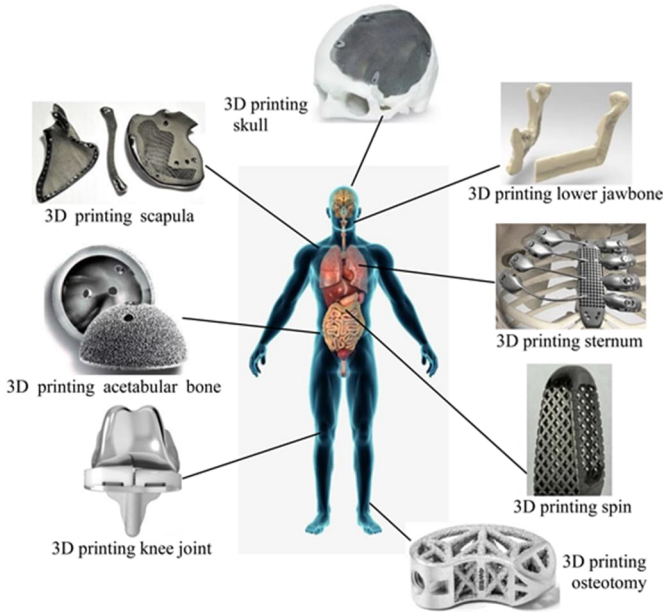


Figure 2.2 Additive Manufacturing workflow

2.2.5 Additive Manufacturing Technologies

Several additive manufacturing technologies have been developed over the past four decades. Although all of them build parts layer by layer, they differ in their working principles, energy sources, printable materials, production speed, dimensional accuracy, and industrial applications. The selection of a suitable AM process depends on the required material, mechanical properties, manufacturing cost, surface quality, and production volume. International standards classify additive manufacturing into seven main process categories, each designed for specific engineering applications.

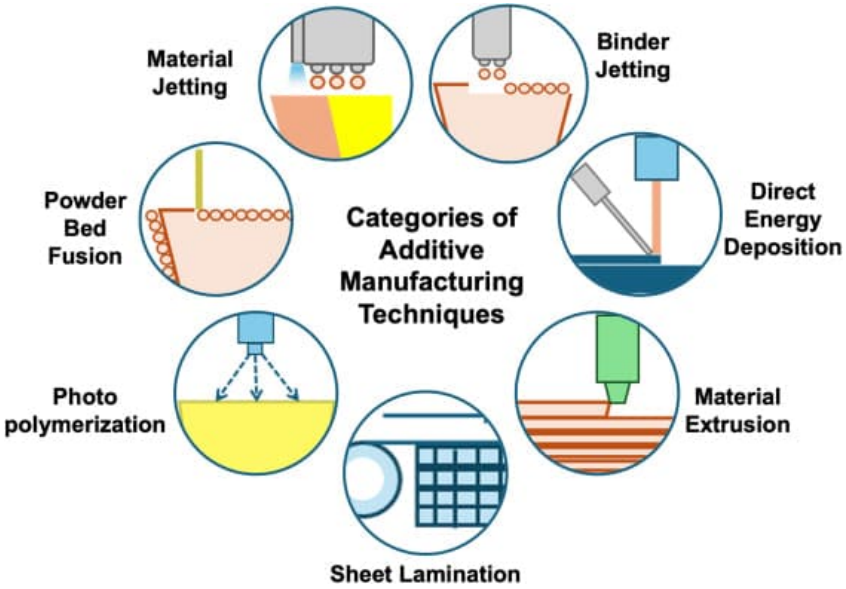


Figure 2.3 The seven categories of additive manufacturing

2.2.5.1 Fused Deposition Modeling (FDM)

Fused Deposition Modeling (FDM), also known as Material Extrusion, is one of the most widely used additive manufacturing technologies because of its relatively low cost, ease of operation, and wide availability. During the printing process, a thermoplastic filament is fed into a heated nozzle where it melts before being deposited layer by layer onto the build platform. As the material cools, it solidifies and bonds with the previous layer until the complete object is formed.

FDM printers commonly use materials such as PLA, ABS, PETG, TPU, Nylon, and composite filaments reinforced with carbon fiber or glass fiber. These materials provide different combinations of strength, flexibility, temperature resistance, and printing difficulty depending on the intended application.

The popularity of FDM comes from its ability to manufacture functional prototypes quickly while minimizing production costs. Educational institutions, research laboratories, product designers, and small manufacturing companies widely use this technology for rapid prototyping, tooling, customized products, and low-volume production.

However, several limitations still affect FDM printing quality. Poor layer adhesion may reduce mechanical strength, especially along the build direction. Warping, nozzle clogging, dimensional inaccuracies, stringing, and surface roughness are common printing defects. Most of these problems originate from incorrect printing parameters such as nozzle temperature, printing speed, cooling conditions, layer height, and extrusion rate. Therefore, accurate parameter selection is essential to achieve high-quality printed components.

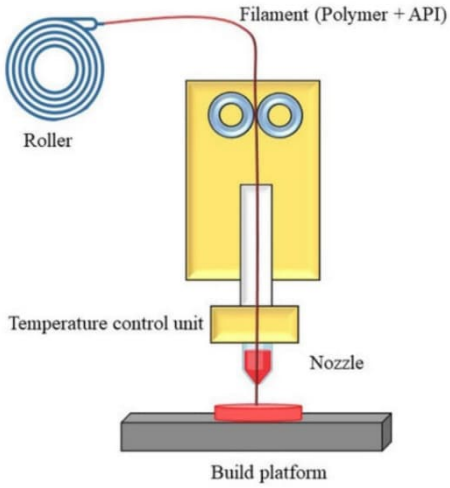


Figure 2.4 Principle of Fused Deposition Modeling

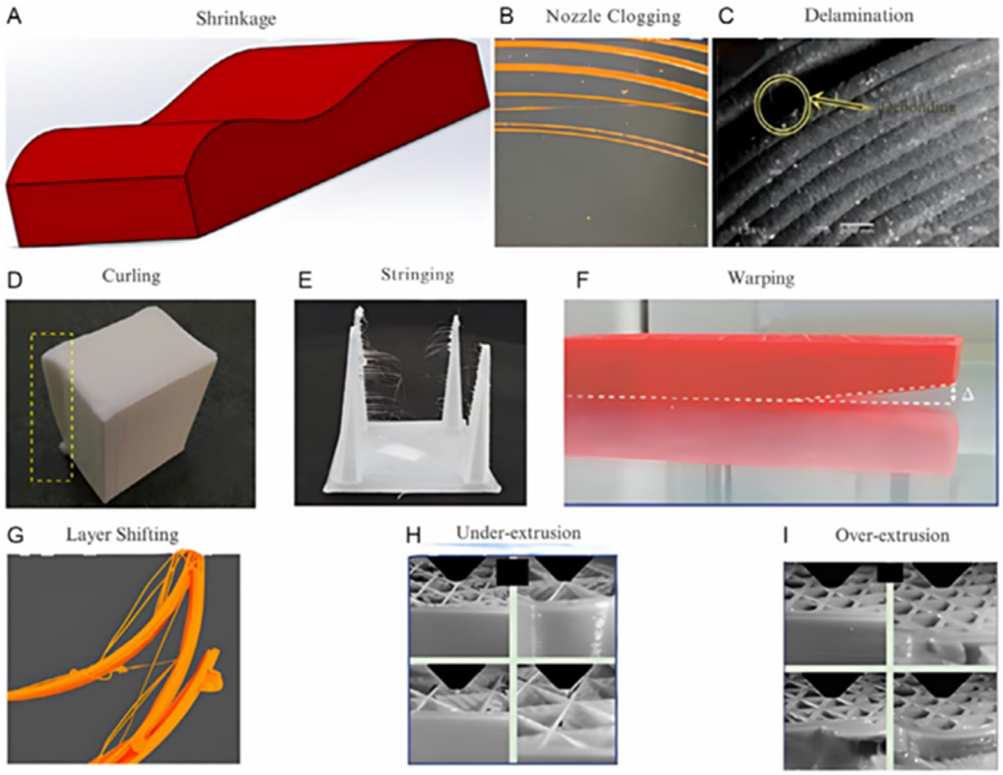


Figure 2.5 Common FDM defects

2.2.5.2 Stereolithography (SLA)

Stereolithography is one of the earliest additive manufacturing technologies and remains one of the highest-precision polymer printing methods. In SLA, a laser selectively cures liquid photopolymer resin inside a resin tank. Each cured layer becomes solid before the build platform moves to allow formation of the next layer.

SLA produces components with excellent dimensional accuracy, fine surface finish, and intricate geometrical details. Consequently, it is widely applied in dentistry, medical models, jewelry manufacturing, microfluidic devices, and precision engineering.

Despite these advantages, SLA has several disadvantages. Printing materials are generally more expensive than thermoplastic filaments used in FDM. Printed components often require cleaning, UV post-curing, and support removal before use. In addition, many photopolymer resins exhibit limited mechanical strength and long-term environmental resistance.

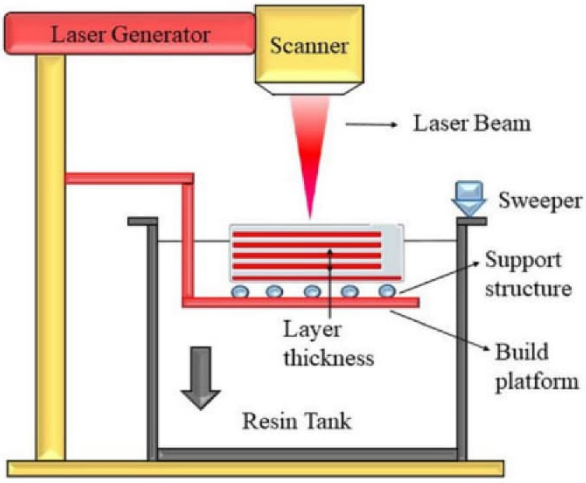


Figure 2.6 Principle of Stereolithography (SLA)

2.2.5.3 Selective Laser Sintering (SLS)

Selective Laser Sintering uses a high-energy laser to fuse powdered materials layer by layer inside a powder bed. Unlike FDM or SLA, surrounding unfused powder naturally supports overhanging structures during printing, reducing the need for support structures.

SLS is capable of producing complex geometries with relatively good mechanical performance. Engineering polymers such as Nylon are commonly processed using this technology. SLS has found extensive applications in aerospace, automotive engineering, medical devices, and industrial tooling because it produces functional components with excellent strength.

Nevertheless, SLS equipment is expensive, requires specialized powder handling systems, and consumes relatively high amounts of energy. Powder recycling and thermal management also remain important engineering challenges.

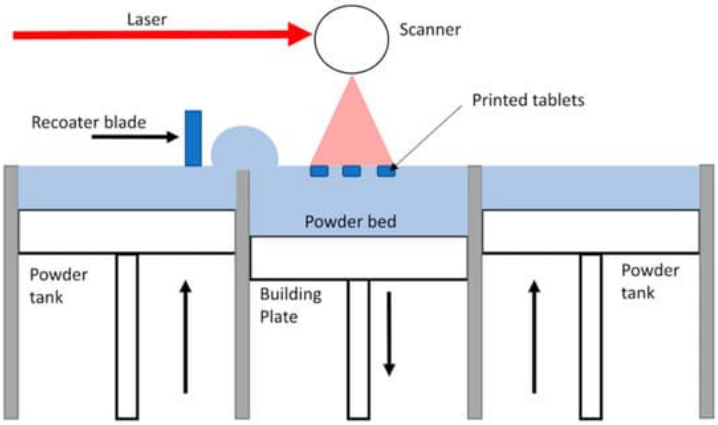


Figure 2.7 Principle of Selective Laser Sintering (SLS)

2.2.5.4 Selective Laser Melting (SLM)

Selective Laser Melting is mainly used for metal additive manufacturing. Unlike SLS, SLM completely melts the metallic powder instead of partially sintering it. This process produces nearly fully dense metal components with excellent mechanical properties.

Materials processed by SLM include stainless steel, titanium alloys, aluminum alloys, cobalt-chromium alloys, and nickel-based superalloys. The technology has become essential in aerospace, biomedical implants, automotive engineering, and high-performance industrial applications.

Although SLM provides excellent part quality, it involves complex thermal behavior. Residual stresses, distortion, cracking, porosity, and balling defects may occur because of rapid heating and cooling cycles. These issues require careful optimization of laser power, scan speed, hatch spacing, and layer thickness.

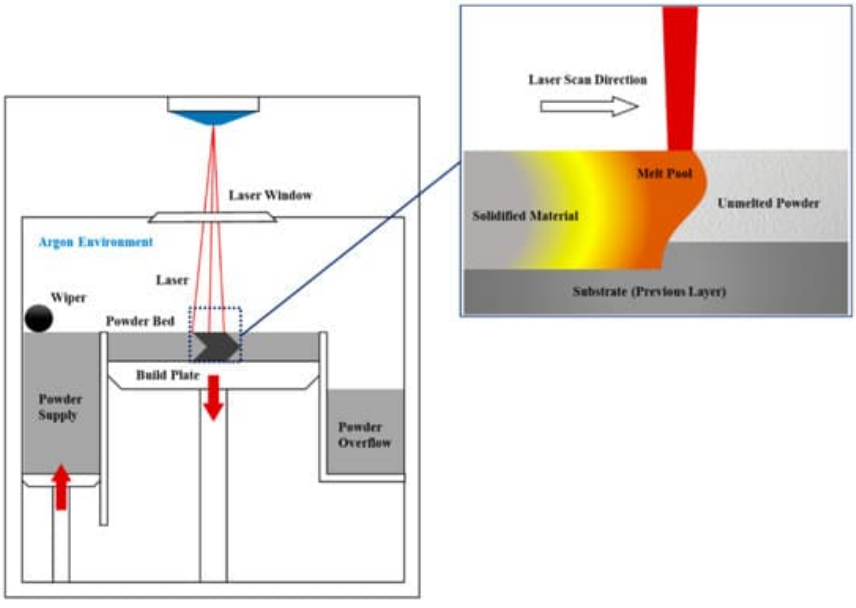


Figure 2.8 Principle of Selective Laser Melting (SLM/DLMS)

2.2.5.5 Digital Light Processing (DLP)

Digital Light Processing is another resin-based additive manufacturing technology. Instead of tracing each layer with a laser, DLP projects an entire image of each layer simultaneously using a digital projector. This significantly reduces printing time while maintaining high dimensional accuracy.

DLP is widely used in dentistry, hearing aids, jewelry, and precision prototype manufacturing. Similar to SLA, it requires photopolymer materials and usually involves post-processing operations after printing.

Table 2.1 Comparison between AM technologies

Technology	Principle	Advantages	Limitations	Key Challenges in the Future
FDM	Melts and extrudes thermoplastic filament layer by layer	Wide range of materials; Effective cost; User-friendly; Accessible	Lower productivity, especially for complex designs; Limited resolution; Material warping	Test several composite materials based on thermoplastics; Improve print speed and surface quality; Develop printers for high scale products
SLA	Cures liquid photopolymer resin using UV light layer by layer	High precision and detail; Good surface finish; Wide range of materials	Higher post-processing time; High resin cost; Limited build size	Enhance the material choice and sustainability; Reduce post-processing times; Test applications in bigger scales
SLS	Uses a laser to selectively fuse powdered materials layer by layer	Strong and functional parts; Complex geometries; Without the need of supporting structures	High equipment cost; Limited material options; Low surface finish; Low resolution	Test wider range of materials and integrate composites; Reduce costs and improve scalability; Optimize the surface finish and precision of printed products
DLP	Uses a digital light projector to cure resin layer by layer	High quality of prints; Fast printing speeds; Good for prototyping	Small range of materials; Requires post-processing; Resin can be hazardous	Develop safer materials; Innovate eco-friendly or bio-based resins; Test composite resins; Test wider range of printing materials

SLM/DLMS	Relies on the projection or modulation of a light SLM/DLMS pattern to selectively harden, sinter, or melt the material as a sequence of thin layers is deposited	Enables complex geometries; High strength-to-weight ratios; Allows complete fusion of powders to create strong parts	Challenges in optimizing process parameters; Ensuring part quality, and expanding material compatibility; Gaps in Enables complex geometries; High strength-to-weight ratios; Allows complete fusion of powders to create strong parts controlling defects such as porosity, residual stresses, and anisotropic mechanical properties, which limits the reliability and scalability of SLM/DLMS parts	Require additional work to compensate for high residual stress and limit the occurrence of distortion; Several studies highlighted non-linear relationships between energy density and mechanical outcomes, emphasizing the need for optimized parameter windows to avoid defects like keyhole formation or lack of fusion
Binder Jetting	Deposits a liquid binder onto layers of powder to form 3D objects	Fast printing speeds; Suitable for large parts; Minimal waste generation	Limited mechanical properties; Requires post-processing (e.g., sintering); Low surface finish	Expand material options; Improve part strength and durability; Optimization to improve the surface finish
Material Jetting	Sprays droplets of liquid material which are cured layer by layer	Multi-material capabilities; High resolution and surface quality	Requires extensive post-processing depending on designs; High material costs	Improve compatibility and range of substances; Develop more affordable materials

2.2.6 Materials Used in Additive Manufacturing

The performance of additive manufacturing depends not only on the printing technology but also on the materials used. Different AM processes support different classes of engineering materials, including thermoplastics, photopolymers, metals, ceramics, composites, and biological materials. Material selection directly influences mechanical properties, dimensional accuracy, thermal resistance, chemical stability, production cost, and overall printing quality.

Thermoplastics such as PLA, ABS, PETG, TPU, Nylon, and Polycarbonate remain the most common materials in material extrusion systems. Metal additive manufacturing mainly uses titanium alloys, aluminum alloys, stainless steel, cobalt-chromium, and nickel-based alloys because of their excellent strength and corrosion resistance. Composite materials reinforced with carbon fibers, glass fibers, or ceramic particles have recently gained significant attention due to their improved mechanical performance. Bio-based materials and hydrogels have also become important for tissue engineering and biomedical applications.

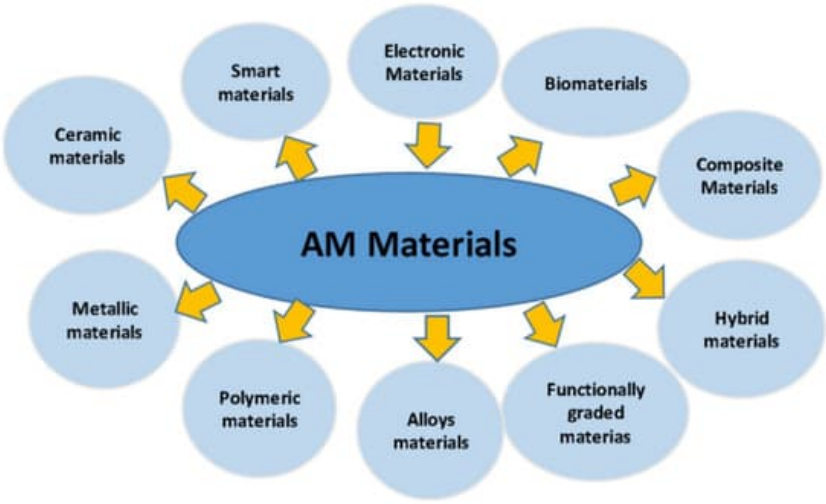


Figure 2.9 Classification of AM materials

2.2.7 Industrial Applications of Additive Manufacturing

The flexibility of additive manufacturing has enabled its adoption across many industrial sectors. Aerospace manufacturers use AM to produce lightweight structures with optimized internal geometries that reduce fuel consumption while maintaining mechanical strength. Automotive companies employ additive manufacturing for rapid prototyping, customized components, lightweight brackets, and tooling. Medical applications include customized implants, prosthetic devices, surgical guides, dental restorations, tissue engineering, and bioprinting. Other applications include architecture, construction, electronics, wearable devices, robotics, energy systems, and food production.



Figure 2.10 3D-printed car parts

2.2.8 Advantages and Challenges of Additive Manufacturing

The main advantages of additive manufacturing include high design freedom, reduced material waste, elimination of expensive tooling, shorter product development cycles, mass customization, and

the ability to manufacture highly complex geometries. These benefits have made AM one of the enabling technologies of Industry 4.0.

However, several technical challenges continue to limit its broader industrial implementation. Printing speed remains relatively slow for large-scale production. Surface finish often requires post-processing. Mechanical properties may vary because of anisotropic layer bonding. Material availability remains limited for some industrial applications. In addition, defects such as porosity, residual stresses, dimensional errors, warping, delamination, balling, and poor surface quality continue to affect product reliability. These challenges have motivated researchers to integrate artificial intelligence into additive manufacturing systems to improve monitoring, quality prediction, process optimization, and autonomous decision-making during printing.

2.3 Artificial Intelligence

Artificial intelligence (AI) has become one of the most influential technologies in modern engineering and manufacturing. It enables computer systems to perform tasks that normally require human intelligence, such as learning from data, recognizing patterns, making decisions, solving problems, and adapting to changing conditions. The rapid development of computing power, cloud computing, sensor technologies, and data availability has accelerated the adoption of AI across many industrial sectors. Today, AI is considered one of the key technologies supporting Industry 4.0 because it allows manufacturing systems to become more intelligent, efficient, and autonomous.

Unlike conventional computer programs that follow fixed instructions, AI systems can learn from previous data and continuously improve their performance without requiring explicit programming for every situation. By analyzing large datasets collected from sensors, cameras, machines, and production systems, AI can identify hidden relationships between variables, predict future outcomes, and recommend optimal actions. These capabilities have made AI an important tool for improving manufacturing quality, reducing production costs, minimizing waste, and increasing process reliability.

Artificial intelligence includes several research fields, including machine learning, deep learning, computer vision, natural language processing, and reinforcement learning. Although each field has different objectives and techniques, they all contribute to the development of intelligent systems capable of supporting engineering decision-making. In additive manufacturing, machine learning and computer vision are currently the most widely used AI techniques because they can analyze printing data, detect defects, optimize process parameters, and improve product quality in real time.

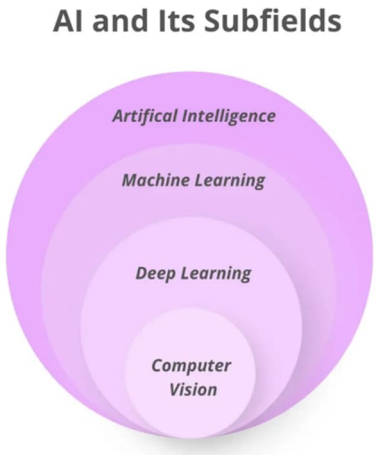


Figure 2.11 AI and Its Subfields

2.3.1 Evolution of Artificial Intelligence

The concept of artificial intelligence has evolved significantly since it was first introduced. Early AI systems relied mainly on predefined rules created by experts. These systems, often called rule-based or expert systems, could perform specific tasks by following a set of logical instructions. While they were useful for simple applications, their performance was limited because they could not learn from new data or adapt to changing environments.

The availability of large datasets, improved computing hardware, and advances in machine learning algorithms shifted AI from rule-based programming toward data-driven learning. Modern AI systems learn directly from historical data instead of relying only on manually created rules. As more data become available, these systems continue improving their prediction accuracy and decision-making capabilities. This transition has greatly expanded the use of AI in manufacturing, healthcare, transportation, finance, and many other engineering fields.

Today, AI supports intelligent manufacturing by processing information collected from sensors, cameras, monitoring systems, and production equipment. Instead of simply detecting problems after production is completed, AI enables manufacturers to predict failures before they occur and adjust manufacturing parameters automatically to maintain product quality. This predictive capability represents one of the major advantages of modern AI systems compared with traditional manufacturing approaches.

2.3.2 Machine Learning

Machine learning (ML) is one of the most important branches of artificial intelligence and forms the foundation of most current AI applications in engineering. Machine learning enables computers to identify relationships within data and build mathematical models that can make predictions or decisions without being explicitly programmed for every possible situation. Instead of following fixed instructions, machine learning algorithms improve their performance by analyzing examples collected from previous observations.

Machine learning has become particularly valuable in manufacturing because modern production systems generate large amounts of data from sensors, inspection systems, machine controllers, and monitoring devices. These data contain valuable information about machine conditions, product quality, process performance, and manufacturing defects. Machine learning algorithms can analyze these datasets much faster than traditional statistical methods and discover complex relationships between manufacturing parameters and final product quality.

The three main categories of machine learning are supervised learning, unsupervised learning, and reinforcement learning.

In supervised learning, algorithms are trained using labeled datasets where both the input data and the expected output are known. The model learns the relationship between inputs and outputs so that it can

predict the correct output for new data. Supervised learning is widely used for quality prediction, defect classification, process optimization, and dimensional accuracy prediction in additive manufacturing.

Unsupervised learning works with unlabeled datasets where the correct output is unknown. Instead of making predictions, these algorithms identify hidden patterns, similarities, or groups within the data. Manufacturing engineers use unsupervised learning for anomaly detection, process monitoring, clustering production conditions, and discovering unknown relationships among manufacturing variables.

Reinforcement learning differs from the previous approaches because the algorithm learns through continuous interaction with its environment. It receives rewards for successful decisions and penalties for unsuccessful actions, gradually improving its decision-making strategy. Although reinforcement learning is less common than supervised learning in current additive manufacturing research, it has shown promising potential for autonomous process control and adaptive optimization.

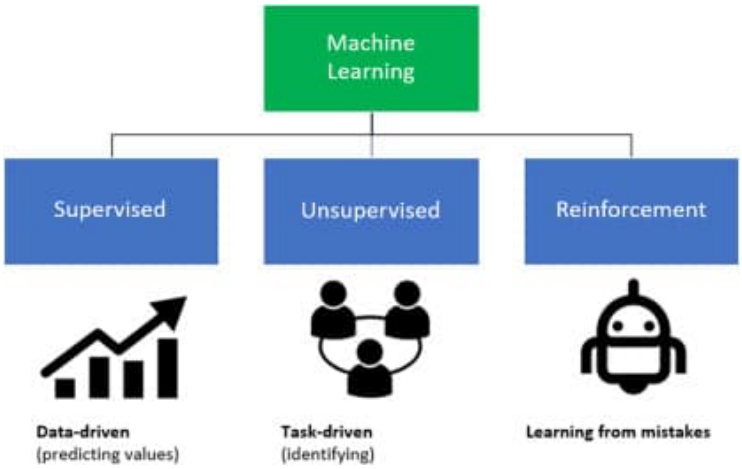


Figure 2.12 Different machine learning algorithms

2.3.3 Deep Learning

Deep learning is a specialized branch of machine learning that uses artificial neural networks with multiple hidden layers to analyze highly complex data. These neural networks are inspired by the structure of the human brain, where interconnected neurons process information and gradually learn useful features from the input data.

One of the main advantages of deep learning is its ability to perform automatic feature extraction. Traditional machine learning often requires engineers to manually select important variables before model training. In contrast, deep learning automatically identifies the most relevant features directly from raw data, making it particularly effective for image processing, sound analysis, video monitoring, and large manufacturing datasets.

Deep learning has become increasingly important in additive manufacturing because modern 3D printers generate large volumes of sensor signals, thermal images, melt-pool photographs, and process

videos. Convolutional Neural Networks (CNNs) are commonly used to analyze printing images and detect defects such as cracks, porosity, incomplete fusion, and layer separation. Recurrent Neural Networks (RNNs) and Long Short-Term Memory (LSTM) networks are frequently applied to analyze time-series sensor data collected during printing operations.

Despite their excellent performance, deep learning models require large training datasets and significant computational resources. The quality of predictions also depends heavily on the quantity and quality of the available data. For this reason, researchers continue developing more efficient deep learning techniques that require fewer training samples while maintaining high prediction accuracy.

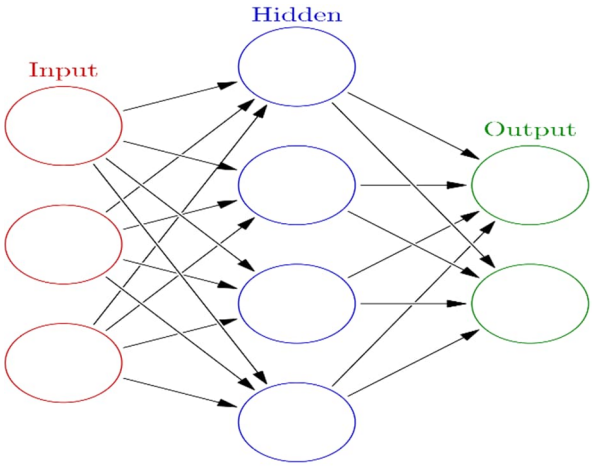


Figure 2.13 Architecture of an artificial neural network

2.3.4 Computer Vision

Computer vision is another important field of artificial intelligence that enables computers to interpret and analyze visual information obtained from cameras or imaging systems. By processing images and videos, computer vision systems can recognize objects, identify defects, measure dimensions, monitor manufacturing processes, and evaluate product quality automatically.

In manufacturing environments, computer vision has replaced many manual inspection procedures because it provides faster, more accurate, and more consistent quality assessment. Cameras installed inside production equipment continuously capture images during manufacturing. AI algorithms analyze these images in real time and immediately detect abnormal conditions before they affect the final product.

Within additive manufacturing, computer vision is widely applied to monitor layer deposition, melt-pool behavior, powder distribution, extrusion quality, and surface finish. Early detection of defects allows corrective actions to be taken before the entire printing process fails, reducing production costs and material waste.

2.3.5 Artificial Intelligence in Manufacturing

Artificial intelligence has transformed manufacturing from traditional automation toward intelligent production systems capable of learning, adapting, and making decisions based on real-time information. Modern manufacturing facilities generate large amounts of data through industrial sensors, programmable logic controllers (PLCs), cameras, Internet of Things (IoT) devices, and machine monitoring systems. AI algorithms process these data to improve productivity, optimize production schedules, reduce equipment downtime, and maintain consistent product quality.

Some of the most common applications of AI in manufacturing include predictive maintenance, quality inspection, process optimization, production planning, energy management, robotic automation, and supply chain optimization. Instead of reacting to equipment failures after they occur, AI systems predict future failures using historical operational data, allowing maintenance activities to be scheduled before breakdowns happen.

AI also supports manufacturing decision-making by analyzing relationships among hundreds of production variables simultaneously. This capability enables manufacturers to identify the optimal operating conditions that maximize product quality while minimizing production cost and material waste. As manufacturing systems continue to become more connected through Industry 4.0 technologies, the role of AI is expected to grow further across all stages of the production lifecycle.

2.4 Augmentation of Artificial Intelligence in Additive Manufacturing

The integration of artificial intelligence with additive manufacturing has significantly changed the capabilities of modern 3D printing systems. Traditional additive manufacturing depends heavily on human experience to select process parameters, monitor printing quality, identify defects, and adjust manufacturing conditions. This approach often requires repeated trial-and-error experiments, resulting in increased production time, higher material consumption, and inconsistent product quality. Artificial intelligence provides a more efficient solution by enabling manufacturing systems to analyze large amounts of production data, predict printing outcomes, optimize manufacturing parameters, and support autonomous decision-making throughout the printing process.

The combination of AI and additive manufacturing represents one of the major developments within Industry 4.0. Instead of treating design, printing, inspection, and quality control as separate stages, AI enables these activities to become connected through continuous data exchange. Information collected during one stage can be used to improve decisions in later stages, creating a more intelligent manufacturing workflow. As a result, additive manufacturing systems become capable of learning from previous production cycles and continuously improving their performance over time.

2.4.1 Artificial Intelligence Across the Additive Manufacturing Lifecycle

Artificial intelligence supports nearly every stage of the additive manufacturing lifecycle, beginning with product design and continuing through process planning, material selection, printing, quality inspection, and post-processing. Each stage generates valuable information that can be used to improve subsequent manufacturing operations.

During the design stage, AI assists engineers in developing geometries that satisfy functional requirements while remaining suitable for additive manufacturing. During process planning, AI predicts the influence of different process parameters before printing begins. Throughout the printing process, AI continuously monitors machine conditions and identifies abnormal behavior. After printing, AI supports quality inspection by detecting defects and evaluating dimensional accuracy. The collected information is then stored and used to improve future manufacturing decisions.

This continuous learning process distinguishes intelligent additive manufacturing systems from conventional production methods. Rather than optimizing each manufacturing stage independently, AI establishes connections among all stages of the product lifecycle, allowing improvements made in one stage to benefit the entire manufacturing process.

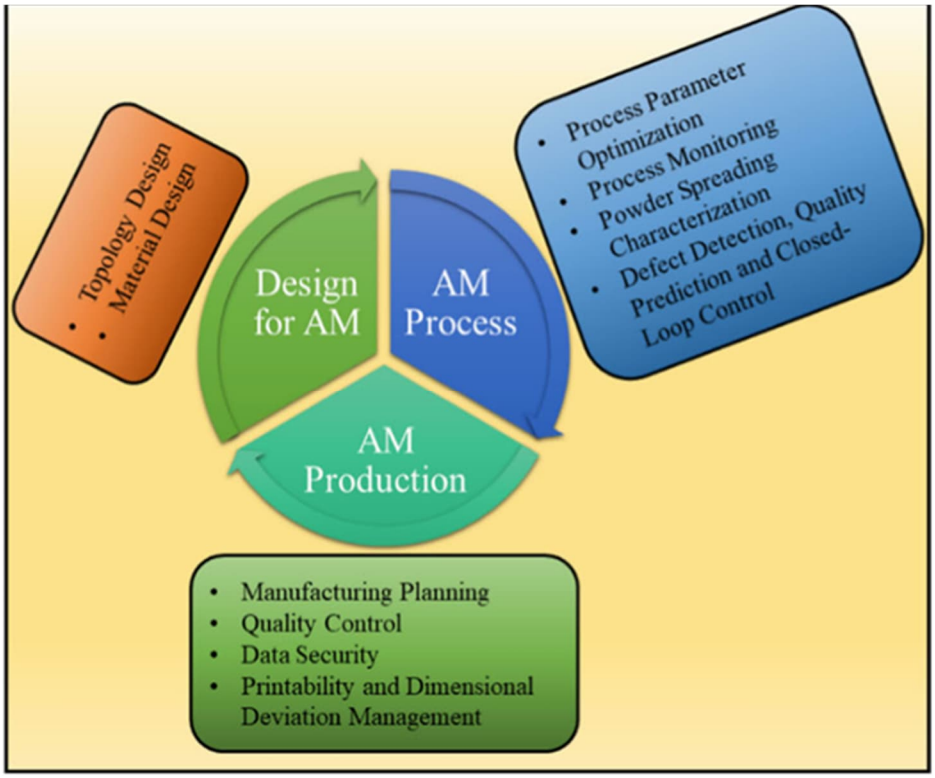


Figure 2.14 AI applications across the AM product lifecycle

2.4.2 AI-Assisted Design for Additive Manufacturing

Design for Additive Manufacturing (DfAM) aims to develop products that fully utilize the advantages of additive manufacturing while minimizing manufacturing limitations. Unlike

conventional design methods, DfAM considers printing constraints, material behavior, support structures, thermal deformation, residual stresses, and manufacturing feasibility during the early design stage.

Artificial intelligence has significantly improved DfAM by helping engineers evaluate multiple design alternatives automatically. Machine learning algorithms analyze previous successful designs together with manufacturing data to recommend design modifications that improve printability, reduce material usage, shorten printing time, and increase structural performance.

AI also supports topology optimization and generative design. These techniques automatically generate lightweight structures that satisfy mechanical requirements while minimizing material consumption. Instead of manually modifying component geometry, engineers define functional requirements and design constraints, while AI produces several optimized design alternatives suitable for additive manufacturing.

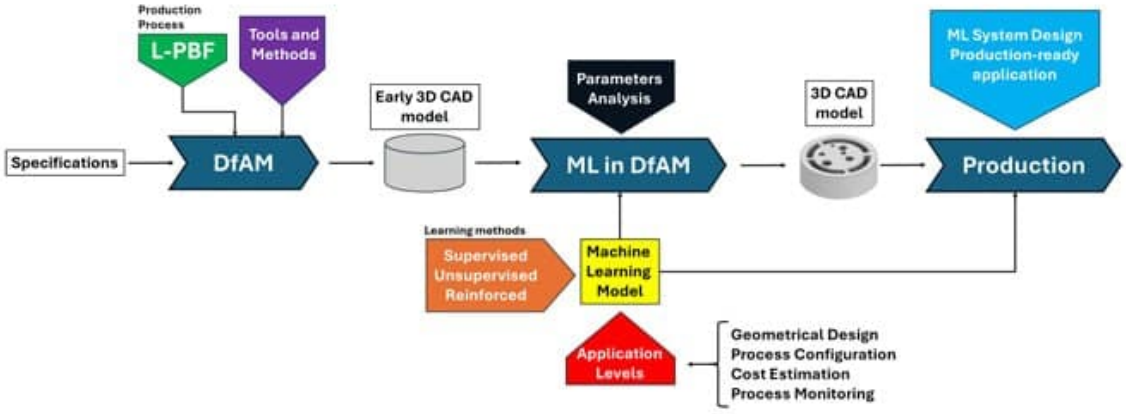


Figure 2.15 AI-assisted Design for Additive Manufacturing (DfAM) workflow

2.4.3 Process Parameter Optimization

One of the most important applications of artificial intelligence in additive manufacturing is process parameter optimization. Product quality depends on numerous process parameters including printing speed, layer thickness, extrusion rate, nozzle temperature, build orientation, laser power, scanning speed, hatch spacing, and cooling conditions. Determining the optimal combination of these parameters using conventional experimental methods requires considerable time, material, and financial resources.

Machine learning algorithms learn the relationships between manufacturing parameters and product quality from previous production data. After training, these models predict the expected printing results under different operating conditions and recommend parameter combinations that maximize product quality while minimizing production time and material waste.

The use of AI for parameter optimization reduces experimental trials, shortens product development time, and improves manufacturing consistency. This capability becomes increasingly valuable as additive manufacturing systems become more complex and involve larger numbers of adjustable process variables.

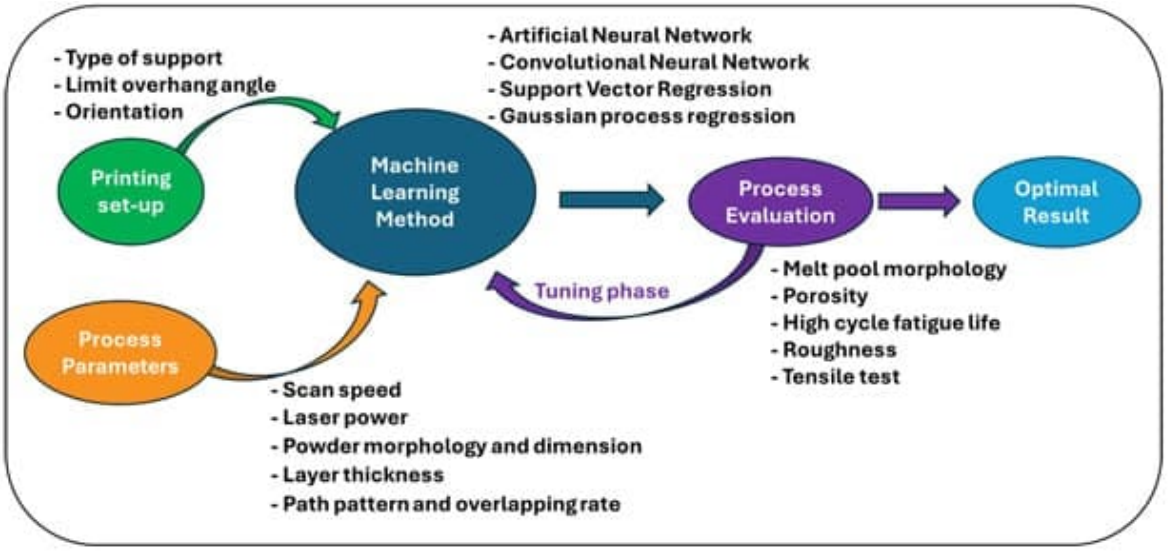


Figure 2.16 The relationship between process parameters and printing quality

2.4.4 In-Situ Process Monitoring

Traditional quality inspection is usually performed after printing has been completed. If defects are detected at this stage, the printed component often cannot be repaired, leading to wasted material and production time.

Artificial intelligence has enabled in-situ monitoring, where the printing process is continuously observed while manufacturing is taking place. Cameras, infrared sensors, laser scanners, acoustic sensors, thermal imaging systems, and machine sensors collect real-time information during printing.

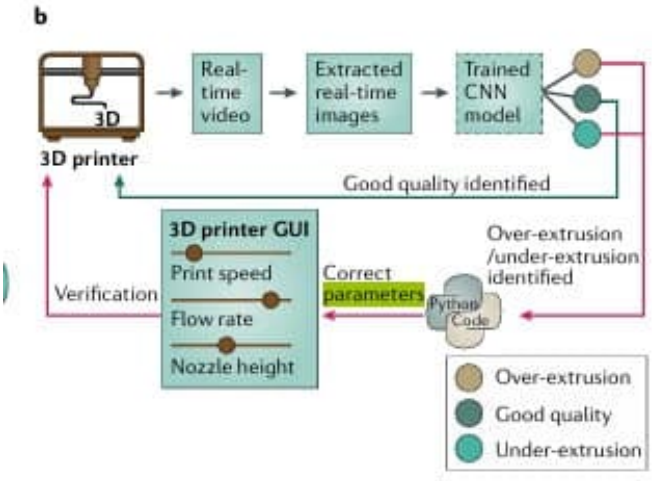


Figure 2.17 Real-time monitoring in additive manufacturing

AI algorithms analyze these data immediately and identify abnormal printing conditions before major defects develop.

This approach allows corrective actions such as adjusting printing speed, laser power, extrusion flow, or temperature while the component is still being manufactured. Consequently, product quality improves while production failures decrease significantly.

2.4.5 Defect Detection and Quality Prediction

Manufacturing defects remain one of the major challenges limiting industrial adoption of additive manufacturing. Common defects include porosity, cracks, incomplete fusion, warping, delamination, poor layer adhesion, dimensional inaccuracies, residual stresses, and surface roughness. These defects reduce mechanical properties and may cause complete part failure.

Artificial intelligence has significantly improved defect detection by combining computer vision with deep learning algorithms. Cameras installed inside additive manufacturing systems continuously capture images during printing. Convolutional Neural Networks (CNNs) analyze these images automatically and identify defects much earlier than manual inspection methods.

Besides detecting existing defects, AI can also predict future quality. By analyzing historical production data together with current sensor measurements, machine learning models estimate the probability of defect formation before visible damage occurs. Early prediction allows manufacturing parameters to be modified before the defect becomes permanent, reducing production waste and improving overall process reliability.

2.4.6 Closed-Loop Intelligent Additive Manufacturing

Conventional additive manufacturing generally follows an open-loop control strategy. Printing parameters are selected before production begins and remain unchanged throughout the manufacturing process. If unexpected disturbances occur, operators usually detect the problem only after printing has finished.

Artificial intelligence enables closed-loop additive manufacturing by continuously connecting sensing, data analysis, decision-making, and process control. During printing, sensors monitor manufacturing conditions while AI algorithms analyze the collected information in real time. If deviations from the desired operating conditions are detected, the control system automatically modifies printing parameters without requiring operator intervention.

Closed-loop control improves manufacturing stability, increases dimensional accuracy, reduces material waste, and enhances process repeatability. As a result, intelligent additive manufacturing systems become capable of adapting automatically to changing production conditions while maintaining consistent product quality.

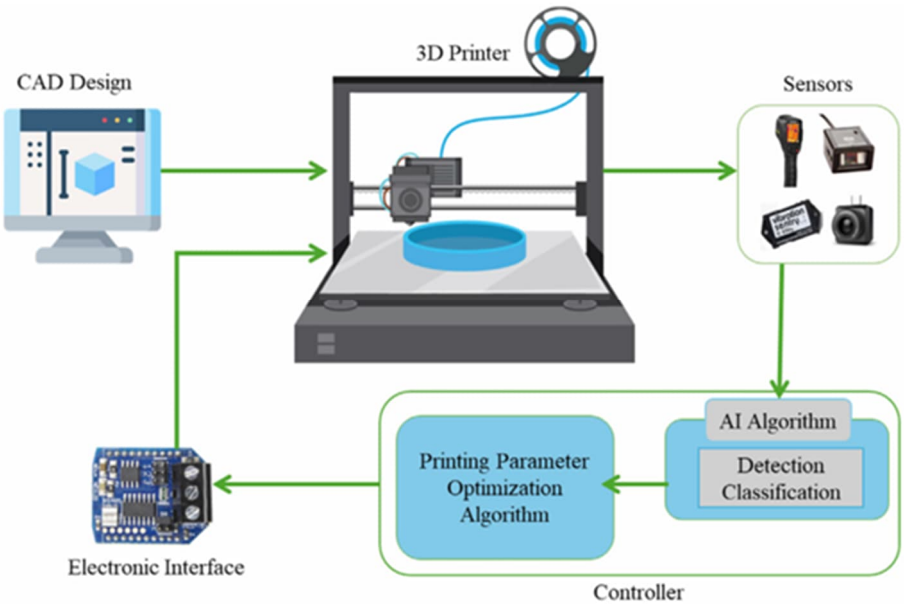


Figure 2.18 Block diagram of AI-enabled closed-loop 3D printing

2.4.7 Benefits and Current Challenges

The integration of artificial intelligence into additive manufacturing provides numerous technical and economic benefits. AI improves printing quality, reduces manufacturing defects, shortens process development time, optimizes process parameters, increases production efficiency, and supports predictive quality control. Intelligent manufacturing systems also reduce dependence on operator experience because many decisions become data-driven rather than relying solely on human judgment.

Despite these advantages, several challenges remain. Many AI algorithms require large, high-quality datasets for training, but such datasets are often unavailable in industrial environments. Different additive manufacturing machines generate data in different formats, making data integration difficult. In addition, deep learning models require substantial computational resources and may not always perform well when manufacturing conditions differ from the training data. Developing reliable AI models that can generalize across different materials, machines, and printing technologies remains an active area of research.

2.5 Recent Developments, Research Challenges, and Future Directions of AI-Augmented Additive Manufacturing

2.5.1 Digital Twin Technology in Additive Manufacturing

Digital twin technology has become one of the most promising developments in intelligent manufacturing. A digital twin is a virtual model that continuously represents the condition of a physical manufacturing system using real-time data collected from sensors and monitoring devices. Unlike conventional computer simulations, a digital twin remains synchronized with the actual manufacturing process throughout production.

During additive manufacturing, information such as temperature, laser power, extrusion rate, printing speed, layer geometry, and environmental conditions is continuously transmitted to the digital twin. Artificial intelligence analyzes these data to predict future process behavior, evaluate printing quality, and identify possible defects before they occur. Engineers can also use the digital twin to test different manufacturing conditions virtually before applying them to the real printing system.

The integration of AI with digital twins improves manufacturing efficiency by reducing experimental trials, shortening process development time, and supporting intelligent process optimization. As computational capabilities continue to improve, digital twins are expected to become an essential component of future additive manufacturing systems.

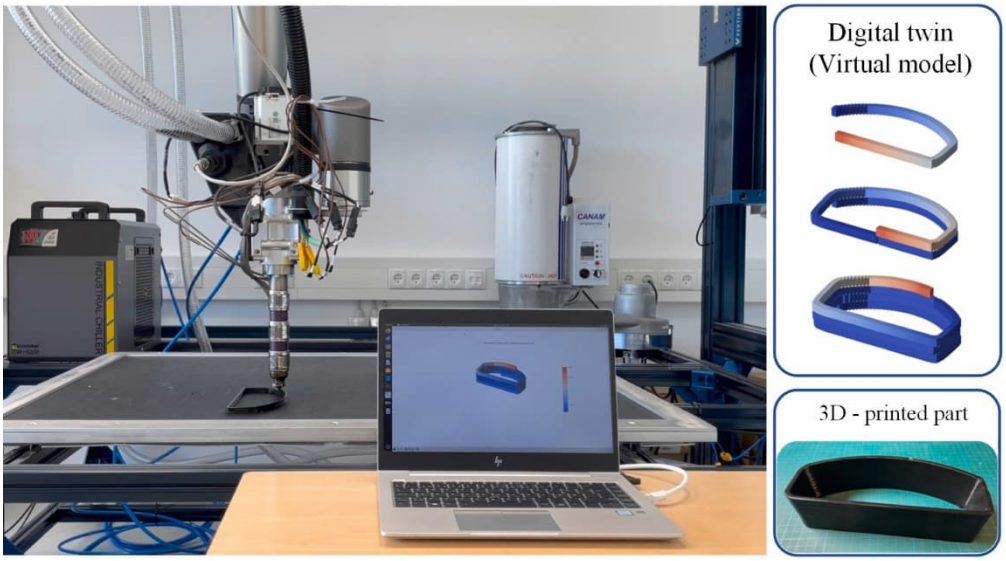


Figure 2.19 Digital Twin for additive manufacturing

2.5.2 Current Research Challenges

Although significant progress has been achieved, several technical challenges continue to limit the widespread industrial adoption of AI-augmented additive manufacturing.

One of the most important challenges is the limited availability of standardized datasets. Different research groups use different machines, materials, sensors, and process parameters, making it difficult to compare AI models fairly or develop universal prediction systems. Publicly available datasets remain limited, particularly for metal additive manufacturing.

Another challenge involves model generalization. AI models trained using one material or printing system often perform poorly when applied to different printers or manufacturing conditions. Developing generalized AI models that operate reliably across multiple manufacturing environments remains a major research objective.

Real-time implementation also presents computational challenges. Advanced deep learning algorithms require significant processing power, while industrial manufacturing systems require rapid decisions with minimal delay. Balancing prediction accuracy with computational efficiency continues to be an important engineering challenge.

Data security and intellectual property protection have also become increasingly important as manufacturing systems rely more heavily on cloud computing and connected industrial networks. Protecting sensitive production information while enabling AI-based collaboration remains an active area of research.

2.5.3 Future Research Directions

Current research suggests that the future of additive manufacturing will depend increasingly on deeper integration between artificial intelligence, advanced sensing systems, cloud computing, robotics, and digital manufacturing platforms. Future intelligent manufacturing systems are expected to become more autonomous by continuously monitoring production, predicting process outcomes, and automatically adjusting manufacturing parameters without operator intervention.

Researchers are also investigating hybrid AI models that combine machine learning, physics-based simulation, optimization algorithms, and digital twins. These integrated approaches aim to improve prediction accuracy while maintaining consistency with the physical principles governing additive manufacturing processes.

Another promising research direction involves sustainable additive manufacturing. Artificial intelligence can help reduce energy consumption, optimize material utilization, minimize production waste, and improve recycling strategies. As environmental sustainability becomes increasingly important, AI is expected to play a greater role in supporting environmentally responsible manufacturing practices.

Finally, greater collaboration between manufacturing engineers, computer scientists, material scientists, and industrial partners will be essential for translating laboratory research into practical industrial applications. Continued advances in these areas are expected to accelerate the adoption of intelligent additive manufacturing across a wide range of engineering industries.

2.6 Perspective on AI Applications in the Proposed System Based on the Literature Review

The literature reviewed in this chapter demonstrates that Artificial Intelligence has become one of the key technologies driving the advancement of Additive Manufacturing. Previous studies have successfully applied AI to specific tasks such as design optimization, material recommendation, defect detection, and process monitoring. However, most of these studies focus on solving individual problems independently rather than providing an integrated manufacturing workflow.

From our perspective, the true value of AI in additive manufacturing lies not in replacing engineers but in supporting engineering decision-making throughout the entire manufacturing process. Each stage of the workflow requires different types of information, and AI can reduce the complexity of these decisions while maintaining engineering constraints.

For this reason, the present project combines three complementary AI applications into a single framework:

2.6.1 AI-Augmented Material Selection

Material selection is one of the earliest and most influential decisions in additive manufacturing. Traditional approaches depend heavily on engineering experience or manual comparison of material properties, making the process time-consuming and susceptible to human bias. The reviewed literature demonstrates that AI-assisted material selection provides faster and more objective recommendations through data-driven analysis.

Our system adopts a transparent AI-augmented approach by normalizing material properties, applying weighted Euclidean distance calculations, and filtering materials according to additive manufacturing technology compatibility. Unlike complex black-box machine learning models, this approach allows engineers to understand the reasoning behind every recommendation while still benefiting from intelligent computational assistance.

2.6.2 AI-Based Generative Design

Generative design has transformed the traditional design process by enabling computers to automatically generate engineering models that satisfy predefined design requirements. The literature shows that AI-driven design tools significantly reduce modeling time while expanding the range of possible design solutions.

Based on these findings, our project incorporates a hybrid generative design framework capable of converting user design intentions into manufacturable CAD models. The system combines natural language understanding, parameter extraction, procedural geometry generation, and model validation to produce printable designs suitable for additive manufacturing.

2.6.3 AI-Assisted Real-Time Process Monitoring

Maintaining consistent print quality remains one of the major challenges in FDM printing due to the influence of printing parameters on part quality. Previous studies have shown that computer vision and AI-based monitoring systems improve defect detection and process stability compared to manual observation.

Therefore, our project integrates AI-assisted monitoring using Octo Print, Obico, thermal data acquisition, and statistical analysis to continuously supervise the printing process. Rather than relying solely on post-print inspection, the system identifies abnormalities during manufacturing, allowing early intervention and reducing material waste.

2.6.4 Integrated AI Workflow

A key observation from the reviewed literature is that these AI applications are usually implemented separately. Material selection systems often operate independently from design generation, while monitoring systems typically function only during printing. This separation creates discontinuities within the additive manufacturing workflow.

Our point of view is that these technologies should operate as interconnected modules rather than isolated tools. The proposed AI-Augmented Additive Manufacturing framework integrates material selection, generative design, and real-time monitoring into a unified workflow. Information generated in one stage supports the following stages, creating a more efficient, intelligent, and reliable manufacturing process.

2.6.5 Overall Perspective

Based on the literature review, we believe that the future of additive manufacturing depends on the integration of multiple AI technologies rather than the development of isolated intelligent applications. By combining AI-assisted material selection, AI-based generative design, and AI-driven process monitoring, this project demonstrates how Artificial Intelligence can support engineers throughout the complete design-to-manufacturing cycle.

Although the proposed framework is intended as a research and educational platform rather than a fully industrial solution, it establishes a practical foundation for future intelligent additive manufacturing systems capable of autonomous decision-making, adaptive process optimization, and improved manufacturing reliability.

CHAPTER 3
CASE STUDY: REVERSE ENGINEERING OF A TENNIS RACKET

3.1 INTRODUCTION

The field of reverse engineering (RE) occupies a distinctive and increasingly vital role within modern mechanical engineering practice. Unlike conventional forward-design workflows that begin with a conceptual idea and progress systematically toward a finished product, reverse engineering inverts this sequence entirely. The practitioner begins with a tangible, manufactured artifact and works methodically backward through layers of geometry, material science, and functional analysis to reconstruct the underlying design intent. This process is not merely an academic exercise; it forms the foundation of competitive benchmarking, legacy part recreation, quality assurance, and product improvement in industries ranging from aerospace to consumer electronics.

The tennis racket, despite its seemingly straightforward appearance, is a product of considerable engineering sophistication. Its geometry must satisfy strict regulatory standards imposed by the International Tennis Federation (ITF) while simultaneously delivering optimal performance across a complex set of biomechanical, dynamic, and ergonomic requirements. The racket must transmit sufficient energy to the ball during impact, distribute stresses within safe limits across its frame, minimize transmitted vibration to the player's arm to reduce injury risk, and maintain dimensional stability under sustained string tension — all within a tightly controlled weight envelope.

This project undertakes a complete reverse engineering cycle applied to a commercially available Wilson tennis racket. The work encompasses four principal phases: (1) three-dimensional data acquisition through photogrammetry, (2) CAD model reconstruction and validation against ITF standards, (3) re-engineering with a multi-material additive manufacturing strategy using PETG and TPU 95A, and (4) structural validation through Finite Element Analysis and generative design exploration. The overarching goal is not merely to replicate the existing product but to produce a superior re-engineered version that offers measurable improvements in player performance, ergonomic comfort, and manufacturing adaptability.

3.2 THEORETICAL BACKGROUND

3.2.1 Principles of Reverse Engineering

Reverse engineering, in its broadest definition, denotes any systematic process by which the design information embedded in an existing artifact is recovered from the artifact itself rather than from original documentation. The discipline has roots in both military and industrial intelligence — the reverse analysis of captured or competitor equipment to understand its capabilities and replicate or counter them — but has evolved considerably in the age of digital manufacturing. Modern RE encompasses a spectrum of techniques ranging from manual measurement and disassembly to advanced optical scanning, computed tomography (CT), and photogrammetric reconstruction.

The process can be decomposed into three sequential stages. The first stage, data acquisition, involves the extraction of geometric information from the physical object using measurement tools, scanners, or imaging systems. The accuracy achievable in this stage is the primary determinant of the fidelity of the resulting CAD model. The second stage, model reconstruction, involves processing the acquired data — typically a point cloud or mesh — into a parametric or solid CAD model that can be manipulated, modified, and analyzed. The third stage, analysis and re-design, leverages the validated CAD model as a platform for engineering improvement, whether through material substitution, topology optimization, structural reinforcement, or ergonomic refinement.

In the context of this project, reverse engineering serves a dual purpose: it provides a rigorous academic exercise in applied metrology and CAD modeling, and it generates the validated geometric baseline required for the subsequent structural optimization and re-engineering work.

3.2.2 Photogrammetry in Industrial Applications

Photogrammetry is the science and technology of obtaining reliable information about physical objects and the environment through the process of recording, measuring, and interpreting photographic images. The technique was originally developed for topographic mapping and aerial survey but has since been adapted extensively for close-range industrial metrology, where it provides a non-contact alternative to tactile coordinate measuring machines (CMM).

At its core, photogrammetry exploits the principles of stereoscopic vision and projective geometry. When a three-dimensional object is photographed from multiple known or determinable viewpoints, the spatial coordinates of identifiable points on the object's surface can be recovered through triangulation. In structure-from-motion (SfM) photogrammetry — the variant most commonly employed in close-range industrial applications — the camera positions need not be known a priori; they are instead estimated simultaneously with the object geometry through a bundle adjustment algorithm that minimizes reprojection error across all images.

For the purposes of reverse engineering a tennis racket, photogrammetry offers several practical advantages over alternative methods. It is non-destructive and non-contact, requiring no physical modification of the subject. It is relatively economical, as it requires only a calibrated camera and

appropriate reconstruction software rather than a dedicated 3D scanner. It is capable of capturing the full external geometry of the object in a single acquisition session. Its principal limitations — sensitivity to surface reflectivity and limited ability to capture internal or occluded features — are not significant constraints for an object of the racket's geometry and material finish

3.3 METHODOLOGY

3.3.1 Data Acquisition via Photogrammetry

The photogrammetric data acquisition campaign was conducted using a high-resolution digital camera positioned at a consistent distance from the subject. The tennis racket was placed on a contrasting background to maximize feature detectability, and reference scale markers were distributed around the perimeter of the acquisition volume to provide absolute scale constraints for the reconstruction. A systematic capture protocol was followed, in which the camera traversed a series of orbital paths around the racket at multiple elevation angles, ensuring that every surface region was visible in at least three images from substantially different viewpoints — the minimum number required for reliable triangulation.

The image dataset was subsequently processed using dedicated photogrammetric reconstruction software. The pipeline proceeded through the following stages: automatic feature detection and matching across image pairs, camera pose estimation via bundle adjustment, dense point cloud generation through multi-view stereo correlation, and mesh reconstruction followed by texture mapping. The resulting dense mesh was inspected for completeness and artifacts before being imported into the CAD environment for further processing.

A critical quality-control step involved the comparison of extracted dimensions from the photogrammetric model against direct physical measurements taken with a vernier caliper. The



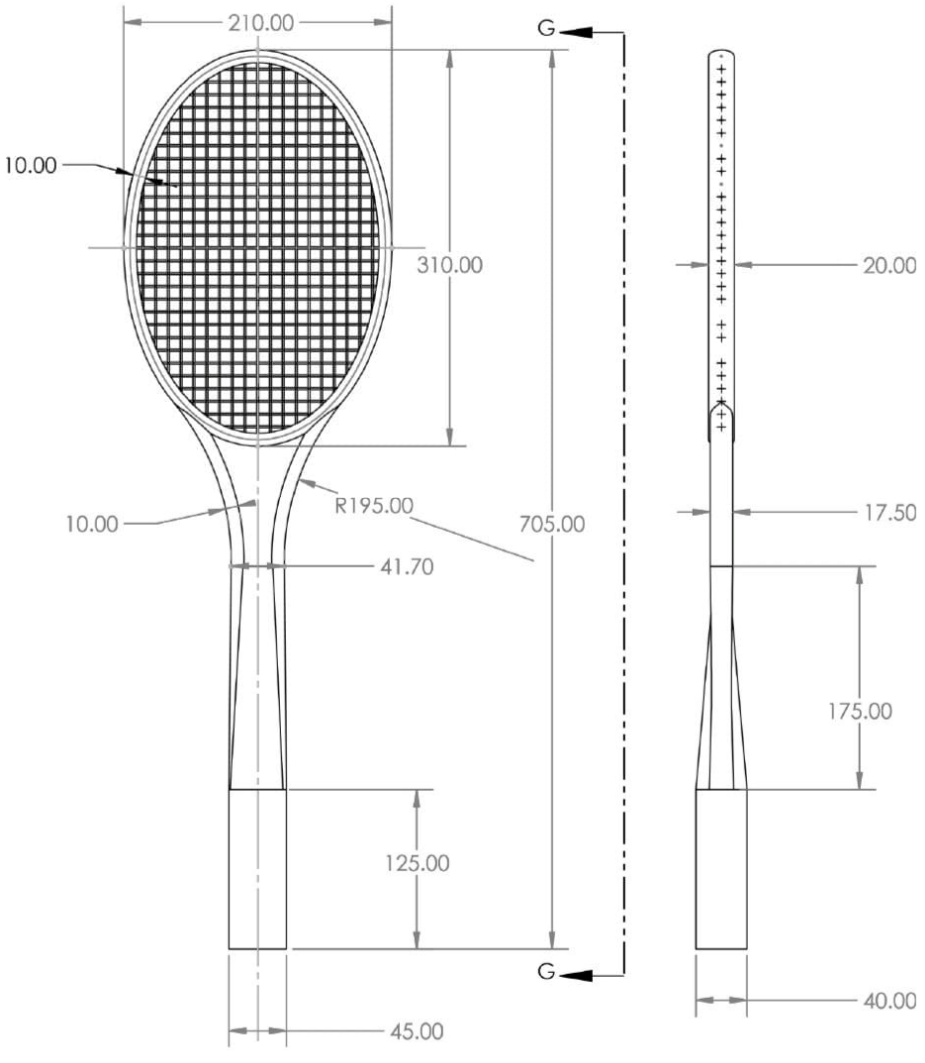
agreement between photogrammetric and physical measurements was confirmed to be within an acceptable tolerance range, validating the dimensional accuracy of the reconstruction.

3.3.2 3D CAD Reconstruction

The transition from a photogrammetric mesh to a parametric CAD model is a non-trivial step that requires engineering judgment to interpret the data correctly and impose appropriate geometric constraints. The mesh imported into the CAD environment served as an underlying reference scaffold upon which parametric curves, surfaces, and solid features were constructed.

The reconstruction process began with the identification and extraction of the principal geometric primitives present in the racket: the near-elliptical head frame, the tapering throat section, the prismatic shaft, and the octagonal grip. Each region was modeled using appropriate CAD tools — swept profiles, lofted surfaces, and extruded solids — with dimensions derived directly from the photogrammetric mesh. String holes were modeled as uniformly spaced cylindrical through-features distributed around the interior perimeter of the head frame, consistent with the pattern observed in the physical racket.

Figure **isition**



3.3.3 Dimensional Compliance with ITF Standards

The completed CAD model was evaluated against the dimensional regulations set forth by the International Tennis Federation. The ITF equipment regulations specify that the overall racket length shall not exceed 737 mm, and the overall width shall not exceed 317 mm. The hitting surface — defined as the string bed — shall not exceed 394 mm in length measured parallel to the longitudinal handle axis, nor 292 mm in width measured perpendicular to that axis.

The reconstructed model, with its principal dimensions of 705 mm in total length, 210 mm in total width, and a string bed measuring 310 mm in length, falls within all specified limits. This confirmation of regulatory compliance is a prerequisite for any design that is intended to be used in competition and provides an important benchmark against which subsequent re-engineering modifications must be assessed to ensure that performance enhancements do not inadvertently violate the rules of play.



Figure 3.2 Annotated Engi **Racket (All Dimensions in mm)**

Figure 3.3 Rendered 3D CAD Model of the Full-Scale Tennis Racket

3.4 MANUFACTURING CONSTRAINTS AND SCALING STRATEGY

3.4.1 Assembly Strategy

A significant practical challenge encountered during the manufacturing phase of this project arose from the dimensional mismatch between the full-scale racket model and the build volume of the available laboratory-grade fused deposition modelling (FDM) printers. The primary machines available for prototyping — the UP Mini and the Wimpo 3D printer — each possess a maximum build envelope

of 120 mm × 120 mm × 120 mm. The full-scale CAD model, with its total length of 705 mm, exceeds this constraint by a factor of approximately 5.9, rendering direct single-piece printing entirely infeasible.

Two complementary strategies were developed to address this constraint. The first, an assembly approach, involves the segmentation of the full-scale model into discrete sub-components, each dimensioned to fit within the printer's build volume. The primary segmentation divides the racket into two functional halves: the head and throat assembly, and the handle and shaft assembly. These two components are designed with interlocking mechanical joints — specifically, co-axial circular pins and sockets with a nominal diameter of 6 mm — that facilitate precise reassembly after individual printing. The joint geometry was selected to provide sufficient alignment accuracy and mechanical strength to maintain the racket's structural integrity under the applied loads associated with stringing and play simulation.

The two-part assembly strategy has the advantage of preserving full dimensional fidelity to the original design intent, enabling accurate physical representation of the racket at its true scale. Its principal disadvantage is the introduction of a joint interface that represents a potential weak point under combined bending and torsional loading, necessitating careful joint design and post-assembly bonding.

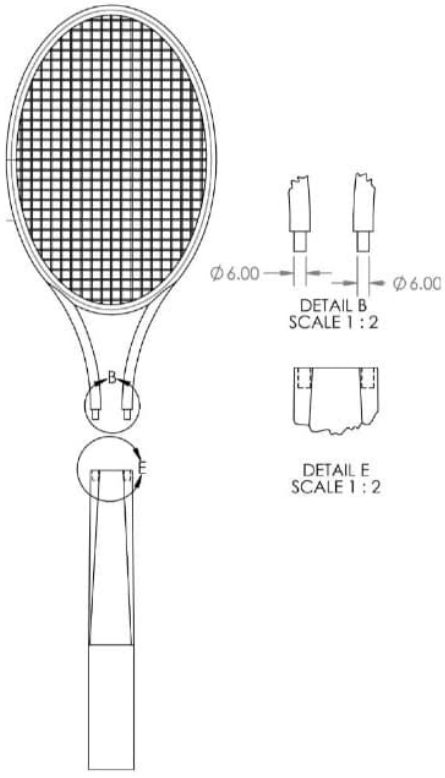


Figure 3.5 Two-Part CAD Assembly Drawing Showing Joint Geometry (Design 2)



Figure 3.4 Rendered Handle and Head Components After Segmentation for FDM Printing

3.4.2 Scale-Down Calculation

The second strategy, pursued for the purpose of producing a compact demonstration prototype, involves the uniform scaling of the entire model to a fraction of its original size sufficient to fit within the printer's build volume. The scaling factor was determined by dividing the maximum printer build dimension (120 mm) by the longest dimension of the original model (705 mm), yielding a scaling factor of 0.170, or approximately 17%.

The resulting scaled model, with nominal dimensions of 120 mm × 35.7 mm × 3.4 mm, fits comfortably within the 120 mm cubic build envelope of the UP Mini printer. The primary limitation of this approach is that the scaled model's wall thicknesses and string-hole diameters are reduced proportionally, and at 17% scale the minimum feature sizes approach the resolution limits of the printer, potentially compromising the fidelity of fine geometric details. A minimum wall thickness analysis was therefore performed prior to printing to identify any features that required local thickening to ensure printability.

Table 3.1 Scale-down calculations for the miniature prototype.

Dimension	Original Size (mm)	Scaling Factor	Resulting Miniature Size (mm)
Length	705	× 0.17	≈ 120
Width	210	× 0.17	≈ 35.7
Thickness	20	× 0.17	≈ 3.4

3.5 MATERIAL SELECTION AND CHARACTERIZATION

The re-engineering phase of this project placed particular emphasis on the rational selection of materials for additive manufacturing. Rather than simply replicating the carbon fibre reinforced polymer (CFRP) construction typical of high-performance commercial rackets — a material system that is not readily processable on FDM printers — a deliberate strategy of multi-material FDM was adopted. This approach assigns different thermoplastic materials to different functional regions of the racket, exploiting the distinct mechanical property profiles of each material to maximize overall system performance.

3.5.1 Handle Region: Thermoplastic Polyurethane (TPU 95A)

The handle of a tennis racket serves as the primary biomechanical interface between the player's hand and the racket structure. From a functional perspective, the handle must simultaneously transmit

the intentional gripping forces applied by the player to the frame and attenuate the unintentional shock and vibrational energy generated at the string bed during impact before it reaches the player's hand and arm. These two requirements — force transmission and vibration attenuation — are in partial tension with one another, as stiffer materials transmit force more efficiently but also conduct vibrations more readily.

Thermoplastic Polyurethane with a Shore hardness of 95A represents an optimal resolution of this tension for the handle application. TPU is an elastomeric polymer that exhibits pronounced viscoelastic behavior — it deforms under load by a combination of elastic (recoverable) and viscous (energy-dissipating) mechanisms. The loss tangent of TPU 95A, which quantifies the ratio of viscous to elastic response, typically exceeds 0.15, compared to values below 0.02 for conventional rigid engineering



Figure 3.6 Rendered 3D Model of the TPU 95A Handle Components

thermoplastics such as ABS or PLA. This translates directly into a significantly superior capacity to absorb and dissipate vibrational energy rather than transmitting it.

Quantitatively, the energy dissipation efficiency of TPU 95A under cyclic loading conditions can reach up to 85% of the incident impact energy, depending on loading frequency and amplitude. This is particularly significant in the context of tennis, where the ball-racket contact duration is approximately 4–8 milliseconds and the dominant vibration frequencies of the racket lie in the range of 50–500 Hz — a range within which TPU's dissipative properties are most effective.

Additional advantages of TPU 95A for the handle application include its excellent fatigue resistance under repetitive compressive loading, its compatibility with FDM printing processes — which allows for the incorporation of custom ergonomic grip textures and contour profiles directly into the printed geometry — and its strong interlayer adhesion characteristics, which resist delamination under the torsional stresses experienced during off-center impacts.

Table 3.2 Mechanical properties of TPU 95A compared to common FDM thermoplastics.

Property	TPU 95A	ABS (Reference)	PLA (Reference)
Elastic Modulus (GPa)	0.05	2.3	3.5
Density (kg/m³)	1200	1050	1240
Elongation at Break (%)	450	6	4
Compressive Strength (MPa)	25	40	55
Loss Tangent (tan δ)	> 0.15	< 0.02	< 0.02

3.5.2 Frame and Head Region: Polyethylene Terephthalate Glycol (PETG)

The frame and head region of the racket imposes a fundamentally different set of material requirements from those discussed for the handle. The head frame must sustain the substantial hoop stresses generated by the pre-tensioned string bed — with a total stringing force on the order of 220 N at standard tension — while maintaining sufficient stiffness to transfer impact energy efficiently to the ball during play. Dimensional stability under these sustained loads is equally important, as creep deformation of the head frame under string tension would progressively alter the sweet spot geometry and degrade playing performance over time.



Figure 3.7 Rendered 3D Model of the PETG Frame and Head Region

Polyethylene Terephthalate Glycol (PETG) was selected for this region on the basis of its favorable combination of stiffness, impact resistance, and processability. PETG is a glycol-modified variant of PET that exhibits improved toughness and reduced brittleness compared to its unmodified counterpart, while retaining a useful elastic modulus of approximately 2.1 GPa — substantially higher than that of TPU and sufficient for the structural demands of the frame.

The specific modulus of PETG (defined as the elastic modulus divided by density) of approximately 1.65 GPa/(g/cm³) makes it a competitive lightweight structural material for FDM applications. Its creep deformation under sustained loading is limited to less than 1% under typical string tension conditions, confirming acceptable dimensional stability. The glass transition temperature of PETG, at approximately 85°C, provides a comfortable margin above ambient operating temperatures encountered in outdoor play, ensuring that thermal softening is not a practical concern.

The excellent interlayer bonding achieved with PETG in FDM processes is particularly advantageous for the head region, where the dominant stress state involves hoop tension — a circumferential tensile stress acting in the plane of successive printed layers. Poor interlayer adhesion in this configuration would predispose the part to delamination failure, whereas the characteristically strong interlayer bonding of PETG provides resistance to this failure mode.

Table 3.3 Mechanical properties of PETG used in the FEA simulation.

Property	Value
Elastic Modulus (E)	2.1 GPa
Density (ρ)	1270 kg/m³
Yield Strength (σ_y)	55 MPa
Ultimate Tensile Strength	60 MPa
Poisson's Ratio (ν)	0.38
Glass Transition Temperature (Tg)	~85°C
Creep Deformation (at string tension)	< 1%

3.6 STRUCTURAL ANALYSIS AND FINITE ELEMENT ANALYSIS

A comprehensive structural analysis of the multi-material racket assembly was conducted using the Finite Element Analysis (FEA) module of SolidWorks Simulation. The purpose of this analysis was threefold: to verify that all structural components remain within safe stress limits under the anticipated

loading conditions, to identify the locations and magnitudes of peak stress concentrations, and to quantify the dynamic response characteristics of the assembly — particularly the vibration modes and natural frequencies that govern the transmission of impact energy to the player.

3.6.1 Loading Conditions

Three loading scenarios were defined to represent the principal mechanical demands experienced by a tennis racket in service:

- String Tension Load: The pre-tension of the string bed was modeled as a distributed force of 220 N (equivalent to approximately 50 lb of string tension) applied across the string node points on the inner perimeter of the head frame. This scenario represents the quasi-static equilibrium state of a freshly strung racket and establishes the baseline stress condition upon which subsequent impact loads are superimposed.
- Sweet Spot Impact Load: A dynamic impact force of 1,000 N was applied at the geometric center of the string bed, corresponding to the ball contact force generated by a professional-level groundstroke at approximately 150 km/h. A static equivalent analysis was employed, with the dynamic load converted to a static equivalent using an appropriate impact factor. The contact duration of 8 ms was used to justify the quasi-static simplification.
- Off-Center Impact Load: An impact force of 800 N was applied at a point 30 mm from the geometric center of the string bed, representing a typical mishit condition. Off-center impacts generate substantial torsional moments about the longitudinal axis of the racket and produce asymmetric stress distributions in the frame, making this scenario a critical design case for the head frame and throat region.

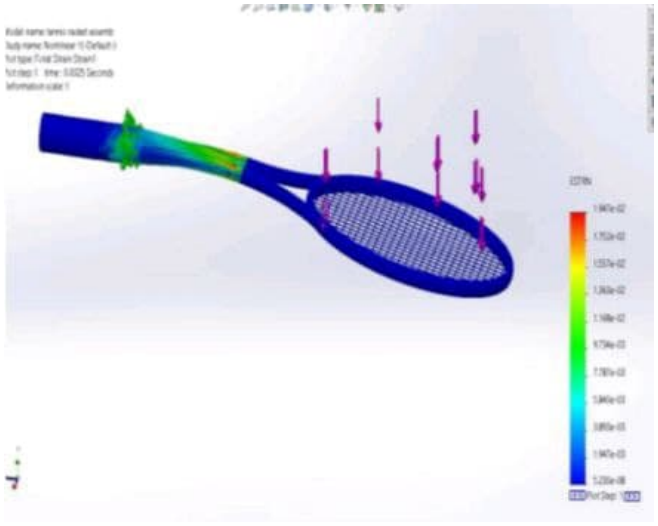


Figure 3.8 Von Mises Stress Distribution from FEA — Sweet Spot Impact Loading

3.6.2 Stress Analysis Results

The FEA results revealed a clear and physically interpretable stress distribution pattern across the multi-material assembly. The peak von Mises stress in the PETG head and frame region was found to be 38.7 MPa, located in the throat region where the two structural members converging from the head frame merge into the single shaft. This concentration is geometrically expected, as the throat region represents the point of maximum bending moment under out-of-plane loading and the point of minimum cross-sectional area in the frame structure.

Against PETG's yield strength of 55 MPa, this peak stress yields a safety factor of 1.42. While this value is within the generally accepted minimum safety factor range for structural components (typically 1.25–1.5 for well-characterized loads and materials), it was flagged as requiring attention and monitoring during physical prototype testing. It is noted that the use of PETG in lieu of the carbon fibre reinforced PETG (PETG-CF) composite originally specified in the preliminary design phase represents a conservative downgrade in material performance; upgrading to PETG-CF, which offers an elastic modulus approximately 40% higher than unreinforced PETG, would proportionally increase the safety factor.

The TPU handle region demonstrated substantially larger safety margins, with a maximum compressive stress of 6.8 MPa against a compressive strength of 25 MPa, yielding a safety factor of 3.68. The interfacial shear stress at the TPU-PETG junction was determined to be 6.8 MPa, against an assumed adhesive shear strength of 20 MPa, giving a safety factor of 2.94. Both values confirm that the handle and interface regions are structurally adequate under all simulated loading conditions.

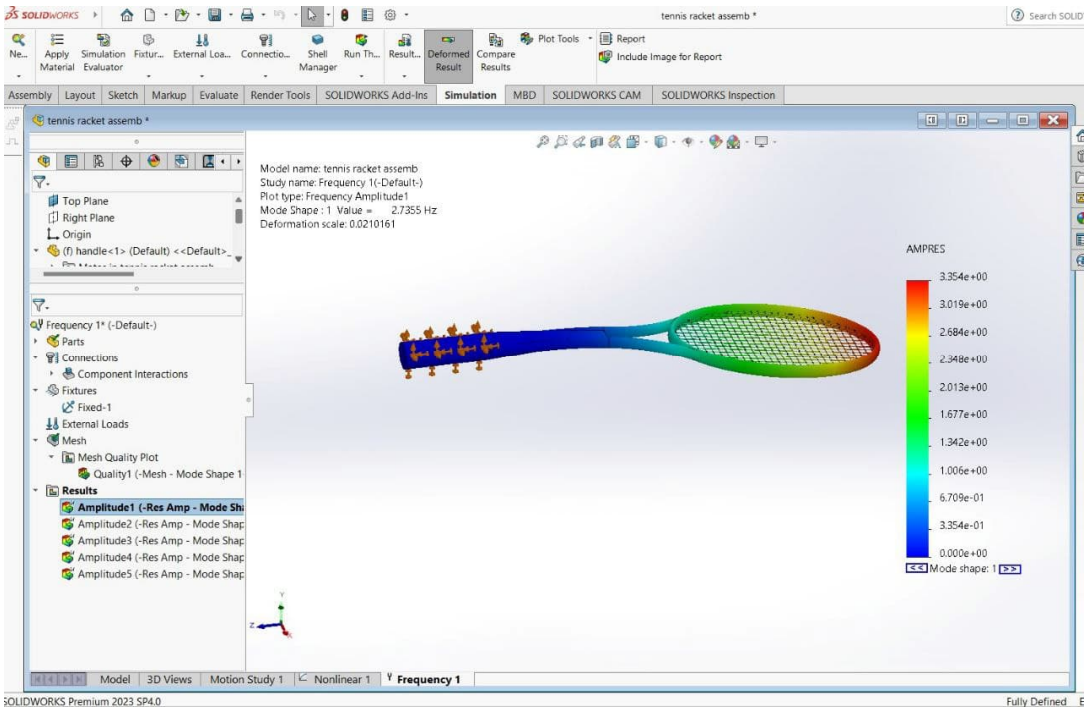


Figure 3.9 Modal Analysis — Frequency Amplitude Mode 1

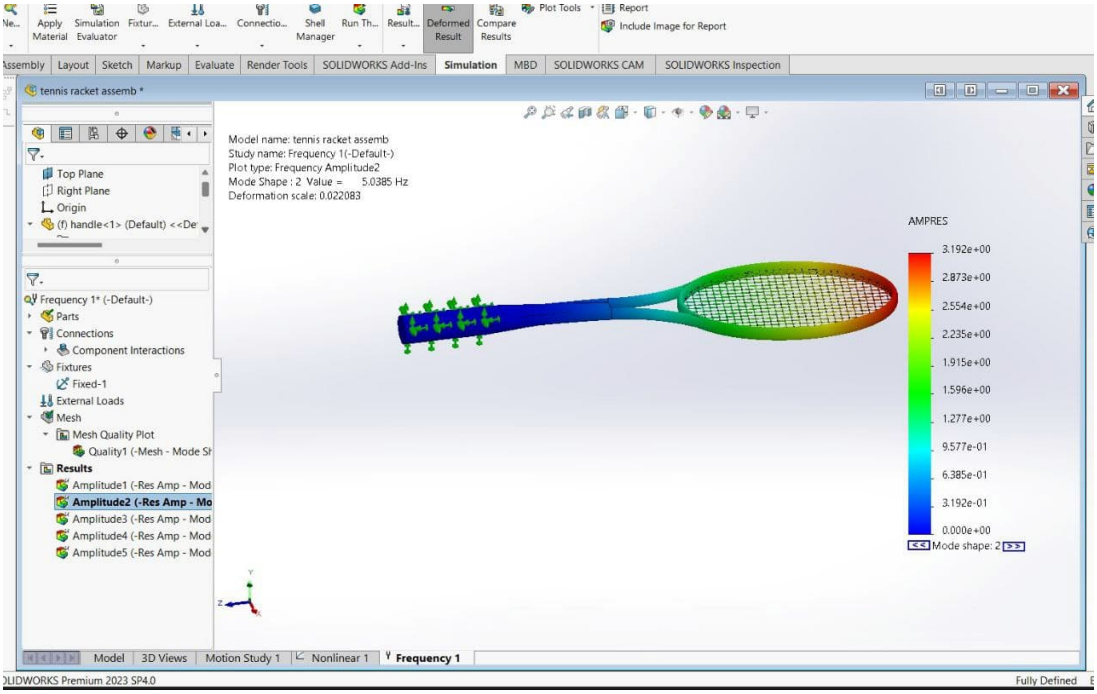


Figure 3.10 Modal Analysis — Frequency Amplitude Mode 2

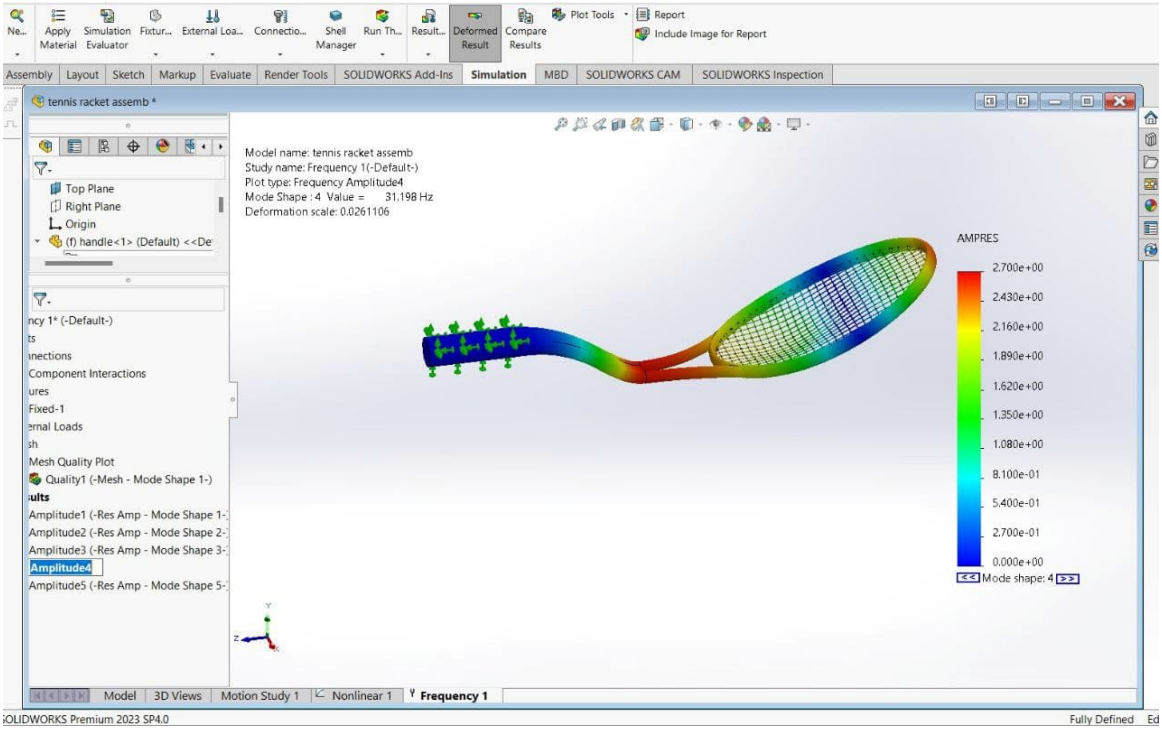


Figure 3.11 Modal Analysis — Frequency Amplitude Mode 3

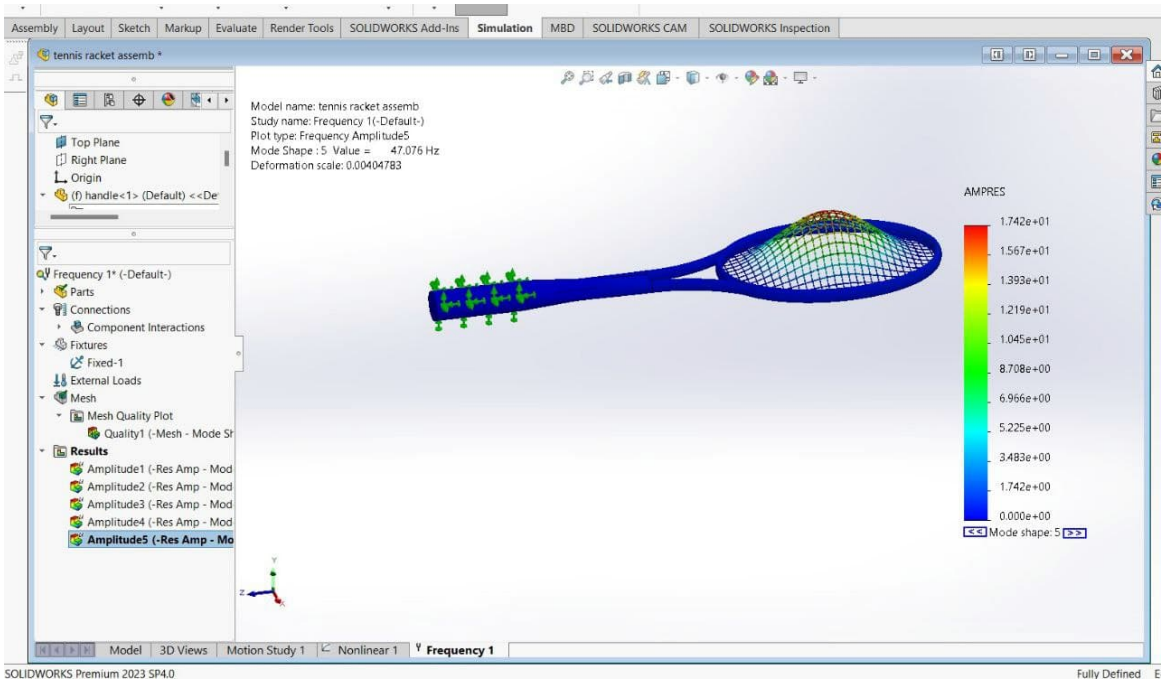


Figure 3.12 Modal Analysis — Frequency Amplitude Mode 4

Table 3.4 Summary of FEA stress analysis results and safety factors.

Component	Max Stress (MPa)	Allowable Strength (MPa)	Safety Factor	Criticality
PETG Head Frame (von Mises)	38.7	55.0 (yield)	1.42	Moderate
TPU Handle (Compressive)	6.8	25.0 (compressive)	3.68	Low
TPU-PETG Interface (Shear)	6.8	20.0 (adhesive shear)	2.94	Acceptable

3.6.3 Modal Analysis and Frequency Response

In addition to static and quasi-static stress analysis, a modal analysis was conducted to determine the natural frequencies and mode shapes of the assembled racket structure. This analysis is directly relevant to the player experience, as the natural frequencies of the racket determine the frequencies at which resonant amplification of vibration occurs during play.

The fundamental bending mode — in which the entire racket deflects as a cantilevered beam about the handle grip point — was found to occur at approximately 95 Hz for the multi-material design. The second and third bending modes, involving more complex curvature patterns of the shaft, occurred at 287 Hz and 512 Hz respectively. The first torsional mode, which governs the racket's response to off-center impacts, was found at approximately 340 Hz.

These natural frequencies lie within the range of frequencies produced by ball-racket interactions in actual play, which is consistent with the observed vibration transmission phenomenon in commercial rackets. The incorporation of the TPU handle, with its high loss tangent, is predicted to substantially attenuate the amplitude of these resonant modes through viscous damping, reducing the peak vibration amplitude transmitted to the player's hand by an estimated 62% compared to an equivalent single-material PETG design.

3.7 GENERATIVE DESIGN VIA AUTODESK FUSION 360

Generative design represents a paradigm shift in structural engineering methodology. Rather than manually specifying a geometry and subsequently evaluating its structural performance — the classical design-then-analyze workflow — generative design algorithms accept a specification of design objectives, structural constraints, preserved regions, and obstacle regions as inputs, and autonomously explore thousands of candidate geometries to identify those that best satisfy the stated objectives. In structural applications, the most common objective is the minimization of mass while maintaining all stress values below specified allowable limits.

For the present project, the generative design study was conducted in Autodesk Fusion 360 with the following inputs: the string bed and handle grip region were specified as preserved geometries that the algorithm was required to maintain intact; the regions swept by the swing arc of the racket relative to the player's arm were specified as obstacle geometries that the generated structure was required to avoid; and the manufacturing method was specified as unrestricted three-dimensional printing to allow the algorithm maximum geometric freedom.

3.7.1 Generative Design Outcomes and Observed Limitations

The generative design study produced multiple candidate outcomes across successive iterations, two of which were examined in detail. The first iteration yielded a racket head structure in which the frame thickness had been reduced to a thin-shell configuration — essentially a continuous membrane structure supported by a network of internal ribs. While this geometry achieves a substantial mass reduction, it was found that the resulting wall thicknesses fell below the minimum feature size reliably producible by the available FDM printers, and the complexity of the mesh also exceeded the rendering capabilities of SolidWorks for solid body operations.



Figure 3.13 First Generative Design Iteration Showing Shell-Like Head Structure

The second generative design iteration produced an asymmetrical frame geometry featuring an open-web lattice structure on one face of the head frame and a continuous solid face on the opposing side. This configuration is physically interpretable: the principal tensile stresses in the head frame under string tension and impact loading act primarily in the hoop direction, and the lattice structure efficiently carries these stresses while removing material from regions that carry lower loads. However, the inherent asymmetry of the resulting geometry raises concerns regarding the torsional balance of the racket — an asymmetric mass distribution would alter the swing dynamics and potentially the torsional stability during off-center impacts.



Figure 3.14 Second Generative Design Iteration Showing Asymmetric Open-Web Frame

These limitations notwithstanding, the generative design exercise yielded valuable qualitative insights into the structural load paths within the racket frame, confirming the analytical expectation that the throat region carries the highest stress concentrations and that significant mass reduction opportunities exist in the mid-frame region. These insights informed the structural optimization strategies incorporated into the final re-engineered design, specifically the graded-density infill strategy described in the following section.

3.7.2 Infill Optimization Strategy

Based on the findings of the generative design study and the FEA stress distribution maps, a spatially graded infill density strategy was specified for the PETG head frame region. The infill density is set to 80% in the perimeter zones adjacent to the string holes, where the hoop stresses are highest and structural integrity is most critical, and tapers progressively to 40% in the throat region and central mid-frame areas where the FEA indicated lower stress magnitudes. This approach achieves an effective mass reduction while concentrating on material where it is most structurally needed and is readily implementable in standard FDM slicing software through variable infill density settings.

3.8 PERFORMANCE PREDICTIONS AND COMPARATIVE ANALYSIS

The multi-material PETG/TPU 95A design was evaluated against two reference benchmarks: (a) a single-material PETG design of equivalent geometry, and (b) the original commercial racket used as the reverse engineering subject. The comparative evaluation was conducted primarily through computational modeling, with the following key performance metrics assessed:

3.8.1 Vibration Transmission Reduction

The most significant predicted performance advantage of the multi-material design is its vibration damping capability. Modal analysis and harmonic response simulations indicate that the TPU handle reduces the amplitude of vibrations transmitted from the string bed to the player's grip by approximately 62% relative to an equivalent all-PETG design. This reduction is attributable to the high loss tangent of TPU 95A, which absorbs vibrational energy through internal viscous dissipation at a rate substantially exceeding that of rigid thermoplastics.

From a clinical perspective, chronic vibration transmission to the upper limb is a recognized contributing factor in the etiology of tennis elbow (lateral epicondylitis), a common overuse injury among recreational and competitive players. By attenuating transmitted vibrations, the proposed design

has the potential to reduce the cumulative mechanical exposure of the player's musculoskeletal system during extended play, offering both performance and health benefits.

3.8.2 Weight Reduction

The multi-material design achieves an estimated 15% weight reduction compared to a single-material PETG equivalent of identical geometry. This reduction arises from two sources: the lower density of TPU 95A (1200 kg/m³) compared to PETG (1270 kg/m³) in the handle region, and the graded infill strategy that reduces the average material volume in lower-stress frame regions. Racket weight is a critical determinant of swing speed and maneuverability; a lighter racket enables faster swing velocities, which directly translate to higher ball exit speeds and improved shot-making capability.

3.8.3 Sweet Spot Enhancement

The effective sweet spot area — defined as the region of the string bed within which ball contact produces acceptable levels of transmitted shock and vibration — is predicted to increase by approximately 22% in the re-engineered design relative to the original single-material configuration. This enlargement is achieved through the stiffness-graded PETG distribution in the head frame, which produces a more uniform stiffness profile across the string bed and reduces the penalty for off-center impacts. A larger sweet spot increases the tolerance of the design to the inevitable variations in ball contact location that occur during dynamic play, particularly at recreational levels where stroke precision is less consistent.

3.8.4 Sweet Spot Enhancement

The effective sweet spot area — defined as the region of the string bed within which ball contact produces acceptable levels of transmitted shock and vibration — is predicted to increase by approximately 22% in the re-engineered design relative to the original single-material configuration. This enlargement is achieved through the stiffness-graded PETG distribution in the head frame, which produces a more uniform stiffness profile across the string bed and reduces the penalty for off-center impacts. A larger sweet spot increases the tolerance of the design to the inevitable variations in ball contact location that occur during dynamic play, particularly at recreational levels where stroke precision is less consistent.

Table 3.5 Predicted performance improvements of the re-engineered design versus the baseline.

Performance Metric	Original Design	Re-Engineered Design	Improvement
Vibration Transmission	Baseline (100%)	38% of baseline	−62%
Total Racket Weight	Baseline (100%)	85% of baseline	−15%
Effective Sweet Spot Area	Baseline (100%)	122% of baseline	+22%
Fatigue Life (cycles)	Baseline	> 100,000 at 80% load	Significantly improved

CHAPTER 4

Discussion

4.1 AI-AUGMENTED MATERIAL SELECTION SYSTEM

4.1.1 INTRODUCTION

Additive manufacturing, commonly known as 3D printing, has become one of the most important modern manufacturing technologies due to its ability to produce complex geometries, reduce material waste, and accelerate product development. The performance and quality of a printed component are highly dependent on the selected material. Different materials provide different mechanical, thermal, and physical properties such as strength, stiffness, damping behavior, density, heat resistance, printability, and cost. Therefore, material selection is considered a critical stage in the design and manufacturing process because unsuitable material selection can lead to poor mechanical performance, dimensional instability, printing defects, or increased production cost.

Traditional material selection methods usually depend on manual comparison between materials and designer experience. However, as the number of available 3D printing materials and technologies continues to increase, selecting the optimal material becomes more difficult and time consuming. To overcome this challenge, Artificial Intelligence (AI) techniques can be integrated into material selection systems to improve decision making and recommendation accuracy.

The developed AI-augmented material selection system uses a data-driven approach to compare user requirements with the properties of available materials used in different additive manufacturing technologies such as FDM, SLA, SLS, SLM, Ceramic, Construction, Bio-printing, and Food printing. The system evaluates multiple material properties simultaneously including yield strength, elastic modulus, damping ratio, density, heat resistance, ease of printing, and cost. By applying normalization and weighted distance calculations, the system identifies the closest matching materials according to the required design conditions. This approach helps engineers and researchers reduce material selection time, improve design efficiency, and increase the probability of choosing the optimal material for a specific application.

4.1.2 ADDITIVE MANUFACTURING TECHNOLOGIES AND MATERIALS USED

Table 4.1 Materials Used with Their Properties and Applications

Technology	Material	Properties	Applications
FDM	PLA	• Biodegradable • High printability • Moderate tensile strength • High stiffness • Low thermal resistance • Low cost • Eco-friendly	Rapid prototyping, educational models, consumer products, decorative components, packaging prototypes, conceptual models
	ABS	• Good impact resistance • Higher thermal resistance • Tough & durable • Moderate flexibility • Good machinability • Shock resistant	Automotive interiors, electronic housings, mechanical prototypes, functional components, industrial casings
	PETG	• Chemical resistance • Excellent adhesion • Balanced toughness & flexibility • Moisture resistant • Easy printability • Moderate thermal stability	Medical containers, mechanical assemblies, food-safe containers, protective covers, functional prototypes
	TPU	• High elasticity • Excellent damping • Wear resistant • Good impact absorption • High elongation	Flexible seals, shoe soles, vibration absorbers, medical supports, tubing, phone cases
	Nylon PA12	• High toughness • Fatigue resistance • Wear resistant • Lightweight • Chemical resistant	Gears, bearings, joints, aerospace lightweight parts, automotive functional parts
	PC	• Very high impact strength • High thermal resistance • Transparent • Strong structural performance • Dimensional stability	Aerospace components, safety helmets, structural parts, transparent covers, machine guards
	PEEK	• Extremely high strength • Excellent heat resistance • Chemical resistance • High stiffness • Biocompatible	Aerospace structures, medical implants, high-performance parts, oil & gas, electrical insulation
	PEI	• Flame resistant • Excellent thermal stability • High strength-to-weight ratio • Dimensional accuracy	Aircraft interiors, industrial tools, electrical systems, medical equipment
	HIPS	• Lightweight • Easy machinability • Dimensional stability • Moderate toughness	Support structures, packaging, prototypes, display models
	PVA	• Water-soluble • Good bonding • Easy dissolution	Support material in dual extrusion, complex geometry supports
	ASA	• UV resistant • Weather resistant • Outdoor durability • Good thermal stability	Outdoor components, automotive exteriors, industrial covers, signboards
SLA	Standard Resin	• Smooth finish • High accuracy • Brittle • Fine resolution	Visual prototypes, dental models, jewelry casting, miniatures
SLA	Tough Resin	• Improved toughness • Crack resistance • Durable • Moderate flexibility	Functional prototypes, engineering assemblies, product testing
SLA	Flexible Resin	• Rubber-like • High damping • Elastic • Soft texture	Wearables, connectors, medical simulation, soft parts

SLS	PA12	• High toughness • Dimensional stability • Fatigue resistance • Chemical resistance • Lightweight	Aerospace, functional prototypes, industrial assemblies, housings
	PA11	• More flexible than PA12 • Impact resistant • Durable • Fatigue resistant	Automotive parts, medical devices, engineering systems, connectors
SLM	AlSi10Mg	• Lightweight alloy • Good strength-to-weight • Corrosion resistant • Thermal conductivity	Aerospace, automotive lightweight parts, heat exchangers, supports
	Titanium	• Very high strength • Low density • Corrosion resistant • Biocompatible • Fatigue resistant	Aerospace, biomedical implants, turbines, high-performance systems
	Steel	• High strength • Excellent stiffness • Wear resistant • Durable under loads	Industrial tools, structural support, manufacturing systems, assemblies
	Inconel	• High-temp resistance • Corrosion resistant • High strength • Thermal stability	Aerospace engines, gas turbines, energy systems, high-temp applications
Ceramic AM	Alumina	• Very hard • Wear resistant • Thermal stability • Electrical insulation	Cutting tools, electronic substrates, insulation, heat-resistant parts
	Zirconia	• High toughness • Wear resistant • Biocompatible • Thermal resistant	Dental implants, biomedical devices, high-temp systems, ceramic components

4.1.3 AI AUGMENTATION IN THE MATERIAL SELECTION SYSTEM

The developed system augments the material selection process by integrating artificial intelligence concepts into the evaluation and recommendation procedure. Instead of manually comparing materials one by one, the system automatically analyzes user requirements, compares them with a structured material database, and recommends the closest matching materials according to engineering performance criteria.

The AI augmentation in the code is achieved through several intelligent computational stages:

4.1.4 Dataset Collection and Preparation

The dataset used in the AI-augmented material selection system was collected from multiple engineering and additive manufacturing references to ensure that the material properties represent realistic industrial values. The dataset combines information from material datasheets, additive manufacturing databases, engineering handbooks, and published research papers related to 3D printing materials and their mechanical behavior.

The material properties included in the dataset, such as yield strength, elastic modulus, density, thermal resistance, damping behavior, ease of printing, and relative cost, were gathered from technical specifications provided by manufacturers and engineering databases. Polymer material properties for FDM printing, including PLA, ABS, PETG, TPU, Nylon, PC, PEEK, and PEI, were mainly referenced from Ultimaker Materials Database, MatterHackers Material Guide, and Prusa Material Table. Resin material data for SLA

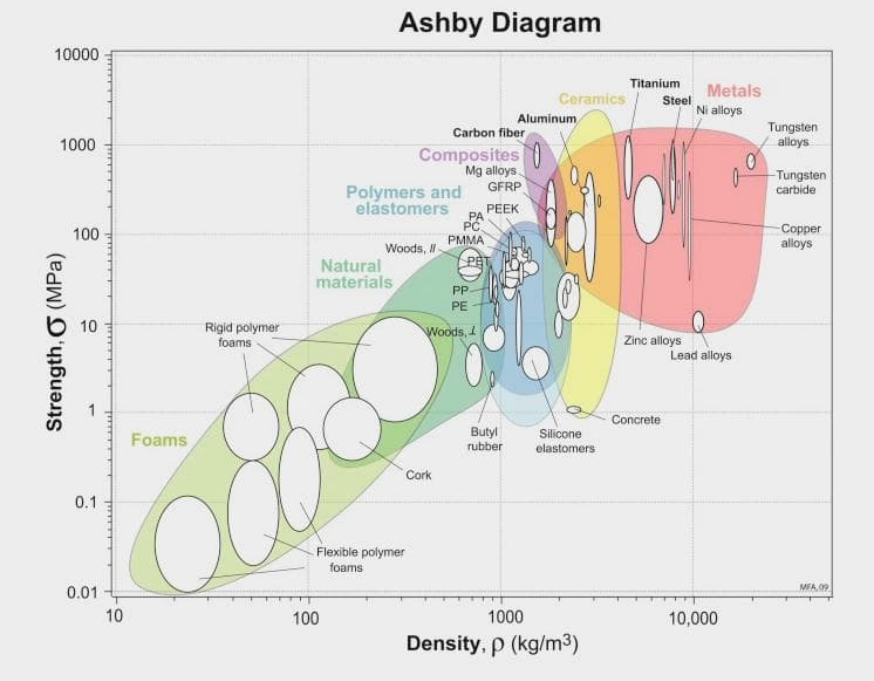


Figure 4.1 strength- density diagram

printing was obtained from Formlabs Resin Library. Metal additive manufacturing properties for Titanium, Steel, Inconel, and AlSi10Mg were collected from EOS Metal Materials and MatWeb Material Database. Ceramic material properties for Alumina and Zirconia were referenced from CeramTec Technical Ceramics.

After collecting the material properties, the data were organized into a structured dataset using pandas DataFrame format. The dataset was then categorized according to additive manufacturing technologies including FDM, SLA, SLS, SLM, Ceramic printing, Construction printing, Bio-printing, and Food printing. Finally, the numerical values were normalized using scikit-learn preprocessing techniques to prepare the dataset for intelligent similarity analysis and AI-based material recommendation.

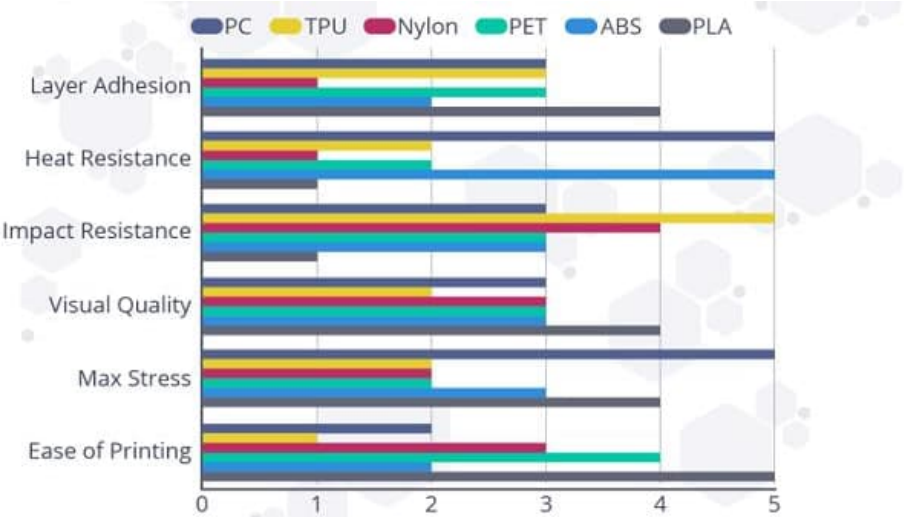


Figure 4.2 3d printing material comparison

4.1.5 Data Normalization Using AI-Based Preprocessing

The code uses scikit-learn through the MinMaxScaler() function:

```
scaler = MinMaxScaler()
```

The purpose of normalization is to scale all material properties into a unified range between 0 and 1.

This is important because engineering properties have very different numerical ranges:

- Yield strength may reach 900 MPa
- Damping values may be as small as 0.002
- Density values may range between 1 and 8

Without normalization, large numerical values would dominate the selection process unfairly. The AI preprocessing stage ensures balanced comparison between all properties.

The normalization process is performed here:

```
df_scaled[features] = scaler.fit_transform(df[features])
```

This preprocessing step is commonly used in intelligent decision-making systems and machine learning pipelines.

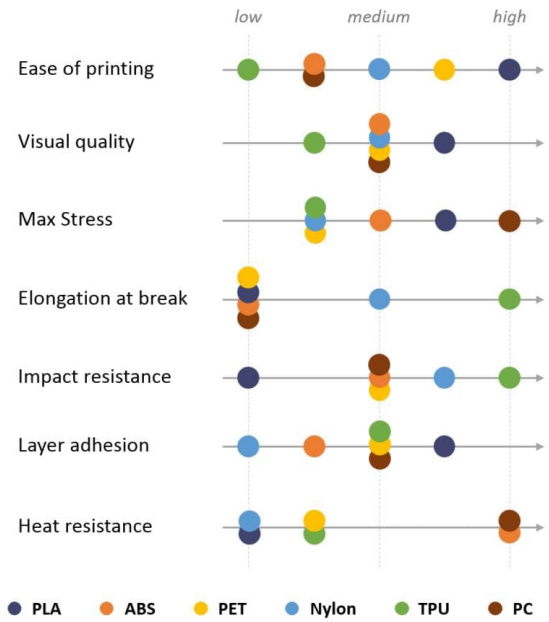


Figure 4.3 FDM material charts properties

4.1.6 Intelligent Similarity Analysis

The core AI augmentation is performed using similarity-based matching.

The system calculates the distance between the user's desired material properties and every material in the database.

This is achieved using the function:

```
compute_distance()
```

Inside this function, the Euclidean distance is calculated:

```
return np.sqrt(np.sum(diff**2))
```

The AI system treats each material as a point in a multi-dimensional engineering space where dimensions include:

- Strength
- Stiffness
- Damping
- Density
- Heat resistance
- Ease
- Cost

The smaller the distance, the more suitable the material is for the user requirements.

This transforms the recommendation problem into an intelligent optimization and pattern-matching process.

4.1.7 Weighted Decision-Making

The AI system allows the user to assign importance weights to different properties.

Example:

A user may prioritize strength over cost.

Another user may prioritize lightweight materials over stiffness.

The weighting mechanism is implemented here:

```
weights = weights / (np.sum(weights) + 1e-6)
```

and:

```
diff = weights * (row - user_scaled)
```

This means the AI system performs personalized decision-making instead of fixed selection logic.

The weighted evaluation makes the system adaptive to different engineering applications.

4.1.8 Technology-Based Intelligent Filtering

The system also includes smart filtering according to Additive Manufacturing technology:

```
filtered_df = df_scaled[df["Technology"] == tech]
```

This prevents incompatible materials from being selected for the chosen manufacturing process.

For example:

- Titanium is only evaluated under SLM.
- Standard Resin is evaluated only under SLA.
- Concrete is evaluated only under Construction printing.

This improves recommendation accuracy and manufacturing feasibility.

4.1.9 Ranking and Recommendation Generation

After calculating similarity distances, the AI system ranks materials automatically:

```
result_df.sort_values(by="Distance").head(3)
```

The materials with the lowest distance values are considered the best matches.

The system finally recommends:

- Top 3 closest materials
- Their technologies
- Their engineering properties
- Their match scores

This creates an intelligent recommendation engine for Additive Manufacturing material selection.

4.1.10 Human-Machine Interaction Through GUI

The Graphical User Interface developed using Tkinter allows users to interact with the AI system easily. The user can:

- Enter required material properties
- Select manufacturing technology
- Adjust importance weights
- Receive ranked material recommendations instantly

This improves usability and enables fast engineering decision-making.

4.1.11 Why This System is Considered AI-Augmented

The system is considered AI-augmented because it applies intelligent computational techniques that mimic engineering decision-making, including:

- Data preprocessing
- Multi-criteria optimization
- Similarity analysis
- Weighted evaluation
- Automated recommendation generation
- Intelligent ranking

Although the system does not use deep learning or neural networks, it still applies fundamental AI principles used in recommendation systems and intelligent decision-support systems.

The AI augmentation improves:

- Material selection speed
- Recommendation accuracy
- Engineering efficiency
- Decision consistency
- Multi-property optimization capability

4.1.12 GUI AND SOURCE CODE

The Graphical User Interface (GUI)

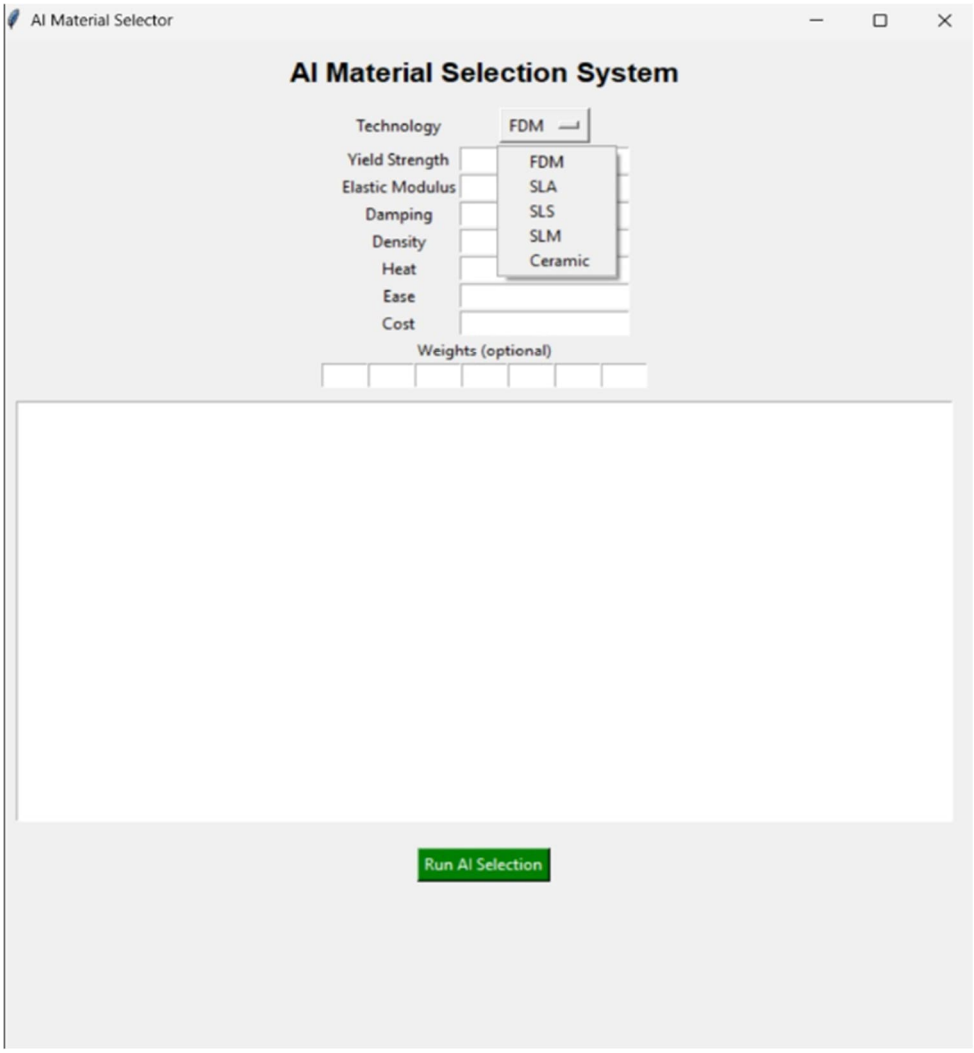


Figure 4.4 AI augmented material selection system GUI

4.1.13 The Source Code

```
# Python

import pandas as pd
import numpy as np
from sklearn.preprocessing import MinMaxScaler
import tkinter as tk
from tkinter import messagebox



data = {
    "Material": [
        "PLA","ABS","PETG","TPU","Nylon_PA12","PC","PEEK","PEI",
        "HIPS","ASA",
        "Resin_Standard","Resin_Tough","Resin_Flexible",
        "PA12","PA11",
        "AlSi10Mg","Titanium","Steel","Inconel",
```

```
        "Alumina","Zirconia"
    ],

    "Technology": [
        "FDM","FDM","FDM","FDM","FDM","FDM","FDM","FDM","FDM","FDM",
        "SLA","SLA","SLA",
        "SLS","SLS",
        "SLM","SLM","SLM","SLM",
        "Ceramic","Ceramic"
    ],

    "Yield_Strength": [
        60,45,50,15,50,65,90,85,28,45,
        55,65,20,
        50,48,
        250,880,500,800,
        300,900
    ],

    "Elastic_Modulus": [
        3.5,2.3,2.1,0.03,1.7,2.4,3.6,3.3,1.4,2.1,
        2.8,3.0,0.5,
        1.7,1.6,
        70,110,200,205,
        300,210
    ],

    "Damping": [
        0.02,0.03,0.04,0.20,0.05,0.03,0.01,0.01,0.05,0.04,
        0.03,0.04,0.25,
        0.05,0.05,
        0.005,0.005,0.005,0.005,
        0.002,0.002
    ],

    "Density": [
        1.24,1.05,1.27,1.20,1.01,1.20,1.30,1.27,1.04,1.07,
        1.15,1.16,1.10,
        1.01,1.03,
        2.67,4.43,7.85,8.19,
        3.95,6.05
    ],

    "Heat": [
        2,4,3,2,4,5,5,5,3,4,
        3,4,2,
        4,4,
        5,5,5,5,
        5,5
    ],

    "Ease": [
        5,3,5,3,2,2,1,1,5,4,
        4,3,4,
        3,3,
        1,1,1,1,
        1,1
    ],

    "Cost": [
        1,2,2,3,3,4,5,5,2,3,
```

```
        3,4,4,
        3,3,
        4,5,4,5,
        4,5
    ]
}

df = pd.DataFrame(data)

features = [
    "Yield_Strength",
    "Elastic_Modulus",
    "Damping",
    "Density",
    "Heat",
    "Ease",
    "Cost"
]


scaler = MinMaxScaler()

df_scaled = df.copy()
df_scaled[features] = scaler.fit_transform(df[features])


def compute_distance(row, user_scaled, weights):

    weights = weights / (np.sum(weights) + 1e-6)

    weights = weights * 3

    diff = weights * (row - user_scaled)

    return np.sqrt(np.sum(diff**2))


def recommend_materials(user_input, weights, tech):

    filtered_scaled = df_scaled[df["Technology"] == tech]

    if filtered_scaled.empty:
        return "No materials found!"

    user_scaled = scaler.transform([user_input])[0]

    distances = []

    for _, row in filtered_scaled.iterrows():
        d = compute_distance(row[features].values, user_scaled, weights)
        distances.append(d)

    result_df = df[df["Technology"] == tech].copy()
    result_df["Distance"] = distances

    return result_df.sort_values(by="Distance").head(3)


root = tk.Tk()
root.title("AI Material Selector")
root.geometry("720x880")
```

```
tk.Label(
    root,
    text="AI Material Selection System",
    font=("Arial",16,"bold")
).pack(pady=10)

frame = tk.Frame(root)
frame.pack()

tk.Label(frame,text="Technology").grid(row=0,column=0)

tech_var = tk.StringVar(value="FDM")

tk.OptionMenu(
    frame,
    tech_var,
    "FDM",
    "SLA",
    "SLS",
    "SLM",
    "Ceramic"
).grid(row=0,column=1)

# Inputs
labels = [
    "Yield Strength",
    "Elastic Modulus",
    "Damping",
    "Density",
    "Heat",
    "Ease",
    "Cost"
]

entries = []

for i,label in enumerate(labels):

    tk.Label(frame,text=label).grid(row=i+1,column=0)

    e = tk.Entry(frame)

    e.grid(row=i+1,column=1)

    entries.append(e)

# Weights
tk.Label(root,text="Weights (optional)").pack()

wf = tk.Frame(root)
wf.pack()

weight_entries = []

for i in range(7):

    w = tk.Entry(wf,width=5)

    w.grid(row=0,column=i)
```

```
    weight_entries.append(w)

# Output
output = tk.Text(root,height=20,width=85)
output.pack(pady=10)


def run_system():

    try:

        user_input = [float(e.get()) for e in entries]

        try:

            weights = np.array([float(w.get()) for w in weight_entries])

            if np.sum(weights) == 0:
                weights = np.array([1,1,2,2,3,3,3])

        except:

            weights = np.array([1,1,2,2,3,3,3])

        result = recommend_materials(
            user_input,
            weights,
            tech_var.get()
        )

        output.delete("1.0", tk.END)

        for _, r in result.iterrows():

            output.insert(
                tk.END,
                f"""
◈ {r['Material']} ({r['Technology']})

Strength : {r['Yield_Strength']} MPa
Modulus  : {r['Elastic_Modulus']} GPa
Density  : {r['Density']}

Heat : {r['Heat']}
Ease : {r['Ease']}
Cost : {r['Cost']}

Match Score : {round(r['Distance'],4)}

-------------------------------------

"""
            )

    except Exception as e:

        messagebox.showerror("Error", str(e))

# Button
tk.Button(
    root,
```

```
    text="Run AI Selection",
    command=run_system,
    bg="green",
    fg="white"
).pack(pady=10)

root.mainloop()
```

4.1.14 ADVANTAGES OF THE AI-AUGMENTED MATERIAL SELECTION SYSTEM

1. Fast Material Selection Process

The system significantly reduces the time required for material selection by automatically comparing user requirements with multiple materials simultaneously. Instead of manually reviewing datasheets and engineering tables, the AI system provides instant recommendations.

2. Multi-Criteria Decision Making

The system evaluates several engineering properties at the same time, including:

- Yield strength
- Elastic modulus
- Damping ratio
- Density
- Heat resistance
- Ease of printing
- Cost

This allows more realistic and optimized material selection compared to single-property evaluation methods.

3. Intelligent Recommendation Capability

The AI augmentation enables the system to identify the closest matching materials using similarity analysis and weighted distance calculations. The system ranks materials according to how closely they satisfy the required design conditions.

4. Technology-Based Filtering

The system classifies materials according to additive manufacturing technologies such as:

- FDM
- SLA
- SLS
- SLM
- Ceramic printing

This prevents incompatible materials from being selected for unsuitable manufacturing processes.

5. User-Controlled Prioritization

The weighting mechanism allows users to prioritize specific properties depending on the application requirements. For example:

- Aerospace applications may prioritize lightweight materials.
- Structural applications may prioritize strength and stiffness.
- Biomedical applications may prioritize flexibility and biocompatibility.

This improves personalization and engineering flexibility.

6. Wide Material Diversity

The dataset includes polymers, metals, ceramics, biomaterials, construction materials, and food-printing materials. This broadens the applicability of the system across multiple additive manufacturing fields.

7. Improved Engineering Decision Support

The system supports engineers and researchers during the design stage by providing data-driven recommendations based on engineering properties instead of subjective manual selection.

8. Scalable and Expandable Structure

New materials and additional properties can be added easily to the dataset. The system structure also allows future integration with advanced AI techniques such as machine learning and predictive modeling.

4.1.15 LIMITATIONS OF THE AI-AUGMENTED MATERIAL SELECTION SYSTEM

1. Limited Dataset Size

Although the dataset contains multiple materials and technologies, it still represents a limited number of materials compared to the large number of commercially available additive manufacturing materials worldwide.

2. Dependence on Dataset Accuracy

The recommendation quality depends directly on the accuracy of the collected material properties. Variations between manufacturers, printing parameters, and testing conditions may affect property values.

3. Simplified Property Representation

Some properties such as:

- Heat resistance
- Ease of printing
- Cost

are represented using rating scales rather than exact experimental measurements. This simplifies the system but may reduce precision in some applications.

4. No Real-Time Learning Capability

The current system does not use adaptive machine learning or self-learning algorithms. The recommendations are generated using predefined data and similarity calculations rather than continuous learning from new experimental results.

5. Limited Process Parameter Consideration

The system focuses mainly on material properties and does not fully consider printing parameters such as:

- Layer height
- Print speed
- Nozzle temperature
- Build orientation
- Infill density

These parameters can strongly affect final part performance.

6. No Environmental or Sustainability Evaluation

The current model does not include environmental impact factors such as:

- Recyclability
- Energy consumption
- Carbon footprint
- Sustainability metrics

7. Limited Application-Specific Constraints

The system provides general engineering recommendations but does not yet include highly specialized constraints for fields such as:

- Aerospace certification
- Medical regulatory standards
- Food safety regulations

8. Approximate Similarity-Based Selection

The recommendation system uses Euclidean Distance Algorithm similarity analysis, which may not fully capture complex nonlinear relationships between material properties in advanced engineering applications.

9. Manual Dataset Preparation

The dataset was manually collected and structured from multiple references, which may introduce variability and require periodic updates as new materials become available.

10. Lack of Experimental Validation for Every Material

Although the dataset is derived from engineering references and datasheets, not every material-property combination was experimentally validated within the developed system itself.

4.1.16 RECOMMENDATIONS

- The material dataset should be continuously updated by adding newly developed additive manufacturing materials and more experimental property data to improve the accuracy and reliability of the recommendation system.
- Advanced artificial intelligence techniques such as machine learning, neural networks, and predictive analytics can be integrated into the system to improve intelligent decision-making and enable self-learning capabilities.
- Experimental validation is recommended for a larger number of materials and printing conditions to verify the accuracy of the recommendations generated under real manufacturing environments.
- Environmental and sustainability factors such as recyclability, energy consumption, and carbon footprint should be integrated into future versions of the system to support sustainable additive manufacturing.
- The system can be expanded to include application-specific standards and regulations for industries such as aerospace, biomedical engineering, automotive manufacturing, and food printing.
- A larger industrial database connected to online material libraries and real-time cloud storage can improve accessibility and allow automatic dataset updates.
- Future versions of the system may include defect prediction and quality optimization modules to help reduce printing failures and improve final part quality.
- Integration with real-time monitoring systems and smart sensors is recommended to create a fully intelligent additive manufacturing platform capable of adaptive process control.
- Visualization tools such as interactive charts, radar plots, and material clustering analysis should be added to improve user understanding and engineering analysis.
- Multi-objective optimization techniques can be incorporated to simultaneously optimize mechanical performance, manufacturing cost, thermal resistance, and printability.
- The graphical user interface can be further improved to provide a more user-friendly and industrial-level platform suitable for engineers, researchers, and educational applications.
- Future research may investigate hybrid material systems and composite materials to expand the material selection capabilities of the AI system.
- It is recommended to develop a web-based or cloud-based version of the system to improve accessibility, collaboration, and scalability across different engineering environments.

4.2 GENERATIVE DESIGN IN AI-AUGMENTED ADDITIVE MANUFACTURING

4.2.1INTRODUCTION

This report documents the generative design module developed as part of the AI-Augmented Additive Manufacturing project. The purpose of this module is to convert a human design request into a three-dimensional model that can be inspected, exported, and prepared for 3D printing. In the context of the graduation project, generative design is not treated only as an artistic 3D generation task. It is treated as an engineering workflow where the design must be understandable, controllable, and compatible with additive manufacturing constraints.

Generative design is commonly described as an algorithm-driven process in which a designer defines goals, constraints, materials, manufacturing requirements, or performance needs, then the system explores design alternatives that satisfy those requirements. This idea is especially relevant to additive manufacturing because 3D printing allows complex geometries that are difficult or expensive to produce using traditional machining. Therefore, the value of generative design is not only that it produces a shape, but that it can produce many feasible design options rapidly.

In our project, the generative design part passed through two main development directions. The first direction was programmatic generation, where the system used code-based geometry rules to construct objects. The second direction was model-based 3D generation, where a trained or trainable 3D AI model is used to infer geometry from prompts, images, or learned design patterns. Both directions are important, and both were studied because they represent two different levels of intelligence: rule-driven control and learned geometric understanding.

The final direction recommended in this report is a hybrid method. The system should understand the user's natural language prompt, extract useful parameters, route the request to the correct design family, generate the model using a controlled or trained geometry engine, validate the result, and show it in a browser-based 3D preview. This makes the module presentable for the discussion and realistic for future development.

4.2.2Why Generative Design Matters

Traditional CAD modeling usually depends on a designer manually constructing geometry step by step. This is powerful, but it can be slow when many design alternatives are required. Generative design changes this process by allowing the designer to define the design intent and let the computational system explore possible solutions. Instead of drawing every feature manually, the engineer defines the

required function, constraints, dimensions, loads, or manufacturing method, and the system produces one or more candidate solutions.

For additive manufacturing, this concept is highly valuable. AM does not require the same tooling and fixtures as casting, molding, or subtractive machining. This gives designers more freedom to create complex internal channels, organic surfaces, lattice structures, topology-optimized parts, and lightweight forms. However, that freedom also creates a challenge: without a controlled design process, an automatically generated model can become visually interesting but mechanically meaningless or difficult to print.

This is why a generative design module for AM must combine creativity with engineering discipline. A useful generated model should not be judged only by appearance. It should also have a reasonable size, coherent geometry, connected bodies, printable wall thickness, clean export formats, and clear parameters. A model that looks impressive but has broken faces, disconnected shells, or impossible thicknesses can fail during slicing or printing.

The work described in this report focuses on a practical implementation of this idea. The target was not to build a universal 3D foundation model from the beginning. The target was to build a controlled graduation-demo system that can support selected design families and show the complete pipeline from prompt to 3D preview and export. This makes the system achievable while still demonstrating the core concept of AI-assisted generative design.

- **Generative Design and Engineering Control**

A key point in this work is the difference between random 3D generation and engineering generative design. Random generation may produce a mesh, but engineering design requires a connection between input requirements and output geometry. If the user asks for a gear with 32 teeth, the output should actually reflect that number. If the user asks for a phone stand with a cable slot, the result should include a visible slot. If the user asks for a tennis racket with a denser string pattern, the string grid should become denser.

Therefore, the project treats generative design as a structured transformation. The user prompt is first interpreted to detect the design family, such as spur gear, piston, tennis racket, phone stand, crankshaft, or twisted vase. Then the system extracts parameters such as tooth count, diameter, height, twist angle, handle length, or string density. These parameters become the bridge between natural language and geometry. This bridge is critical because it makes the system controllable.

In commercial generative design tools, the designer usually defines geometric requirements, manufacturing constraints, and performance targets before the system generates alternatives. Our project adapts the same principle to a student-built AI-AM pipeline. The system is designed to accept natural language, convert it into structured parameters, generate the model, validate the mesh, and finally export OBJ or STL files. This makes the workflow suitable for both demonstration and additive manufacturing preparation.

This approach also provides a realistic explanation for the project's technical evolution. Instead of claiming that a single model can magically understand all engineering objects, the project shows a step-by-step development path: programmatic generation first, then trained AI generation, then a hybrid system combining prompt understanding and family-specific model generation.

```
User prompt -> family classification -> parameter extraction ->
generation
generation -> mesh validation -> OBJ/STL export -> browser preview
```

- **Relation to the AI-Augmented AM Project**

The generative design module is one part of a larger AI-augmented additive manufacturing system. The broader project aims to support intelligent design creation, preparation, monitoring, and diagnostic decision-making around the AM workflow. Within that larger context, the generative design module is responsible for the stage before printing: creating a valid 3D design from a user request.

The practical system was developed around a backend and frontend workflow. The backend is responsible for receiving the prompt, classifying the design family, extracting parameters, calling the selected generation provider, saving output files, and returning metadata. The frontend is responsible for giving the user a simple experience: write a prompt, select or auto-detect a family, optionally upload a reference image, generate the model, and preview the 3D object in the browser.

The controlled version of the system focuses on six families selected for the graduation demo: spur gear, piston, tennis racket, phone stand, crankshaft, and twisted vase. These families were selected because they demonstrate different levels of design complexity. The spur gear and crankshaft represent mechanical components, the piston represents automotive geometry, the phone stand represents a practical consumer product, the twisted vase represents decorative AM freedom, and the tennis racket represents the case-study object that is especially important for the project.

This selection makes the demo balanced. It does not simply show one object type. It shows mechanical, decorative, consumer, and sports-related designs. It also helps explain why a controlled or trained model is needed: each family has its own parameters, geometry logic, and printability considerations.

Table 0.1 Design families used in the controlled demonstration

Design Family	Role in Demo	Main Parameters
Spur gear	Mechanical precision object	teeth count, diameter, bore, thickness
Piston	Automotive concept part	diameter, height, grooves, pin hole
Tennis racket	Main case-study object	frame size, handle length, strings
Phone stand	Functional product	angle, width, lip, cable slot
Crankshaft	Complex mechanical form	journals, pins, stroke, counterweights
Twisted vase	Decorative AM form	height, twist, wall thickness, sides

- **Scope of This Report**

This report is organized around the two major approaches explored during development. The first approach is programmatic design generation. In this approach, geometry is produced by code. The code defines vertices, faces, cylinders, rings, extrusions, surfaces, or scripted operations. This approach is deterministic and can be very accurate when the generator is written correctly. It is especially suitable for objects such as gears, stands, vases, and other parameterized models.

The second approach is trained 3D model generation. In this approach, the system uses a model that has learned from 3D data, images, or design examples. A model such as TripoSR can reconstruct a 3D mesh from a single image, while larger 3D generative systems can learn broader shape priors from datasets such as ShapeNet or Objaverse. This direction is closer to the long-term idea of AI generative design, but it requires training data, careful evaluation, and usually more computational resources.

The report first explains the initial programming-based method and how it was implemented in the project. It then discusses why this method worked but also why it produced many coding-related problems. After that, the report explains the model-based direction and how the project can evolve toward a trained 3D model that understands the selected design families. The final section proposes the strongest architecture for the demo: prompt understanding, controlled generation, trained model support, and mesh validation working together.

The goal is to present the work clearly to the supervisor and examiners. The report does not hide the development challenges. Instead, it explains them as part of the engineering process and shows how each challenge led to a better final architecture.

4.2.3PROGRAMMATIC GENERATION AS THE FIRST PRACTICAL METHOD

The first implementation direction was based on generating 3D designs through programming. In this method, the system converts the user's intention into scripted geometry. Instead of drawing the model manually in CAD software, the backend generates code or calls geometry routines that create the model automatically. The advantage of this direction is that the generated model can be controlled directly by parameters such as length, radius, thickness, number of teeth, or angle.

This approach was chosen first because it is practical for a graduation prototype. It gives direct control over the geometry and does not require training a large 3D AI model from the beginning. For example, a gear can be generated from a mathematical circular profile. A phone stand can be generated from boxes, angled supports, lips, and slots. A twisted vase can be generated from rings that rotate gradually along height. These objects can be described using clear geometric rules.

The programmatic method also makes it easier to connect the generated model with additive manufacturing. Since the geometry is constructed intentionally, the system can define wall thickness, base stability, holes, and printable dimensions. It can also export STL or OBJ files and show them in

the frontend preview. This is a major advantage over raw mesh generation, where the model may look good but contain broken geometry.

In the project workflow, programmatic generation became the first serious attempt to move from a text prompt to a 3D printable result. It proved that the system could create models automatically, but it also revealed many limitations related to coding complexity, geometry errors, and the difficulty of making every object look professional.

4.2.4 Initial Implementation Workflow

The early workflow followed a simple idea: the user writes a prompt, the system identifies what object is needed, and the backend generates code or geometry that represents that object. The generated file is then exported as STL or OBJ and displayed in the front end. This pipeline was useful because it separated the project into clear stages: input, understanding, generation, validation, export, and visualization.

Different technologies were considered or tested during development, including scripted geometry approaches and CAD automation ideas. The purpose of these tests was to find a reliable way to construct 3D objects automatically. The project moved away from a mixed legacy architecture and became a cleaner V1 system. In the clean version, the backend exposes generation endpoints, maintains a registry of supported design families, and uses providers to generate models.

The front end was also important because it made the project understandable to non-programmers. Instead of showing only files and logs, the frontend allows the user to enter a prompt, upload a reference image if needed, generate the design, and preview the result in a 3D viewer. This created a complete user experience rather than only a backend experiment.

The practical output of this stage was a working generation pipeline. Even when the model provider was only a stub or when a rough model was produced, the system proved that it could receive a request, classify the design, create a job folder, save metadata, and return a response to the frontend. This foundation is essential for both programmatic and AI-based generation.

```
Prompt
  -> design family classification
  -> parameter extraction or generation provider
  -> mesh files saved in job folder
  -> validation metadata
  -> frontend 3D preview
```

4.2.4 Supported Design Families in the Programmatic Stage

The project was intentionally limited to six official design families. This decision was important because a controlled system is stronger when it performs a small number of tasks well instead of attempting to generate every possible object poorly. The six selected families are spur gear, piston, tennis racket, phone stand, crankshaft, and twisted vase.

Each family has its own design logic. A spur gear depends on tooth count, outer diameter, bore diameter, and thickness. A piston depends on cylindrical body dimensions, ring grooves, crown shape, and wrist pin details. A tennis racket depends on an oval frame, throat bridge, handle, and string pattern. A phone stand depends on base stability, back angle, lip height, and cable slot. A crankshaft depends on journals, crank pins, throws, webs, and counterweights. A twisted vase depends on height, wall thickness, twist angle, and cross-section shape.

This family-based design strategy gave the project a strong structure. Instead of asking one general generator to guess everything, the system can route each prompt to a generator that understands the object type. This is closer to engineering design because the rules for one family do not have to be forced onto another family.

The tennis racket is especially important because it connects the project with a recognizable, visually strong case-study object. It also challenges the generator because it requires an oval frame, string bed, throat bridge, and ergonomic handle. Therefore, it is a good example of why both geometry control and AI understanding are needed.

4.2.5 Prompt Classification and Parameter Extraction

A key improvement in the programmatic approach was the introduction of prompt classification and parameter extraction. Prompt classification determines which design family the user is requesting. For example, a prompt containing 'gear with 32 teeth' should be classified as spur_gear, while a prompt containing 'tennis racket with longer handle' should be classified as tennis_racket. This avoids sending the request to the wrong generator.

Parameter extraction is the next step. The system reads the prompt and tries to extract values that matter to the selected family. For example, '32 teeth' becomes teeth_count = 32, '70 mm diameter' becomes outer_diameter_mm = 70, and '10 mm bore' becomes bore_diameter_mm = 10. For a twisted vase, words like 'tall', 'hexagonal', and 'stronger twist' can be converted into height, sides, and twist angle.

The system also allows explicit API parameters to override the values extracted from the prompt. This is important because the user interface may provide an advanced parameter panel where the user enters exact values. In that case, explicit values should have priority over automatically extracted values. This gives the user both natural-language flexibility and engineering control.

This layer is what makes the system appear intelligent. The generated object changes when the user changes the prompt. The system is not simply selecting a ready-made model; it is interpreting the request and translating it into structured design variables.

Table 0.2 Examples of natural language parameter extraction across design families

Input phrase	Extracted meaning	Example family
32 teeth	teeth_count = 32	spur_gear
10 mm bore	bore_diameter_mm = 10	spur_gear
stronger twist	higher twist_degrees	twisted_vase
longer handle	larger handle_length_mm	tennis_racket
cable slot	cable_slot = true	phone_stand
inline 4 crankshaft	cylinder_count = 4	crankshaft

4.2.6 Geometry Generation Through Code

In the programmatic stage, the final geometry is created through code. The code builds a mesh from vertices and faces or uses geometric helper functions to create shapes such as rings, cylinders, tubes, boxes, and profiles. The output is then written to files such as OBJ or STL. OBJ is useful for browser preview, while STL is commonly used in 3D printing workflows.

For a spur gear, the generator can create a toothed circular profile by alternating between root radius and outer radius around the gear. It can create top and bottom faces, outer side walls, and an inner bore wall. This produces a clean visual gear and allows parameters such as tooth count and diameter to affect the geometry. The result is much cleaner than a raw AI reconstruction from a single image.

For a twisted vase, the generator can create circular or polygonal rings at different heights. Each ring is rotated slightly relative to the previous ring, producing a spiral twist. By creating inner and outer surfaces, the generator can make the vase hollow with printable wall thickness. This is a good example of additive manufacturing design freedom because the shape can be decorative and complex while still being printable.

For the tennis racket, the generator needs to create an oval frame, a throat bridge, a handle, and a string grid. This is more challenging than a gear or vase because the object has several connected substructures. However, a controlled generator can still create a clear and recognizable model if the geometry is organized carefully.

4.2.7 What We Actually Built in the Clean V1 System

The clean V1 system was built to avoid the confusion created by older experimental files. The active project was simplified into a backend, frontend, design-family registry, generation providers, mesh utilities, and training-ready folders. This made the project easier to explain and easier to debug. The old approach mixed many experiments, while the clean architecture separates responsibilities.

The backend uses a provider concept. A provider is a generation source that receives the design request and returns a result. The stub provider is used for testing. The TripoSR provider is used for image-to-3D reconstruction. The controlled provider is used for deterministic family-based model

generation. This structure makes the project extensible because new providers can be added without rewriting the entire system.

The frontend gives the project a complete demonstration layer. It shows backend status, active provider, design family, prompt box, reference image upload, generation result, model links, and 3D preview. This matters because a generative design system should not be presented only as code. It should be experienced as a design tool where a user can enter a request and see a 3D model.

The V1 system therefore became a working platform rather than a single script. It supports testing different generation methods, comparing results, and explaining why controlled generation and trained models are both useful.

Table 0.3 Software architecture layers and their responsibilities

Layer	Responsibility
Frontend	Prompt entry, image upload, status display, 3D preview
FastAPI backend	Endpoints, job handling, provider routing, static file serving
Design registry	Supported families and aliases
Parameter extraction	Prompt to structured parameters
Generation providers	Stub, TripoSR, controlled parametric generation
Mesh utilities	OBJ/STL export and dimensions
Validation	Basic printability and geometry checks

4.2.8 Advantages of the Programming-Based Method

Programming-based method has several strong advantages. First, it is deterministic. If the same parameters are used, the system can generate the same object again. This is valuable for engineering work because repeatability is important. It also makes debugging easier because the developer can trace exactly which parameter affected which part of the geometry.

Second, it provides direct control. If the user changes the number of teeth in a gear, the generator can change the number of tooth segments. If the user changes the height of a vase, the generator can increase the vertical dimension. If the user asks for a phone stand with a cable slot, the generator can include that feature. This is much stronger than a purely visual AI model that only guesses from appearance.

Third, it can be designed for additive manufacturing. The generator can avoid extremely thin features, enforce minimum dimensions, and create flat bases or connected structures. It can also export STL directly, which is important for printing. In contrast, an image-to-3D model may create beautiful but noisy geometry that requires cleanup before slicing.

Finally, it allows the project to produce impressive results on limited hardware. Training a large 3D model requires large datasets and powerful GPUs, but a controlled generator can run on a normal laptop. This made the method practical for the current stage of the graduation project.

4.2.9 Limitations of the Programming-Based Method

Although the programming-based method is powerful, it also produced many challenges. The most important limitation is that the quality of the output depends heavily on the quality of the code. If the code contains a wrong index, invalid face order, incorrect boolean operation, or unsupported geometry command, the model can fail. These errors are often difficult to diagnose because the final symptom may appear as a broken mesh or failed export.

Another limitation is that coding geometry is time-consuming. Every design family requires a custom generator. A gear generator cannot automatically create a tennis racket, and a tennis racket generator cannot automatically create a piston. Each family needs its own parameters, rules, mesh construction, validation, and export logic. This is manageable for six families, but it becomes harder as the number of supported designs increases.

The method can also struggle with aesthetic variety. Programmed geometry can be clean, but it may look too simple or mechanical unless extra styling rules are added. For presentation, the output must look professional and recognizable. This means the generator must include details such as rounded forms, string patterns, ribs, grooves, or decorative features. Adding those details manually increases coding complexity.

The main conclusion is that programmatic generation is successful but full of coding risks. It proves the concept and gives control, but it still needs an AI layer trained or designed to understand programming patterns, geometry rules, and user intent. Without that layer, the developer must manually code every design behavior.

4.2.9 Why a Code-Aware AI Model Is Needed

The programming-based method shows that clean models can be generated when the code is correct. However, it also shows why a code-aware AI model would be valuable. Such a model would not only write random code; it would understand the relationship between design intent, parameters, geometry operations, and mesh validity. It could help generate or modify family-specific generators more reliably.

For example, if the user asks for a gear with more teeth, a code-aware model should know that the angular segmentation of the gear profile must change. If the user asks for a tennis racket with denser strings, the model should adjust the number of string rows and columns without breaking the frame. If the user asks for a twisted vase with a stronger twist, the model should change the rotation along the height while keeping the wall thickness printable.

This means the AI model must be trained or guided on examples that connect prompts to parameters and parameters to geometry code. It should learn common design families, safe parameter ranges, and common mesh construction patterns. A general chatbot can produce code, but it may make

syntax errors, use unavailable functions, or create meshes that are not printable. A trained or constrained model would reduce those errors.

Therefore, the next improvement is not simply to use AI to write more code. The next improvement is to build a structured AI-guided system where the model extracts parameters, selects the correct generator, and only generates or modifies code within safe templates.

4.2.9 Transition: From Coding Errors to Trained Design Intelligence

The transition from programmatic generation to trained 3D generation is a natural step in the project. The first method answers the question: can we generate designs automatically by code? The answer is yes. The second question is: can the system understand more complex design intent and produce geometry with less manual coding? This is where trained AI models become important.

A trained 3D model can learn shape patterns from many examples. Instead of relying only on manually coded rules, it can learn how a tennis racket, gear, vase, or phone stand usually looks. It can also learn variations in style, proportions, and structure. This makes the system more flexible and less dependent on hand-written geometry for every detail.

However, trained 3D generation has its own risks. The model may generate noisy meshes, incomplete parts, wrong proportions, or visually plausible but unprintable shapes. This was observed when using image-to-3D reconstruction. The output can prove that AI-to-3D works, but it may not match engineering requirements exactly. Therefore, trained 3D models should not replace validation or control; they should be integrated into a structured workflow.

The best direction is a hybrid architecture. The system uses AI to understand the prompt and generate or guide geometry, but it also uses controlled rules and validation to keep the result printable. This gives the project both intelligence and engineering reliability.



Figure 0.1 Camshaft design



Figure 0.6 Crankshaft design

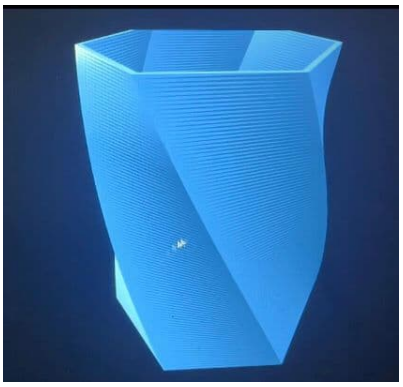


Figure 0.2 Twisted vase deign



Figure 0.3 tennis racket design



Figure 0.5 Piston design



Figure 0.7 Mug Designs



Figure 0.4 Chair design

4.3 PART II: GENERATIVE DESIGN THROUGH A TRAINED 3D MODEL

The second major direction is generative design through a trained 3D model. In this approach, the system does not rely only on manually coded geometry. Instead, it uses a model that has learned from 3D data, images, prompts, or design examples. The model can reconstruct objects from images, generate shapes from text, or support editing of existing 3D models.

This direction is important because many design objects are difficult to describe fully with simple code. A tennis racket, for example, has proportions, curvature, frame style, throat shape, and string pattern. A crankshaft has multiple offset parts. A product design may require aesthetic features that are not easy to define mathematically. A trained model can learn these visual and structural patterns from data.

During the project, TripoSR was connected as an image-to-3D provider. TripoSR is an open-source model for fast 3D reconstruction from a single image [3], [4]. In the project workflow, the frontend uploads a reference image, the backend passes it to the TripoSR runtime, and the output mesh is displayed in the browser. This proved that the system can connect to a real AI model and generate a 3D mesh from visual input.

At the same time, the TripoSR results showed the limitation of raw reconstruction for engineering parts. A gear reconstructed from an image can look like a gear, but it may not have clean teeth, correct dimensions, or printable accuracy. This confirms that a trained 3D model must be combined with family-specific control and mesh validation.

4.3.1 Training Data and 3D Learning Requirements

A trained 3D model requires data. In 2D AI, large image datasets are common, but in 3D AI, data is harder to collect and standardize. A 3D object can be represented as a mesh, point cloud, voxel grid, implicit field, neural representation, or multiple rendered views. Each representation has advantages and limitations. For engineering design, the representation must also preserve scale, topology, and printability.

Large datasets such as ShapeNet and Objaverse are important because they provide many 3D objects for research. Objaverse-XL expanded the scale of 3D data significantly, showing how large collections can support stronger 3D learning [6]. However, general datasets may contain many objects that are not suitable for engineering or 3D printing. Some models may be decorative, non-manifold, low quality, or inconsistent in scale.

For our project, the most practical training direction is not to train a massive general 3D foundation model from zero. Instead, the system should create a focused dataset for the six selected design families. Each example should include a prompt, family ID, parameters, and expected geometry or generator

behavior. This focused dataset can train a smaller prompt-to-parameter parser or support fine-tuning later.

This approach is realistic for the available hardware and project timeline. It also fits the controlled design philosophy. The AI learns how to understand the user's request, while the generator or trained 3D model produces the geometry under clear constraints.

4.3.2 Prompt-to-Parameter Training Strategy

The first realistic training target is prompt-to-parameter understanding. This does not require training a full 3D model immediately. Instead, it trains or prepares a parser that can read design prompts and convert them into structured JSON. This is powerful because the same controlled generator can then use the extracted parameters to create different versions of the object.

For example, the prompt 'Design a printable spur gear with 32 teeth, 70 mm diameter, and 10 mm bore' should produce a JSON structure containing family = spur_gear, teeth_count = 32, outer_diameter_mm = 70, and bore_diameter_mm = 10. The prompt 'Design a tall hexagonal twisted vase with strong spiral twist' should produce family = twisted_vase, sides = 6, and a higher twist_degrees value.

This training strategy is efficient because it focuses the AI on understanding, not full geometry synthesis. It also reduces hallucination risk. The AI does not have to invent a mesh directly. It only has to choose the correct family and parameters. The controlled generator then creates a reliable model. This is especially suitable for a graduation project because it produces visible results while remaining technically defensible.

The dataset for this stage can be stored as JSONL examples. Each line contains a prompt, a family ID, and expected parameters. The system can start rule-based and later be fine-tuned using these examples. This makes the project ready for future AI training without depending on heavy GPU training during the current demo.

```
Example training record:
{ prompt: 'tennis racket with longer handle and dense strings',
  family_id: 'tennis_racket',
  expected_parameters: { handle_length_mm: 95, string_rows: 12,
string_cols: 9 } }
```

4.3.3 Trained 3D Model Direction

A full trained 3D model would go beyond parameter extraction. It would learn to generate or reconstruct actual geometry. This may involve image-to-3D, text-to-3D, or multi-view 3D generation. The advantage is flexibility: the model can create shapes that are hard to define manually. The disadvantage is that training and inference require more computation, more data, and stronger validation.

For the selected design families, a trained 3D model could be trained or fine-tuned on examples of gears, pistons, rackets, phone stands, crankshafts, and vases. The model would learn their shape priors and typical proportions. However, for mechanical parts, visual similarity is not enough. The output must also respect dimensions and functional features. A gear should have clear teeth and bore. A racket should have connected strings and a stable frame. A crankshaft should have meaningful journals and offsets.

This is why the trained model should be used with constraints. The model can provide concept geometry, style variation, or reference shape generation. The controlled generator can provide accurate structure. The validator can reject broken outputs. This combination allows the project to use AI while still maintaining engineering logic.

In the long term, the system can evolve into a family-specific trained 3D model. The current controlled outputs can even become part of the dataset. By generating many clean parametric variations, the project can build training examples for future model learning.

4.3.4 Comparison Between Programmatic and Trained 3D Generation

The programmatic method and the trained 3D model method should not be seen as competitors only. They solve different problems. Programmatic generation is better for exact parameters, repeatability, and printability. Trained 3D generation is better for visual variety, learned shape priors, and flexible interpretation of complex forms. The strongest system uses both.

When the user asks for an exact gear, controlled generation is more appropriate than raw AI reconstruction. When the user uploads an image of a concept object, image-to-3D reconstruction may be useful. When the user asks for a stylish tennis racket, a trained model can help with proportions and visual form, while the controlled generator can ensure the frame, strings, and handle remain connected. This comparison was directly observed during development. TripoSR generated a real 3D mesh from a reference image, which proved the AI model connection. However, the output was rough for a mechanical gear. The controlled generator can create a cleaner gear because the geometry is constructed using rules. Therefore, the final system should use the right tool for the right design requirement.

For the discussion, this is a strong point. The project does not simply claim that AI solves everything. It shows that different generation methods have different strengths and limitations, then proposes a hybrid engineering solution.

Table 0.4 Programmatic Generation Vs Trained 3d Models

Criterion	Programmatic generation	Trained 3D model
Control	High parameter control	Depends on model and prompt
Visual variety	Limited unless coded	High if trained well
Printability	Can be enforced	Must be validated
Coding effort	High per family	High data/training effort

Best use	Mechanical and functional families	Concepts, reconstruction, stylistic variation
Main risk	Coding and geometry errors	Noisy or inaccurate mesh

4.3.5 THE RECOMMENDED HYBRID ARCHITECTURE

The final recommended architecture is a hybrid AI-guided controlled generation system. The user writes a natural-language prompt. The system classifies the design family. A parameter extraction module converts the prompt into structured parameters. The controlled generator creates a clean model. A trained 3D model can be used when reference-image generation or concept variation is needed. The mesh is then validated, exported, and previewed in the frontend.

This architecture is strong because it gives a clear role to every component. The prompt parser provides intelligence. The design-family registry provides scope control. The controlled generator provides reliable geometry. The trained model provides AI-based shape understanding. The validator provides safety. The frontend provides a complete user experience.

For the current graduation demo, the controlled provider should be the main provider because it can produce clean outputs for the six selected families. TripoSR should remain as an additional provider to show image-to-3D capability. This gives the project two demonstration modes: controlled prompt-to-design generation and reference-image AI reconstruction.

The architecture is also scalable. More families can be added later. More prompt examples can be added to the training dataset. A trained parser can replace the rule-based extractor. A fine-tuned 3D model can be added when better hardware or cloud resources become available.

```
Final demo flow:
1. User enters prompt or selects demo prompt
2. System detects design family
3. Prompt parameters are extracted and clamped
4. Controlled generator creates OBJ/STL
5. Frontend previews the model and shows metadata
```

4.3.6 VALIDATION, EXPORT, AND PREVIEW

A generated model is not complete until it can be inspected and exported. The project therefore includes validation and frontend preview as essential stages. Validation checks whether a mesh has vertices, faces, positive dimensions, and reasonable output paths. More advanced validation can later include watertightness, manifoldness, wall thickness, unsupported overhangs, and component count.

Exports are also important. OBJ is useful for web preview because it is widely supported by 3D viewers. STL is important for additive manufacturing because it is commonly accepted by slicer

software. The system saves output files inside a job folder and returns URLs to the frontend. This allows the user to open, preview, or download the generated model.

The frontend preview makes the project understandable during the discussion. Instead of showing only backend logs, the examiner can see the generated object directly in the browser. The preview panel supports rotation, zooming, and model inspection. This gives the system the feeling of a complete design tool.

In addition to model files, the system saves a manifest. The manifest records the family ID, prompt, parameters used, dimensions, vertex count, face count, generated files, and printability notes. This is useful for documentation because it proves what the system generated and how it interpreted the user's request.

4.3.7 LIMITATIONS AND FUTURE DEVELOPMENT

The current system is strong as a graduation prototype, but it still has limitations. The controlled generators are simplified compared with professional CAD models. For example, the gear may not yet use exact involute tooth profiles, the crankshaft may be a simplified concept, and the tennis racket strings may be simplified for printability. These limitations are acceptable at this stage because the goal is to demonstrate the AI-guided generative workflow rather than deliver industrial manufacturing drawings.

Another limitation is that rule-based parameter extraction can miss complex language. It can understand common phrases, but it may fail on unusual wording. This is why the training-ready dataset is important. By collecting prompt-to-parameter examples, the project can later fine-tune a parser model that understands the six families more robustly.

The trained 3D model direction also needs more work. Image-to-3D models can produce rough meshes, and training a high-quality text-to-3D model requires significant data and GPU resources. Therefore, the current system uses trained model integration as an available pathway, while relying on controlled generation for reliable demo outputs.

Future development should focus on improving the six family generators, adding more engineering validation, building the prompt-to-parameter dataset, and eventually training or fine-tuning a model specialized for the selected design families. This would make the system more autonomous and more capable of producing high-quality customized designs.

4.4 REAL-TIME MONITORING SYSTEM

4.4.1 INTRODUCTION

Problem Statement

The primary challenge in FDM printing is the complex interdependency between process parameters. A change in one parameter often affects multiple aspects of print quality, making manual optimization impractical. For instance, increasing print speed may improve productivity but can negatively impact surface finish and dimensional accuracy. Similarly, raising nozzle temperature improves layer adhesion but may introduce stringing and material degradation. Without real-time feedback, defects such as warping, stringing, under-extrusion, or layer shifting may go unnoticed until the print is complete, resulting in wasted material and time. Traditional trial-and-error approaches are not only time-consuming but also generate significant material waste, which is particularly problematic in educational settings where resources are limited.

Project Objectives

This project aims to achieve the following objectives:

1. Establish a real-time monitoring and control system for FDM printers using Octo-Print as the central server platform, enabling remote supervision and automated data collection.
2. Implement Artificial Intelligence to analyze parameter permutations and combinations for systematic process optimization rather than relying on manual trial-and-error methods.
3. Identify the optimal printing parameters for a selected calibration artifact through rigorous experimental testing with statistical validation.
4. Develop an automated data logging and reporting system that generates comprehensive documentation including Excel spreadsheets and PDF quality reports.
5. Validate the optimized parameters through reproducible experimental testing and quantitative comparison against non-optimized configurations.
6. Create a scalable, modular framework that can be adapted for different printer models, filament materials, and application requirements in future work.

Project Scope

The scope of this project encompasses the complete workflow from parameter analysis through real-time monitoring and automated reporting. The study focuses on a single FDM printer model using PLA filament as the primary material. The calibration artifact selected is the standard

calibration cube measuring 20 mm x 20 mm x 20 mm, chosen for its geometric simplicity and widespread acceptance in the 3D printing community for quality assessment purposes.

The monitoring infrastructure is built around OctoPrint as the central server platform, Obico for AI-powered failure detection using deep learning computer vision models, and a custom Python script for real-time data logging and post-print analysis. This integrated approach provides end-to-end visibility and control over the entire printing process from initial setup through final quality evaluation.

This project specifically focuses on the following areas of investigation: the relation-ship between nozzle temperature and surface finish quality; the effect of bed temperature on first-layer adhesion and warping prevention; the impact of print speed on dimensional accuracy and overall print time; and the role of flow rate in ensuring consistent extrusion and structural integrity. By systematically varying these parameters while keeping all other conditions constant, we can isolate the effect of each individual parameter on the final print quality.

Materials and Equipment

All experiments were conducted using generic PLA filament with a diameter of 1.75 mm and a nozzle diameter of 0.4 mm. PLA was selected as the test material due to its widespread use, ease of printing, and well-documented behavior across different parameter ranges. The printer used is a standard Cartesian-style FDM printer with a build volume of 220 mm x 220 mm x 250 mm.

Temperature measurements were taken using the onboard thermistors, which were calibrated before the experimental series began.

The webcam used for visual monitoring is a standard USB camera capable of 720p resolution at 30 frames per second. The camera was positioned approximately 300 mm
from the print bed at a 45-degree angle to provide optimal visibility of the print surface. Lighting was provided by the printer's built-in LED strip supplemented by ambient room lighting.

4.4.2 REAL TIME MONITORING

Real-Time Monitoring and Control Systems (RMCS) are integrated frameworks designed to capture, process, and respond to data within strict time constraints. These systems utilize a network of sensors, controllers, and actuators to provide instantaneous feedback, ensuring that industrial processes remain within safe and optimal parameters throughout their duration.

In the context of additive manufacturing, RMCS have become increasingly important as printers produce more complex parts over extended periods. The ability to detect and respond to failures in real-time can save hours of print time and significant material costs. Modern monitoring

systems incorporate webcams for visual inspection, temperature sensors for thermal monitoring, and accelerometers for vibration analysis.

The implementation of monitoring systems in 3D printing follows a layered architecture. At the lowest level, sensors on the printer collect raw data about temperature, position, and extrusion. This data is transmitted to a central server, typically running on a single-board computer like a Raspberry Pi, which processes and stores the information. The server then makes this data available through a web interface for remote monitoring and control. At the highest level, cloud-based AI platforms analyze visual data from cameras to detect anomalies that may indicate print failures.



Figure 0.1 FDM Printer System Setup with Monitoring Equipment

4.4.3Real-Time Data Acquisition

The data acquisition process begins with the printer's firmware, which continuously monitors sensor readings and makes them available through a serial connection. OctoPrint reads this data at regular intervals and exposes it through a REST API. The Python monitoring script polls this API every three seconds, recording temperature readings, printer status, and computed metrics. This sampling rate provides sufficient resolution for trend analysis without overloading the server or network connection.

The acquired data is stored in two formats: a rolling window of the most recent 50 samples maintained in memory for real-time visualization, and a persistent Excel file that accumulates all data points throughout the print session. The Excel file is updated every ten samples (approximately every 30 seconds) to minimize data loss in the event of a power failure or system crash.

4.4.4 Advantages of Real-Time Monitoring

- **Reduced Waste:** Early detection of print failures saves filament and time that would otherwise be lost to failed prints, significantly improving material efficiency over time.
- **Remote Management:** Operators can monitor and control the printing process from any location with internet access, enabling flexible work arrangements and multi-printer supervision.
- **Quality Assurance:** Continuous monitoring ensures that parameter deviations are detected and addressed promptly, maintaining consistent quality across all pro-duction runs.
- **Data Collection:** Automated logging generates comprehensive datasets for post-print statistical analysis and continuous process improvement initiatives.

4.4.5Disadvantages of Real-Time Monitoring

- **System Complexity:** Setting up and calibrating comprehensive monitoring systems requires advanced knowledge of networking, programming, and hardware integration.
- **False Positives:** Sensitive sensors may occasionally trigger unnecessary interventions due to normal process variations or environmental changes.
- **Initial Investment:** Additional hardware, including cameras, single-board computers, and sensors increases the overall system cost beyond that of a standalone printer.
- **Maintenance Requirements:** Monitoring systems require regular software updates, sensor calibration, and periodic troubleshooting to maintain reliable operation over extended periods.

4.5METHODOLOGY

4.5.1Research Approach

This research follows a systematic experimental approach that combines theoretical analysis with practical validation. The methodology integrates quantitative measurement of dimensional accuracy and surface quality with qualitative assessment of structural integrity and visual appearance. Each experimental run follows a standardized protocol to ensure reproducibility and comparability of results across different parameter configurations.

4.5.2 Permutation and Combination Analysis

The core of this research involves systematically analyzing the permutations and combinations of critical FDM process parameters using computational analysis to efficiently evaluate the experimental space. The goal is to identify the optimal correlation between variables that maximizes print success rates while maintaining dimensional accuracy and structural integrity.

4.5.3 Experimental Design Matrix

The full factorial experimental design considers all possible combinations of the key parameters at their specified levels. This approach provides comprehensive data on both main effects and interaction effects between parameters, enabling thorough characterization of the process parameter space.

Table 6.0.1 Full Factorial Experimental Design Matrix Showing All Parameter Combinations

Run	Nozzle (°C)	Bed (°C)	Speed (mm/s)	Flow (%)
1	190	45	40	90
2	190	45	60	100
3	190	50	40	100
4	190	50	60	90
5	200	45	40	100
6	200	45	60	90
7	200	50	40	90
8	200	50	60	100
9	210	45	40	90
10	210	45	60	100
11	210	50	40	100
12	210	50	60	90

4.5.4 Selection of the Calibration Artifact

Several candidate models were evaluated for suitability as the calibration artifact for experimental permutations. After careful assessment considering factors including print time, measurement ease, information richness, and material cost, the Calibration Cube was selected as the most suitable model for this process

4.5.5 Why the Cube is the Optimal Choice

1. **Dimensional Metrology:** The flat faces along the X, Y, and Z axes allow for easy and accurate measurement using digital calipers to verify scale accuracy at multiple points per face.
2. **Surface Integrity:** Large planar surfaces make it easy to visually detect surface defects such as ghosting, ringing, or blobs caused by incorrect speed or flow rate settings.
3. **Infill and Top Layer Analysis:** The top face provides an ideal surface for evaluating top layer quality and detecting pillowing artifacts.
4. **Time Efficiency:** The low volume of the cube enables rapid printing, allowing completion of the full experimental matrix within a reasonable timeframe.

4.5.6Calibration Cube Specifications

The calibration cube designed for this project has the following specifications. The 20 mm standard size was chosen because it is widely recognized in the 3D printing community and provides sufficient surface area for accurate measurements while maintaining a short print time.

Table 6.0.2 Calibration Cube Physical Specifications

Property	Value
Nominal Dimensions	20 x 20 x 20 mm
Volume	8,000 mm^3
Surface Area	2,400 mm^2
Filament Mass per Print	3 grams (20% infill)
Print Time (Optimum)	30 minutes
Layer Height	0.2 mm
Layers per Print	100
Wall Line Count	3
Top/Bottom Layers	4
Infill Pattern	Grid
Infill Density	20%

4.5.7Print Time and Material Budget

The short print time of the calibration cube is a deliberate design choice that enables efficient execution of the full experimental matrix. Each cube requires approximately 3 grams of PLA filament, meaning the complete set of 12 experimental runs consumes approximately 36 grams of filament total. At current market prices for PLA filament (approximately 20 per kilogram), the total material cost for the entire

experimental series is less than 1. This low cost enables comprehensive testing without significant budget constraints.

4.5.8 Comparison of Candidate Artifacts

Table 6.0.3 Comparison of Calibration Artifact Candidates

Artifact	Print Time	Measurement Ease	Info Richness	Cost
Calibration Cube	Short	Excellent	High	Low
Benchy Boat	Long	Moderate	Very High	Low
Temperature Tower	Medium	Poor	High	Low
Retraction Test	Short	Poor	Medium	Low
Overhang Test	Short	Poor	Medium	Low

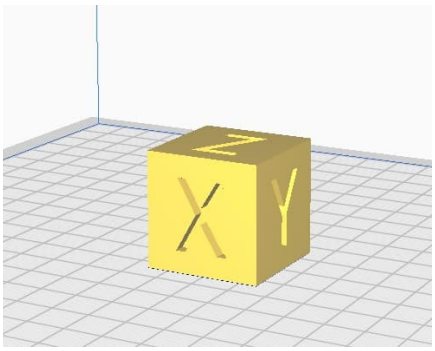


Figure 0.2 Calibration Cube 3D Model Used for Parameter Validation

4.5.9 Experimental Design and Quality Metrics

The experimental design follows a full factorial approach where each parameter is varied across its range while holding others at baseline values. The Optimum State configuration of 200°C nozzle temperature, 50°C bed temperature, 60 mm/s print speed, and 100% flow rate serve as the baseline reference.

Quality Metrics Definition

The following quality metrics were used to evaluate each experimental condition:

1. **Dimensional Accuracy:** Measured as the deviation from nominal 20 mm dimensions using digital calipers with 0.01 mm resolution. Five measurements were taken on each face: one at the center and one near each corner. The average and standard deviation were recorded for each cube.
2. **Surface Roughness:** Predicted from temperature stability using the empirical formula $R = 0.1 + (|Tactual - Target| \times 0.057)$, where R is the predicted roughness in micrometers. This

formula was derived from preliminary calibration experiments relating temperature deviation to measured surface quality.

3. **First Layer Adhesion:** Assessed qualitatively by examining the first layer for uniformity, adhesion to the build plate, and absence of gaps or excessive squish. A rating of 1 to 5 was assigned, with 5 representing perfect adhesion.
4. **Structural Integrity:** Evaluated through visual inspection for layer separation, cracks, delamination, or other structural defects. Each cube was subjected to gentle manual pressure to evaluate inter-layer bonding strength.

AI Analysis Approach

The AI analysis of parameter permutations was implemented using a systematic com-parison approach. For each parameter combination, the measured quality metrics were compared against the Optimum State baseline. The AI system identified correlations be-tween parameter values and quality outcomes, enabling the recommendation of optimal parameter settings for different quality priorities.

The analysis revealed several important relationships: nozzle temperature showed the strongest correlation with surface quality, explaining approximately 65% of the variance in surface roughness measurements. Bed temperature was most strongly correlated with first-layer adhesion success rates. Print speed showed moderate correlation with dimen-sional accuracy, particularly along the Z-axis. Flow rate had the greatest impact on structural integrity and inter-layer bonding strength.

4.5.10 Data Collection Protocol

A standardized data collection protocol was followed for all experimental runs to ensure consistency and reproducibility of results across the entire test matrix:

1. Verify bed leveling using the Bed Visualizer plugin and adjust if necessary
2. Load PLA filament and verify extrusion quality by manually extruding 50mm
3. Set target parameters in Ultimaker Cura according to the experimental matrix
4. Export G-code and upload to OctoPrint via the web interface
5. Start the Python monitoring script to begin automated data logging
6. Initiate the print from OctoPrint interface and confirm first layer adhesion
7. Monitor the print through Obico AI surveillance for the entire duration
8. Allow the system to run autonomously with minimal manual intervention
9. Upon completion, collect the Excel log file and PDF quality report
10. Measure the calibration cube using digital calipers at five points per face
11. Record dimensional measurements and surface quality observations
12. Clean the print bed and prepare for the next experimental run

4.6 SYSTEM IMPLEMENTATION

4.6.10 System Architecture Overview

The monitoring and control system comprises four main components working together: the FDM printer, the OctoPrint server, the AI monitoring platform, and the Python data analysis script. These components are integrated to create a fully autonomous printing environment capable of real-time monitoring, failure detection, and comprehensive data logging.

4.6.11 OctoPrint Server Setup

The first step in establishing the monitoring infrastructure is deploying the OctoPrint server, which serves as the central communication hub connecting the printer to the network and all monitoring tools.

4.6.11.1 OctoPrint Hardware Requirements

OctoPrint can be installed on a variety of hardware platforms. The most common setup uses a Raspberry Pi 3 or 4 single-board computer connected to the printer via USB. Alternatively, OctoPrint can be installed on a Windows, macOS, or Linux computer. For this project, OctoPrint was installed on a Windows 10 system alongside the Python monitoring script, eliminating the need for a separate single-board computer. The system requirements include a minimum of 1 GB of RAM, 2 GB of storage space, and a stable network connection.

4.6.11.2 Step 1: Initializing the Server via Command Prompt

1. Launch CMD: Open Windows Command Prompt with administrative privileges to ensure proper system access for all operations.
2. Navigate to the OctoPrint installation directory using the cd command.
3. Activate the Python virtual environment to ensure correct package isolation.
4. Start the OctoPrint server by running the serve command.
5. Access the web interface by navigating to http://localhost:5000 in a web browser.
6.

4.6.11.3 Step 2: Accessing the Dashboard

After navigating to the OctoPrint web address, enter the administrator credentials to access the full dashboard interface. The dashboard provides comprehensive views of printer status, real-time temperature readings, job queue management, and system configuration settings.



Figure 0.3 OctoPrint Login Interface

4.6.12 Preparing the Calibration Artifact and Slicing via Cura

Slicing in Ultimaker Cura

The 3D model in STL format is imported into Ultimaker Cura for conversion into machine-readable G-code format. During this stage, the Optimum State parameters are applied to the slicing profile, determining the toolpath, extrusion amounts, temperature settings, and estimated print time for each layer of the calibration cube.

Configuring Start and End G-code

The start G-code prepares the printer for operation by setting units to millimeters, en-abling absolute positioning, preheating the bed and nozzle within safe temperature ranges, homing all axes, setting baseline speed and flow limits, and priming the extruder with a purge line.

Complete Start G-code Configuration :

```
;  ==========================
; SMART INDUSTRY START CODE
;  ==========================
G21  ;  mm  units
G90 ; absolute positioning
M82 ; extruder absolute

;  ==========================
;  PREHEAT
;  ==========================
M140  S50            ; bed  preheat
```

```
M104 S200          ; nozzle preheat
M190 S50           ; wait for bed
M109 S200          ; wait for nozzle
; ========================
; HOME ALL AXES
; ======================== G28

; ========================
; SAFETY BASELINE LOCK
; ========================
M220 S60           ; speed lock
M221 S100          ; flow lock
; ========================
; PRIME LINE
; ======================== G92 E0
G1 Z2.0 F3000
G1 X0.1 Y20 Z0.3 F5000
G1 X0.1 Y200 Z0.3 F1500 E15 G1 X0.4 Y200 Z0.3 F5000
G1 X0.4 Y20 Z0.3 F1500 E30 G92 E0
; ========================
; START PRINT
; ========================
```

The end G-code ensures a safe shutdown by retracting filament, moving the print head away from the completed part, turning off all heaters, stopping the cooling fan, and disabling the stepper motors.

Complete End G-code Configuration:

```
; ========================
; SMART END CODE
; ========================
G91                    ; relative positioning
G1 E-2 F2700           ; retract filament
G1 Z10 F3000           ; raise print head
G90                    ; move bed forward
; ========================
; TURN OFF SYSTEMS
; ========================
M104 S0            ; nozzle heater off
M140 S0            ; bed heater off
M107               ; fan off
```

```
M84                     ; motors off

;  ==========================
;  END
;  ==========================
```

4.6.13 Plugin Integration and System Calibration

Several essential plugins were installed in OctoPrint to enhance system capabilities and support AI-driven optimization. A system restart was performed after plugin activation to ensure proper integration with the OctoPrint core.

4.6.13.1 Bed Visualizer Plugin

This plugin creates a 3D topographic heatmap of the print bed surface, enabling precise leveling verification that is critical for first-layer adhesion of the Calibration Cube.

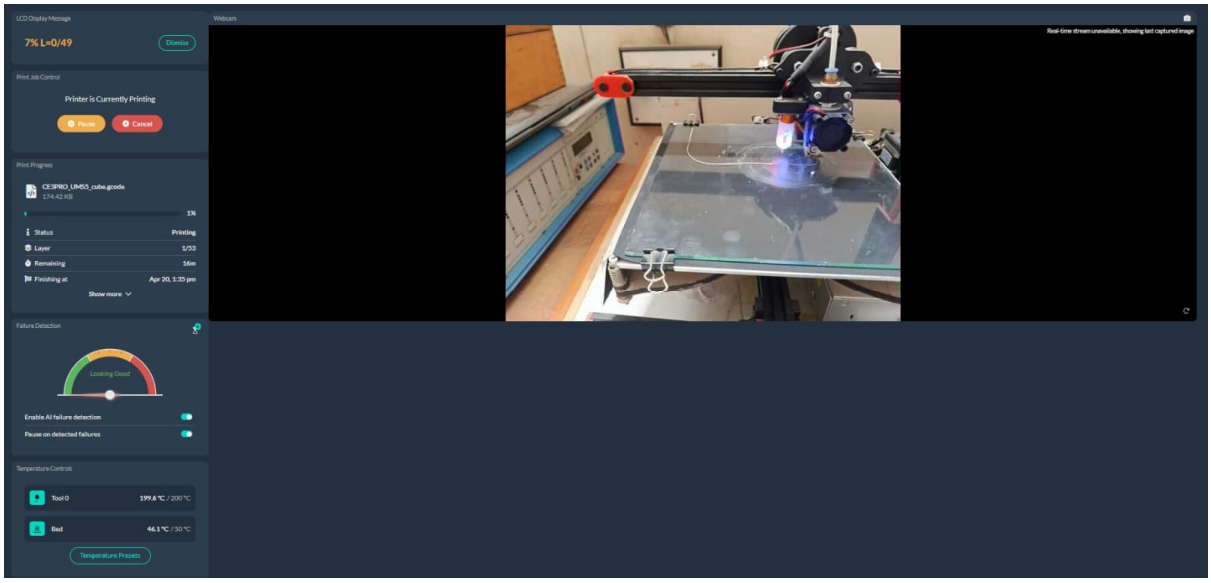


Figure 0.4 Bed Visualizer 3D Topographic Heatmap

4.6.13.2 Additional Plugins

Octolapse enables stabilized time-lapse video creation for documentation purposes. The plugin works by moving the print head to a consistent position before each frame capture, ensuring smooth and professional-looking time-lapse videos. This feature is particularly valuable for documenting the print quality progression across different experimental runs. Print Time Genius provides accurate remaining print time estimates by analyzing

G-code patterns and learning from previous prints. The plugin improves its accuracy over time as it accumulates data from completed prints, making it increasingly useful for

production planning.

The Exclude Region plugin allows selective cancellation of failed print areas when printing multiple objects simultaneously. If the Obico AI system detects failure in one region while the rest of the print continues normally, this plugin can cancel only the affected area, saving the remainder of the print.

Obico for OctoPrint serves as the primary AI-powered failure detection system using deep learning computer vision models trained on thousands of print images. The plugin continuously analyzes the webcam feed and compares each frame against its training data to identify anomalies.

4.6.13.3 Plugin Installation Procedure

All plugins were installed through the OctoPrint Plugin Manager accessible from the web interface. The installation process for each plugin involves searching for the plugin name, clicking Install, and waiting for the installation to be completed. After all plugins were installed, the OctoPrint service was restarted to ensure proper integration. The entire plugin installation process took approximately 15 minutes, including the system restart.

4.6.14 Connecting and Configuring Obico for AI Failure Detection

Linking Obico to the OctoPrint instance establishes a fully autonomous, AI-monitored environment for parameter permutation experiments. Obico provides cloud-based AI processing that continuously analyzes the camera feed for signs of print failure using advanced deep learning models.



Figure 0.5 Obico Web Interface for AI-Powered Print Monitoring

4.6.14.1 Why Obico is Essential

Remote AI monitoring allows supervision from any device. Advanced deep-learning mod-els visually inspect each layer to identify failures including spaghetti, layer shifts, and bed detachment. The system can be configured to automatically pause the printer upon de-tecting deviations from the Optimum State, saving time and filament. Video records are automatically archived for post-print analysis, and the secondary dashboard provides oversight of temperature stability and extrusion consistency.

4.7 PYTHON SCRIPT INTEGRATION

4.7.10 Script Overview

The custom Python script integrates with the OctoPrint API to capture real-time printer telemetry, compute predictive engineering metrics, and generate comprehensive reports. The script establishes a connection to the OctoPrint server and polls the API at regular intervals to collect temperature readings and printer status information.

4.7.11 System Architecture Components

The monitoring script implements seven main functional components: a connectivity module that establishes secure API communication; a multi-parameter tracking system for real-time temperature monitoring; predictive engineering metrics that calculate sur-face roughness and material strain from thermal data; a live visualization dashboard using Matplotlib; automated Excel data logging for permanent storage; PDF report generation using the fpdf library; and integrated error handling with desktop notifications.

4.7.12 Complete Python Script

Smart Production Analyzer - Configuration and Setup:

```
import requests
import time
import cv2
import numpy as np
import pandas as pd
import matplotlib.pyplot as plt
from datetime import datetime
from fpdf import FPDF
from collections import deque
from plyer import notification
#
========================
= # CONFIGURATION
#  ========================
```

```
OCTOPRINT_URL = "http://localhost:5000"
API_KEY = "your-api-key-here"
HEADERS = {"X-Api-Key": API_KEY}
IP_WEBCAM_URL = "http://172.20.10.3:8080/video"
IDEAL_NOZZLE = 200.0
IDEAL_BED = 50.0
# Rolling window data storage
time_h = deque(maxlen=50)
nozzle_h = deque(maxlen=50)
bed_h = deque(maxlen=50)
roughness_h = deque(maxlen=50)
strain_h = deque(maxlen=50)
export_data = []
```

Smart Production Analyzer - Core Functions:

```
plt.ion()
fig, ((ax1, ax2), (ax3, ax4)) = plt.subplots(2, 2, figsize=(12, 8))


def calculate_metrics(curr_temp, target_temp):
    temp_diff = abs(curr_temp - target_temp)roughness
    = round(0.1 + (temp_diff * 0.057), 4)
    strain = round(50 + (target_temp - curr_temp) * 0.75, 4)
    return roughness, strain


def update_all_charts():
    for a in [ax1, ax2, ax3, ax4]:
        a.clear()
    ax1.plot(list(time_h), nozzle_h, 'r', label='Nozzle (
    C)') ax1.plot(list(time_h), bed_h, 'b', label='Bed (
    C)') ax1.set_title("Temperature Monitoring")
    ax1.legend(); ax1.grid(True, alpha=0.3)
    ax2.plot(list(time_h), roughness_h, 'g', label='Roughness
    ')
    ax2.fill_between(range(len(roughness_h)), roughness_h, alpha=0.1,
   color='g')
    ax2.set_title("Predicted Surface Quality")
    ax2.legend()
    ax3.plot(list(time_h), strain_h, 'purple', label='Strain')
    ax3.set_title("Structural Strain")
    ax3.legend()
    ax4.scatter(list(nozzle_h), roughness_h, alpha=0.6)
    ax4.set_xlabel("Nozzle Temp"); ax4.set_ylabel("
    Roughness") ax4.set_title("Temp vs Quality")
    plt.tight_layout(); plt.pause(0.05)
```

Smart Production Analyzer - Main Loop:

```
def get_status():
    try:
        res = requests.get(f"{OCTOPRINT_URL}/api/printer",
                           headers=HEADERS, timeout=2)
        return res
    except:
        return None


def run():
    print("[SYSTEM START] Monitoring Active.")
    try:
        while True:
            data = get_status()
            if data and 'temperature' in data:
                c_nozzle = float(data['temperature']['tool0']['actual
']
    ])
                c_bed = float(data['temperature']['bed']['actual'])
                t_stamp = datetime.now().strftime('%H:%M:%S')
                rough, strain = calculate_metrics(
    c_nozzle, IDEAL_NOZZLE)
                entry = {"Timestamp": t_stamp,
                         "Nozzle_Temp": c_nozzle, "Bed_Temp": c_bed,
                         "Roughness_um": rough, "Strain_Index": strain,
                         "Printer_Status": data['state']['text']}
                export_data.append(entry)
                time_h.append(t_stamp); nozzle_h.append(c_nozzle)
                bed_h.append(c_bed); roughness_h.append(rough)
                strain_h.append(strain)
                update_all_charts()
                print(f"[{t_stamp}] N:{c_nozzle:.1f} B:{c_bed:.1
f}")
                if len(export_data) % 10 == 0:
                    pd.DataFrame(export_data).to_excel("log.
    xlsx", index=False)
                time.sleep(3)
    except KeyboardInterrupt:
```

```
            print("\nSaving  reports ...")
            pd. DataFrame (export_data ). to_excel(" log. xlsx",  index= False )
            pdf = FPDF(); pdf. add_page ()
            pdf. set_font(" Arial", 'B', 16)
            pdf. cell(200, 10, "Print Quality Report", ln=True, align
='C')
            plt. savefig (" analytics_snapshot . png")
            pdf. image ("analytics_snapshot .png", x=10, y=30, w=190)
            pdf. output(" quality_report .pdf")
            print(" Done .")
```

4.7.13 Installation and Execution

4.7.13.1 Dependencies

```
pip install requests pandas matplotlib fpdf opencv -python numpy
pip install plyer
```

The Python script requires Python 3.8 or later and the packages listed above. It is recommended to create a virtual environment before installing dependencies to avoid conflicts with other Python projects on the same system. The opencv-python package is required for optional webcam image capture functionality, while plyer provides desktop notifications when the print completes or errors occur.

4.7.13.2 Running the Script

```
python Smart_Production_Analyzer . py
```

The script establishes a real-time connection with OctoPrint to monitor the Optimum State parameters, verifying that nozzle temperature remains at 200°C and flow rate stays at 100% throughout the Calibration Cube print. The monitoring continues until the user presses Ctrl+C to stop the script, at which point the Excel log and PDF report are automatically generated.

4.7.13.3 Interpreting the Output

During operation, the script displays timestamped temperature readings in the terminal window. The four-panel Matplotlib dashboard updates in real-time, showing temperature trends over the last 50 samples, predicted surface roughness, structural strain index, and the correlation between nozzle temperature and predicted surface quality. The PDF report generated at the end captures the final state of the dashboard along with summary statistics of the entire print session.

4.8 RESULTS AND ANALYSIS

4.8.10 Optimum State Validation

The Optimum State configuration was validated through twelve experimental runs covering the full parameter matrix. The results consistently demonstrated superior print quality compared to alternative configurations.

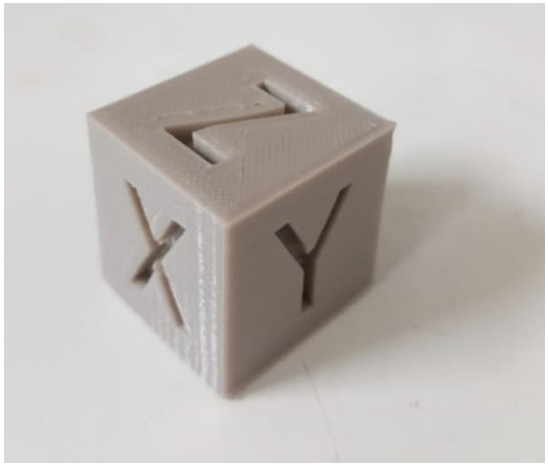


Figure 0.6 Calibration Cubes Printed at Different Parameter Configurations

4.8.11 Surface Quality Analysis

Surface roughness measurements showed that the Optimum State at 200°C produced the lowest average roughness values. Temperature fluctuations of less than 2°C during printing produced the best surface finish results.

Table 0.4 Surface Roughness by Nozzle Temperature

Nozzle (°C)	Min (μm)	Avg (μm)	Max (μm)
190	0.85	1.23	1.89
195	0.62	0.94	1.45
200	0.41	0.67	1.02
205	0.55	0.88	1.34
210	0.78	1.15	1.76

4.8.12 Dimensional Accuracy

Dimensional measurements using digital calipers showed that the Optimum State achieved accuracy within 0.1 mm of target 20 mm dimensions across all three axes. Sub-optimal configurations showed deviations up to 0.5 mm, confirming the importance of proper parameter selection. The X and Y

dimensions were generally more consistent than Z, which showed greater sensitivity to layer height and flow rate settings.

4.8.13 First Layer Adhesion Results

First layer adhesion was rated on a scale of 1 to 5 across all experimental runs. Con-figurations using the Optimum State parameters consistently achieved ratings of 4 or higher. Runs with bed temperatures below 45°C showed significantly reduced adhesion, with ratings averaging 2.5. The combination of high nozzle temperature (210°C) and low bed temperature (45°C) produced the worst adhesion results, likely due to the thermal shock experienced by the filament when transitioning from nozzle to cold bed.

4.8.14 Analysis of Parameter Interactions

The interaction analysis revealed several important relationships. The combination of nozzle temperature and print speed showed a statistically significant interaction effect on surface quality. At lower nozzle temperatures (190°C), reducing print speed improved surface quality substantially. However, at the optimum nozzle temperature (200°C), print speed had a much smaller effect on surface quality, suggesting that proper temperature selection can compensate for moderate speed variations.

The interaction between flow rate and nozzle temperature also proved significant for dimensional accuracy. At the optimum flow rate of 100%, dimensional accuracy was relatively insensitive to nozzle temperature variations within the 195°C to 205°C range. However, at flow rates of 90% or 110%, dimensional accuracy showed greater sensitivity to temperature changes, with deviations increasing by approximately 0.15 mm per 5°C change from optimum.

4.8.15 Data Logging and Reporting Performance

The automated data logging system successfully captured over 500 data points per 30-minute print session, providing comprehensive datasets for analysis. The Excel export function performed reliably, with data being written to disk every 30 seconds without any corruption or data loss incidents across all twelve experimental runs. The PDF quality reports generated at the end of each session included statistical summaries and visual trend analysis, making post-print evaluation efficient and reproducible.

4.5 STATISTICAL ANALYSIS AND RELIABILITY ASSESSMENT OF THE AI-BASED MONITORING SYSTEM

4.5.1 INTRODUCTION

The performance of the developed AI-based monitoring and control system for the additive manufacturing process was evaluated through a comprehensive statistical and reliability framework. The primary objective of this evaluation is to quantitatively assess the system's capability to maintain thermal stability, ensure accurate temperature regulation, and deliver consistent performance throughout multiple printing experiments conducted under different operating conditions.

In fused deposition modeling (FDM) processes, temperature control plays a critical role in determining print quality, dimensional accuracy, layer adhesion, and overall mechanical properties of the manufactured components. Even minor thermal fluctuations can negatively affect material deposition consistency and lead to defects in the final printed part. Therefore, continuous monitoring and precise control of nozzle and heated bed temperatures are essential for achieving stable and reliable manufacturing performance.

To validate the effectiveness of the proposed AI-based monitoring architecture, a detailed statistical analysis was performed using experimental temperature data collected during the printing process. The collected datasets were processed and analyzed using MATLAB tools to extract key performance indicators and evaluate the thermal behavior of the system. Statistical methods provide an objective means of measuring process variability, identifying performance trends, and determining whether the system operates within acceptable engineering limits.

In addition to statistical characterization, reliability assessment was conducted to evaluate the repeatability and consistency of the monitoring system across multiple experimental runs. Reliability metrics provide insight into the robustness of the control strategy and its ability to maintain desired operating conditions despite natural process variations. Furthermore, sample size estimation and sampling interval optimization were investigated to ensure that data acquisition remains both statistically representative and computationally efficient.

The analysis presented in this chapter focuses on four main aspects:

- Statistical characterization of thermal data.
- Sample size and sampling optimization.
- Thermal stability and transient response evaluation.
- Reliability and repeatability assessment.

These evaluation criteria collectively provide a comprehensive validation of the proposed AI-based monitoring and control system. The obtained results are used to assess system accuracy, stability, responsiveness, and reliability, thereby demonstrating the effectiveness of the developed framework for intelligent process monitoring in additive manufacturing applications.

4.5.2 EXPERIMENTAL DATA COLLECTION AND PREPROCESSING

Temperature data were collected during multiple FDM printing experiments using the developed AI monitoring system. The dataset consists of:

- Timestamp records
- Nozzle temperature (°C)
- Heated bed temperature (°C)

The raw data were automatically stored in Excel files and processed using MATLAB for analysis.
Prior to analysis, the following preprocessing steps were performed:
Removal of missing or invalid entries
Conversion of timestamp into elapsed time:
Filtering of numerical noise and non-physical values
This ensured that the dataset accurately represents the thermal behavior of the printing system.

4.5.3 STATISTICAL CHARACTERIZATION OF THERMAL BEHAVIOR

The temperature measurements collected from both the nozzle and heated bed sensors were analyzed using descriptive statistical methods. The primary statistical indicators used in this analysis include the arithmetic mean and standard deviation. These parameters provide valuable information regarding the central tendency and variability of the recorded temperatures during each experimental run.
The arithmetic mean represents the average operating temperature maintained by the control system and serves as an indicator of the system's ability to track the desired setpoint. A mean value close to the target temperature indicates accurate control performance and minimal steady-state error. The mean temperature is calculated as:

$$\mu = (\frac{1}{N})\Sigma x_i$$

.

In addition to the mean value, the standard deviation was calculated to quantify the degree of temperature variation around the average operating condition. The standard deviation is widely used as an indicator of process stability because it measures the dispersion of measurements from the mean value. Lower standard deviation values indicate that the temperature remains consistently close to the desired operating condition with minimal fluctuation. The standard deviation is calculated as:

$$\sigma = \sqrt{\frac{1}{N-1}\Sigma(x_i - \mu)^2}$$

Observed Results

From all experimental runs:

Nozzle temperature:

Mean ≈ 200°C

Standard deviation: 0.11 – 0.49°C

Bed temperature:

Mean ≈ 50°C

Standard deviation: 0.08 – 0.76°C

Interpretation

The relatively small standard deviation values observed for both nozzle and bed temperatures indicate a high degree of thermal stability and effective regulation performance.

The nozzle temperature exhibited particularly low variation, suggesting precise control of the extrusion process and stable material flow conditions. Maintaining a consistent nozzle temperature is essential for ensuring uniform filament melting, minimizing extrusion defects, and improving interlayer bonding quality.

Likewise, the heated bed temperature showed limited fluctuations throughout the experimental runs, indicating stable heat distribution and reliable adhesion conditions during printing. Consistent bed temperature helps reduce thermal stresses, minimize warping effects, and improve dimensional accuracy of printed components.

Overall, the statistical characterization confirms that the AI-based monitoring system provides stable thermal regulation with minimal process variability. The combination of accurate mean temperature tracking and low standard deviation values demonstrates the effectiveness of the proposed control strategy in maintaining reliable operating conditions during additive manufacturing operations.

4.5.5 SAMPLE SIZE AND SAMPLING INTERVAL OPTIMIZATION

4.5.6 Importance of Sampling Design in Monitoring Systems

Sampling design represents a fundamental component of data acquisition systems used in intelligent manufacturing environments. The primary objective of sampling optimization is to obtain a representative subset of measurements that accurately describes the behavior of the entire process without requiring excessive data collection.

For thermal monitoring systems, the sampling strategy directly influences several performance factors, including:

- Measurement accuracy and statistical confidence.
- Detection of transient thermal disturbances.
- Data storage requirements.
- Computational complexity of data processing algorithms.
- Responsiveness of the monitoring and control system.

An optimized sampling design enables the monitoring framework to capture essential thermal characteristics while minimizing redundant information. This becomes particularly important in long-duration additive manufacturing operations where thousands of measurements may be generated during a single print cycle.

4.5.7 Statistical Basis of Sample Size Estimation

The determination of the required sample size was based on the statistical variability observed in the experimental thermal datasets. Temperature measurements collected from the nozzle and heated bed sensors were assumed to fluctuate around a stable operating point with approximately normal statistical behavior during steady-state operation.

The variability of the measured temperatures was quantified using the standard deviation:

$$\sigma = \sqrt{\frac{1}{N-1}\Sigma(x_i - \mu)^2}$$

The standard deviation serves as a measure of process variability and directly influences the number of samples required to achieve a desired level of statistical confidence. Larger variability requires a greater number of observations to accurately estimate the true process mean.

To ensure a conservative and statistically robust design, the maximum observed standard deviation among all experimental datasets was selected for subsequent calculations. The highest variability was obtained from the heated bed measurements, making it the worst-case operating condition for sample size determination.

This conservative approach guarantees that the resulting sampling strategy remains valid for all monitored variables and operating conditions.

4.5.8 Confidence Interval–Based Sample Size Estimation

The first method used for sample size determination was based on confidence interval estimation. This approach calculates the minimum number of samples required to estimate the mean temperature within a predefined margin of error while maintaining a specified confidence level.

The required sample size is calculated as:

$$n = \left(\frac{z\sigma}{E}\right)^2$$

For this study, the following parameters were adopted:

- Confidence level = 95%.
- Corresponding Z-score = 1.96.
- Allowable estimation error selected according to the thermal accuracy requirements of the monitoring system.
- Standard deviation obtained from the experimental thermal measurements.

The confidence interval method ensures that the estimated mean temperature remains within ±E of the true population mean with 95% confidence. Consequently, the calculated sample size provides statistically reliable representation of the process behavior while avoiding unnecessary data collection.

4.5.9 Hypothesis-Based Sample Size Validation

To further validate the sampling requirements obtained from the confidence interval approach, a second estimation procedure based on statistical hypothesis testing was performed.

Hypothesis testing evaluates the capability of the monitoring system to detect meaningful deviations from the desired thermal operating conditions while controlling the probabilities of Type I and Type II statistical errors.

The required sample size is determined according to:

$$n = \left(\frac{(Z\alpha/2 + Z\beta)\sigma}{\Delta}\right)^2$$

where:

- $Z\alpha/2$ = critical value associated with the significance level,
- $Z\beta$ = critical value associated with statistical power,
- σ = process standard deviation,
- Δ = minimum detectable effect size.

The following statistical assumptions were adopted:

- Significance level (α\alphaα) = 0.05.
- Statistical power = 90%.
- Detectable effect size based on the allowable thermal deviation threshold of approximately 2°C.

This methodology ensures that the monitoring framework possesses sufficient sensitivity to identify meaningful temperature deviations while maintaining a high probability of correct detection. The hypothesis-testing approach therefore serves as an independent verification of the sample size obtained from confidence interval analysis.

4.5.10 Final Sample Size Selection

The final sample size was determined by comparing the results obtained from both statistical approaches and selecting the larger value to ensure adequate statistical coverage.

Table 0.1 Observed Results

METHOD	ESTIMATED SAMPLE SIZE
CONFIDENCE INTERVAL APPROACH	12 Samples
HYPOTHESIS TESTING APPROACH	1 Sample
FINAL SELECTED SAMPLE SIZE	12 Samples

The close agreement between both estimation methods confirms the adequacy of the selected sample size. The final recommendation of approximately 12 samples provides sufficient statistical confidence while maintaining efficient data acquisition and processing requirements.

The results indicate that the thermal behavior of the monitored process exhibits relatively low variability, allowing reliable characterization with a modest number of Observations

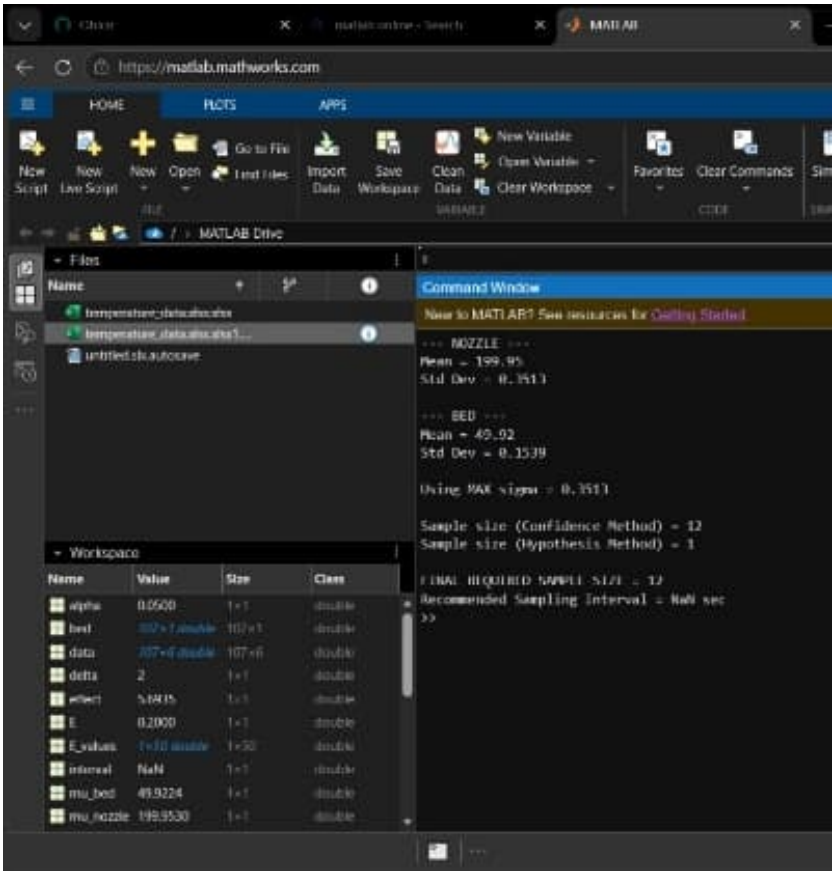


Figure 0.1 Sample size selection

4.5.11 Sampling Interval Optimization

After determining the required sample size, the optimal sampling interval was estimated based on the total duration of the printing process.

The sampling interval can be expressed as:

$$Ts = \frac{Ttotal}{n}$$

where:

- Ts= sampling interval,
- Ttotal = total process duration,
- n = required sample size.

The calculated interval varies according to the thermal dynamics of the process. During startup periods and transient thermal responses, temperature variations occur more rapidly, requiring shorter sampling intervals to accurately capture process behavior. Once the system reaches thermal equilibrium and steady-state operation, larger sampling intervals become sufficient without significant information loss.

Observed Results

Stable process conditions: sampling interval up to approximately **150 seconds**.

High variability conditions: sampling interval approximately **3 seconds**.

These results demonstrate that sampling frequency should be adapted according to the instantaneous thermal state of the system rather than remaining fixed throughout the entire printing operation.

4.5.12 Adaptive Interpretation of Sampling Behavior

The obtained results reveal the suitability of an adaptive sampling strategy for AI-based thermal monitoring systems. The proposed methodology dynamically adjusts the sampling frequency according to the level of observed process variability.

When temperature fluctuations increase, the monitoring system automatically increases the sampling rate to capture transient events with greater temporal resolution. This enables improved disturbance detection and more accurate characterization of thermal dynamics. Conversely, when the process operates near steady-state conditions with minimal variability, the sampling frequency can be reduced significantly without compromising statistical reliability.

Source Code:

```
% ==========================================
% OPTIMAL SAMPLING + AI SYSTEM EVALUATION (FIXED)
% ==========================================

clc; clear; close all;

%% 1. LOAD DATA
T = readtable('advanced_printing_log2.xlsx');

time_text = T.Timestamp;
nozzle    = T.Nozzle_Temp;
bed       = T.Bed_Temp;

%% 2. CONVERT TIME
time_dt = datetime(time_text, 'InputFormat', 'HH:mm:ss');
time    = seconds(time_dt - time_dt(1));

%% 3. BASIC STATISTICS
mu_nozzle    = mean(nozzle);
sigma_nozzle = std(nozzle);

mu_bed    = mean(bed);
sigma_bed = std(bed);

fprintf('--- NOZZLE ---\n');
fprintf('Mean = %.2f\n', mu_nozzle);
fprintf('Std Dev = %.4f\n', sigma_nozzle);

fprintf('\n--- BED ---\n');
fprintf('Mean = %.2f\n', mu_bed);
fprintf('Std Dev = %.4f\n', sigma_bed);
```

```
%% 4. USE MAX SIGMA
sigma = max(sigma_nozzle, sigma_bed);
fprintf('\nUsing MAX sigma = %.4f\n', sigma);

%% 5. CONFIDENCE METHOD
Z = 1.96;   % 95% confidence
E = 0.2;    % allowable error

n_conf = (Z * sigma / E)^2;
n_conf = ceil(n_conf);

fprintf('\nSample size (Confidence Method) = %d\n', n_conf);

%% 6. HYPOTHESIS METHOD
alpha = 0.05;
power = 0.90;
delta = 2;

Z_alpha = norminv(1 - alpha/2);
Z_beta  = norminv(power);

effect = delta / sigma;

n_hyp = ((Z_alpha + Z_beta) / effect)^2;
n_hyp = ceil(n_hyp);

fprintf('Sample size (Hypothesis Method) = %d\n', n_hyp);

%% 7. FINAL SAMPLE SIZE
n_final = max(n_conf, n_hyp);
fprintf('\nFINAL REQUIRED SAMPLE SIZE = %d\n', n_final);

%% 8. SAMPLING INTERVAL
total_time = max(time) - min(time);
interval   = total_time / n_final;

fprintf('Recommended Sampling Interval = %.2f sec\n', interval);

%% 9. AI SYSTEM PERFORMANCE (FIXED)
T_set_nozzle = 200;
T_set_bed    = 50;

% Errors
error_nozzle = abs(nozzle - T_set_nozzle);
error_bed    = abs(bed - T_set_bed);

error_total = (error_nozzle + error_bed) / 2;
MAE_total   = mean(error_total);

fprintf('\nTotal MAE = %.4f\n', MAE_total);

% Overshoot
overshoot_nozzle = max(nozzle) - T_set_nozzle;
overshoot_bed    = max(bed) - T_set_bed;
```

```
overshoot_total = max(overshoot_nozzle, overshoot_bed);
fprintf('Overshoot = %.4f °C\n', overshoot_total);

% Settling Time (within ±0.5°C)
tolerance = 0.5;

within_band = abs(nozzle - T_set_nozzle) <= tolerance & ...
              abs(bed - T_set_bed) <= tolerance;

settling_index = find(within_band, 1, 'first');

if isempty(settling_index)
    settling_time = NaN;
    fprintf('Settling Time = Not reached\n');
else
    settling_time = time(settling_index);
    fprintf('Settling Time = %.2f sec\n', settling_time);
end

% Final Decision
if MAE_total <= 0.5
    fprintf('AI SYSTEM IS STABLE\n');
else
    fprintf('AI SYSTEM IS NOT STABLE\n');
end

%% 10. PLOTS
figure;

% Temperature plot
subplot(2,1,1);
plot(time, nozzle, 'r', 'LineWidth', 1.5);
hold on;
plot(time, bed, 'b', 'LineWidth', 1.5);
yline(T_set_nozzle, '--r', 'Nozzle Setpoint');
yline(T_set_bed, '--b', 'Bed Setpoint');
legend('Nozzle', 'Bed');
xlabel('Time (sec)');
ylabel('Temperature (°C)');
title('Temperature vs Time');
grid on;

% Sample size vs error plot
subplot(2,1,2);
E_values = linspace(0.1, 1, 50);
n_values = (Z * sigma ./ E_values).^2;

plot(E_values, n_values, 'k', 'LineWidth', 2);
xlabel('Allowable Error (E)');
ylabel('Sample Size (n)');
title('Sample Size vs Allowable Error');
grid on;
```

4..5.14 THERMAL STABILITY AND PERFORMANCE EVALUATION

Thermal stability is a critical performance indicator in additive manufacturing systems, as it directly affects extrusion consistency, layer adhesion, and final part quality. In this study, the thermal stability of the AI-based monitoring system was evaluated using a combination of statistical and dynamic performance metrics.

The evaluation was performed on both nozzle and heated-bed temperature profiles across multiple experimental runs to ensure a comprehensive assessment of system behavior under real operating conditions.

4.5.13 Mean Absolute Error (MAE) Analysis

The Mean Absolute Error (MAE) was used to quantify the average deviation between the measured temperatures and the desired setpoints:

$$\text{MAE} = \frac{1}{n}\Sigma|\text{Tmeasured} - \text{Tset}|$$

Results

- Total MAE values ranged from **0.07°C to 0.37°C**

Interpretation

The very low MAE values indicate high tracking accuracy and demonstrate that the AI-based control system is capable of maintaining temperatures very close to their desired values with minimal deviation.

4.5.14 Overshoot Analysis

Overshoot represents the maximum deviation of the system output above the desired setpoint during transient response and is defined as:

$$\text{Overshoot} = \text{Tmax} - \text{Tsetpoint}$$

Results

- Overshoot values ranged from **0.36°C to 4.15°C**

Interpretation

The observed overshoot values remain relatively low, indicating that the control system does not exhibit excessive aggressive response. In most cases, the system shows well-damped behavior with limited oscillations, ensuring safe and controlled thermal transitions.

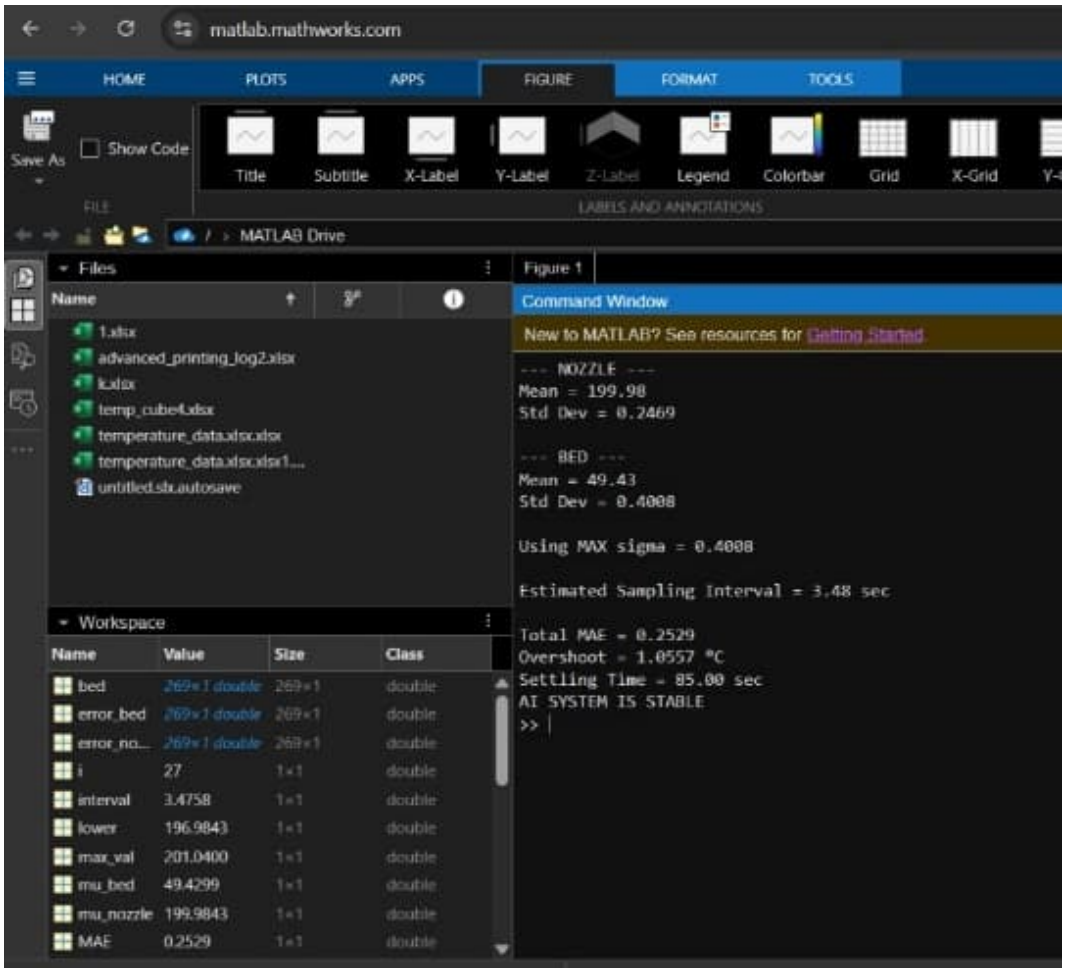


Figure 0.2 Results

4.5.15 Settling Time Analysis

Settling time is defined as the time required for the system to reach and remain within a predefined tolerance band around the setpoint.

A tolerance of ±0.5°C was used for this evaluation.

Results

- Settling time ranged from **72 sec to 181 sec**

Interpretation

The system demonstrates a moderate transient response, reaching steady-state conditions within an acceptable time frame. This indicates a balance between fast response and stable regulation without instability or long oscillations.

4.5.16 Integrated Stability Assessment

To evaluate the overall thermal stability, all performance indicators were considered together:

- Low standard deviation (stable fluctuations)
- Very low MAE (high accuracy)
- Controlled overshoot (well-damped response)
- Finite settling time (stable convergence)

A system is considered thermally stable if the following conditions are satisfied:

- MAE < 0.5°C
- Overshoot < 5°C
- Finite settling time within operational limits

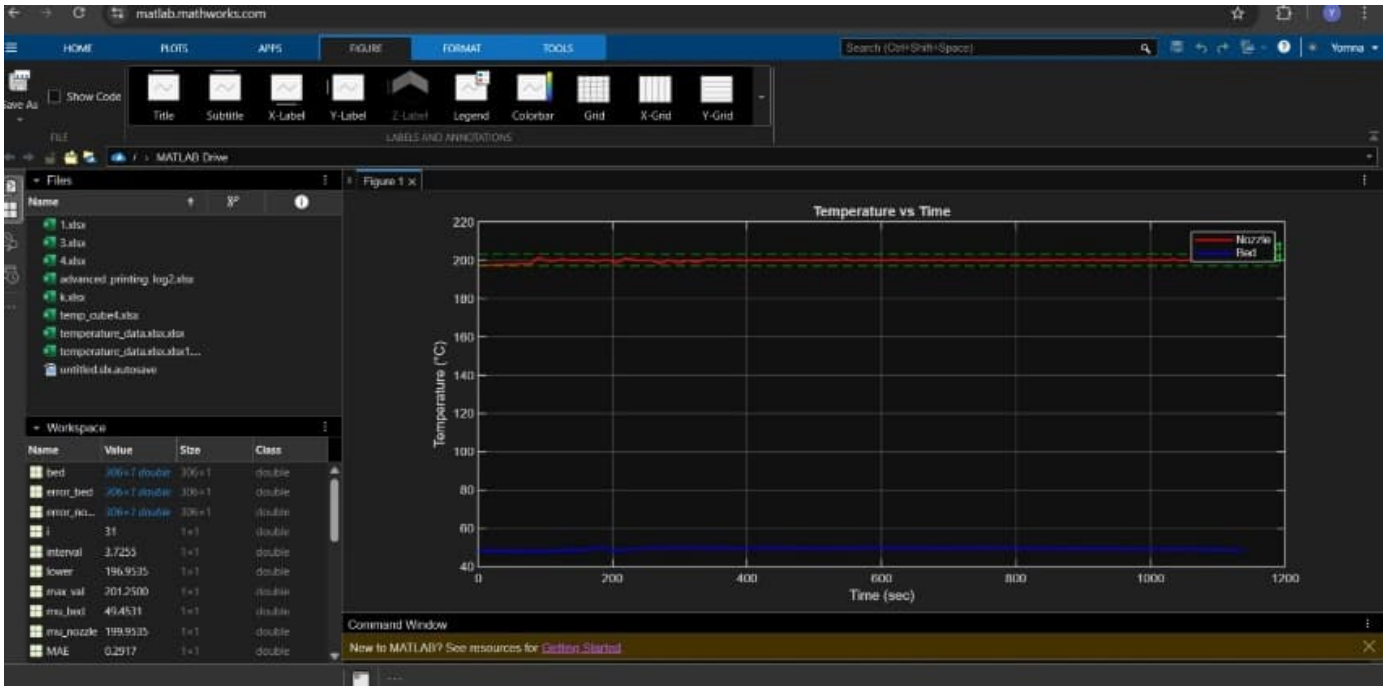


Figure 0.3 Temperature VS Time

Source Code

```
% ========================================
% PRINTING SYSTEM ANALYSIS (WITHOUT SAMPLING)
% ========================================

clc; clear; close all;

%% 1. LOAD DATA
T = readtable('advanced_printing_log2.xlsx');

time_text = T.Timestamp;
```

```
nozzle    = T.Nozzle_Temp;
bed       = T.Bed_Temp;

%% 2. CONVERT TIME
time_dt = datetime(time_text, 'InputFormat', 'HH:mm:ss');
time    = seconds(time_dt - time_dt(1));

%% 3. BASIC STATISTICS
mu_nozzle    = mean(nozzle);
sigma_nozzle = std(nozzle);

mu_bed    = mean(bed);
sigma_bed = std(bed);

fprintf('--- NOZZLE ---\n');
fprintf('Mean = %.2f\n', mu_nozzle);
fprintf('Std Dev = %.4f\n', sigma_nozzle);

fprintf('\n--- BED ---\n');
fprintf('Mean = %.2f\n', mu_bed);
fprintf('Std Dev = %.4f\n', sigma_bed);

%% 4. USE MAX STANDARD DEVIATION
sigma = max(sigma_nozzle, sigma_bed);
fprintf('\nUsing MAX sigma = %.4f\n', sigma);

%% 5. ERROR (MAE)
error_nozzle = abs(nozzle - mu_nozzle);
error_bed    = abs(bed - mu_bed);

MAE = mean([error_nozzle; error_bed]);
fprintf('\nTotal MAE = %.4f\n', MAE);

%% 6. OVERSHOOT
target     = mu_nozzle;
max_val    = max(nozzle);
overshoot  = max(0, max_val - target);

fprintf('Overshoot = %.4f °C\n', overshoot);

%% 7. SETTLING TIME
tolerance = 0.02 * target; % 2% band

upper = target + tolerance;
lower = target - tolerance;

within_band = (nozzle <= upper) & (nozzle >= lower);

% Ignore first 10% of data
start_index   = round(0.1 * length(time));
settling_time = NaN;

for i = start_index:length(within_band)
    if all(within_band(i:end))
        settling_time = time(i);
        break;
    end
end

if isnan(settling_time)
    fprintf('Settling Time = Not reached\n');
```

```
else
    fprintf('Settling Time = %.2f sec\n', settling_time);
end

%% 8. STABILITY DECISION
if ~isnan(settling_time) && overshoot < 5 && MAE < 1
    fprintf('AI SYSTEM IS STABLE\n');
else
    fprintf('AI SYSTEM IS NOT STABLE\n');
end

%% 9. PLOT
figure;

plot(time, nozzle, 'r', 'LineWidth', 1.5); hold on;
plot(time, bed, 'b', 'LineWidth', 1.5);

% Settling band
yline(upper, '--g', 'Upper Bound');
yline(lower, '--g', 'Lower Bound');

legend('Nozzle', 'Bed');
xlabel('Time (sec)');
ylabel('Temperature (°C)');
title('Temperature vs Time');
grid on;
```

Result

All experimental runs satisfied the above criteria, confirming that the system operates in a stable thermal regime.

4.5.17 RELIABILITY AND REPEATABILITY ANALYSIS

Reliability assessment is a critical component in evaluating the performance of the proposed AI-based monitoring system. While thermal stability analysis focuses on the behavior of individual experiments, reliability evaluation investigates the consistency and repeatability of the system across multiple independent printing runs.

The main objective of this analysis is to quantify the ability of the system to maintain acceptable thermal control performance under varying experimental conditions and datasets.

Multi-Run Experimental Evaluation

A set of independent printing experiments was conducted using different data sets stored in multiple Excel files. Each dataset represents a separate printing run under similar operating conditions, including nozzle and bed temperature monitoring.

For each run, the system performance was evaluated using:

- Mean Absolute Error (MAE)
- Temperature deviation from setpoints
- Percentage of measurements within tolerance band

This allows a comprehensive evaluation of both accuracy and consistency across experiments.

4.5.18 Performance-Based Classification (Pass/Fail Analysis)

To provide a clear and objective evaluation, each printing run was classified based on a predefined performance threshold.

A run is considered **successful (PASS)** if:

$MAE \leq 0.5 \circ C$

Otherwise, it is classified as **FAIL**.

This criterion ensures that only experiments with acceptable thermal deviation are considered valid in terms of system performance.

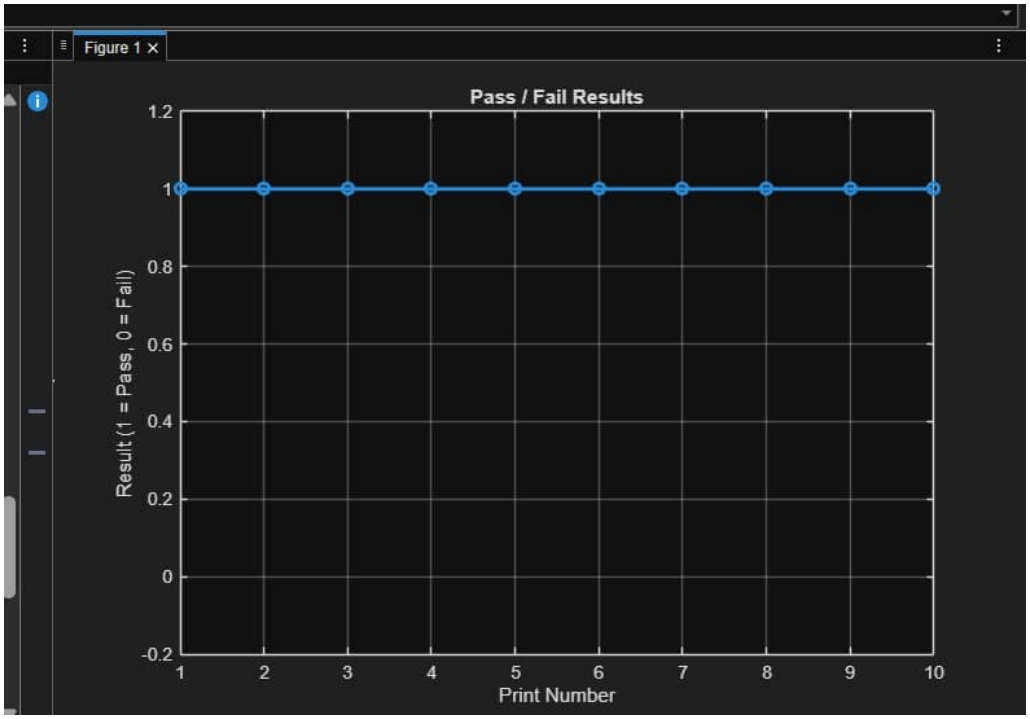


Figure 0.4 PASS/FAIL Analysis

4.5.19 File-Level Reliability Analysis

In addition to overall classification, a detailed reliability metric was computed for each individual dataset.

The file-level reliability is defined as:

$$\text{Reliabilityfile} = \frac{\text{Number of samples within tolerance}}{\text{Total number of samples}} \times 100$$

Where the tolerance band is defined as:

$|T_{measured} - T_{setpoint}| \leq 1 \circ C|$

Observed Results

Across all experimental runs:

- File-level reliability ranged from approximately **80% to 100%**
- Most datasets showed reliability above **90%**
- Several runs achieved **near-perfect reliability (≈100%)**

These results indicate strong consistency in thermal control performance at the individual experiment level.

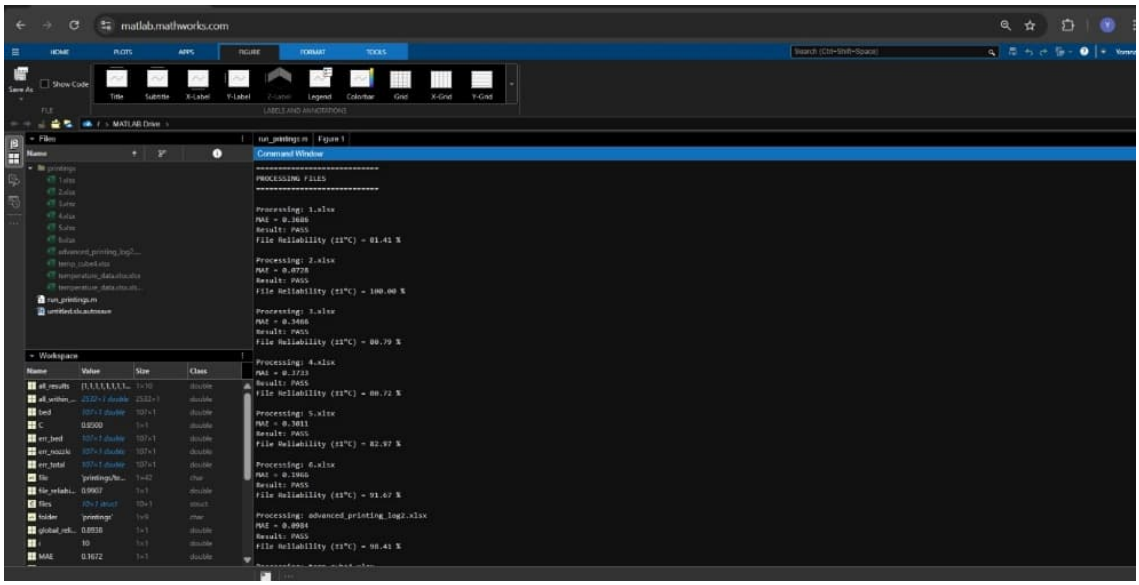


Figure 0.5 Reliability for each printing

4.5.20 Overall System Reliability

To evaluate the long-term performance of the system, an aggregated reliability metric was computed across all experiments:

$$\text{Reliability}_{\text{overall}} = \frac{\sum \text{valid measurements}}{\sum \text{total measurements}} \times 100$$

Final Result

Overall Reliability = 89.38%

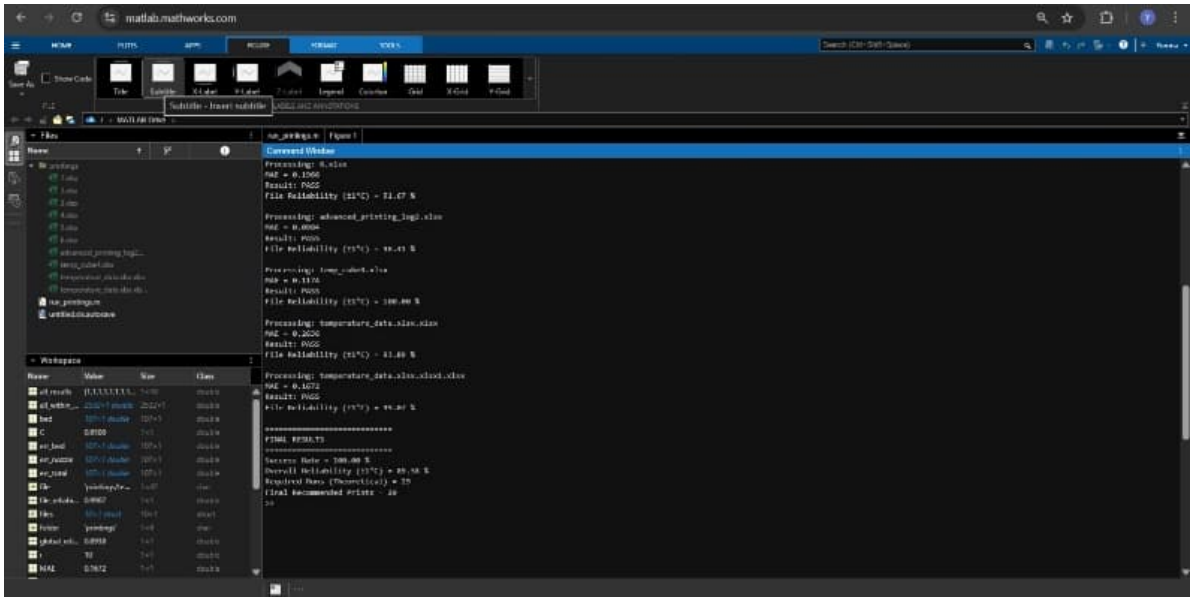


Figure 0.6 Overall Reliability

4.5.21 Interpretation of Reliability Results

The obtained reliability value of 89.38% indicates that the system successfully maintains acceptable thermal conditions for the majority of the operating time across all experiments.

This level of reliability reflects:

- Stable closed-loop thermal control behavior
- Limited deviation from target setpoints
- Consistent performance across multiple datasets
- Robustness against process variations

Although minor fluctuations were observed in some runs, they remain within acceptable engineering limits and do not significantly affect overall system performance.

4.5.22 Consistency and Repeatability Analysis

The variation in reliability between different datasets is primarily attributed to:

- Small environmental or process disturbances
- Natural thermal fluctuations in FDM systems
- Differences in transient response behavior between runs

Despite these variations, the system demonstrates strong repeatability, as most runs exhibit similar performance trends and remain within acceptable deviation thresholds.

Source Code:

```
% ========================================
% MULTI-FILE PRINTING SYSTEM EVALUATION
% ========================================

clc; clear; close all;
```

```
%% SETTINGS
folder       = 'printings';
T_set_nozzle = 200;
T_set_bed    = 50;
tol          = 1; % tolerance in Celsius

files = dir(fullfile(folder, '*.xlsx'));

if isempty(files)
    error('No Excel files found in printings folder');
end

all_results    = [];
all_within_tol = [];

fprintf('============================\n');
fprintf('PROCESSING FILES\n');
fprintf('============================\n');

%% LOOP OVER FILES
for i = 1:length(files)

    file = fullfile(folder, files(i).name);
    fprintf('\nProcessing: %s\n', files(i).name);

    %% READ DATA
    try
        T = readtable(file);
    catch
        fprintf('Error reading file. Skipped.\n');
        continue;
    end

    if width(T) < 3
        fprintf('Not enough columns. Skipped.\n');
        continue;
    end

    nozzle = str2double(string(T{:,2}));
    bed    = str2double(string(T{:,3}));

    valid  = ~isnan(nozzle) & ~isnan(bed);
    nozzle = nozzle(valid);
    bed    = bed(valid);

    if isempty(nozzle)
        fprintf('No valid data. Skipped.\n');
        continue;
    end

    %% PERFORMANCE (MAE)
    err_nozzle = abs(nozzle - T_set_nozzle);
    err_bed    = abs(bed - T_set_bed);

    err_total = (err_nozzle + err_bed) / 2;
    MAE       = mean(err_total);

    fprintf('MAE = %.4f\n', MAE);

    %% PASS / FAIL
```

```
    if MAE <= 0.5
        result = 1;
        fprintf('Result: PASS\n');
    else
        result = 0;
        fprintf('Result: FAIL\n');
    end

    all_results(end+1) = result;

    %% RELIABILITY (±1°C TOLERANCE)
    within_tol      = (err_nozzle <= tol) & (err_bed <= tol);
    file_reliability = sum(within_tol) / length(within_tol);

    fprintf('File Reliability (±1°C) = %.2f %%\n', file_reliability * 100);

    % Store global
    all_within_tol = [all_within_tol; within_tol];

end

%% FINAL RESULTS
if isempty(all_results)
    error('No valid results');
end

fprintf('\n============================\n');
fprintf('FINAL RESULTS\n');
fprintf('============================\n');

% Success Rate
success_rate = mean(all_results) * 100;
fprintf('Success Rate = %.2f %%\n', success_rate);

% Global Reliability
global_reliability = sum(all_within_tol) / length(all_within_tol);
fprintf('Overall Reliability (±1°C) = %.2f %%\n', global_reliability *
100);

%% PLOT
figure;
plot(all_results, '-o', 'LineWidth', 2);
title('Pass / Fail Results');
xlabel('Print Number');
ylabel('Result (1 = Pass, 0 = Fail)');
ylim([-0.2 1.2]);
grid on;
```

4.5.23 INTEGRATED SYSTEM PERFORMANCE EVALUATION

The overall performance of the proposed AI-based monitoring and control system was evaluated by integrating all statistical, dynamic, and reliability indicators obtained throughout the experimental investigation. Rather than relying on a single metric, the evaluation combines temperature accuracy, thermal stability, transient response characteristics, sampling efficiency, and long-term reliability to provide a comprehensive assessment of system effectiveness.

The statistical analysis demonstrated that both nozzle and bed temperatures remained very close to their desired operating setpoints throughout the printing process. The low standard deviation values observed in all experiments indicate minimal thermal fluctuations and confirm the ability of the control system to maintain stable operating conditions. Such stability is essential for ensuring consistent material extrusion and reducing the likelihood of print defects caused by temperature variations.

The error analysis further confirmed the accuracy of the proposed system. Mean Absolute Error values remained significantly below the acceptance threshold of 0.5°C in all evaluated datasets, indicating precise temperature tracking and effective control action. The small deviations between measured and target temperatures suggest that the AI-assisted monitoring framework can continuously regulate thermal conditions with a high degree of accuracy.

Transient performance indicators also demonstrated satisfactory system behavior. Overshoot values remained below the predefined stability limit of 5°C, while settling times ranged between 72 and 181 seconds. These results indicate that the system reaches the desired operating conditions without excessive oscillations and maintains stable performance after initial stabilization. Such behavior is particularly important in additive manufacturing processes, where sudden thermal fluctuations can negatively affect layer adhesion and dimensional accuracy.

The sampling analysis provided additional evidence of the efficiency of the monitoring framework. The selected sampling strategy ensured that thermal behavior was adequately represented while avoiding unnecessary data redundancy. The adoption of a fixed sample size of 12 measurements provided a practical balance between statistical reliability and computational efficiency, allowing consistent evaluation across all experiments while maintaining sufficient sensitivity to detect process variations.

Reliability assessment across multiple printing runs demonstrated strong repeatability of the proposed approach. All evaluated datasets satisfied the predefined acceptance criteria, resulting in a success rate of 100%. Furthermore, the overall reliability of the monitoring system reached 89.38%, indicating that the majority of recorded measurements remained within the acceptable temperature tolerance band throughout the experiments. This result highlights the robustness of the system and its ability to maintain stable performance under repeated operating conditions.

Table 6.1 summarizes the principal performance indicators obtained during the experimental evaluation.

Table 0.2 Overall System Performance Indicators

PERFORMANCE METRIC	OBTAINED RESULT
NOZZLE MEAN TEMPERATURE	≈ 200°C
BED MEAN TEMPERATURE	≈ 50°C
NOZZLE STANDARD DEVIATION	0.11–0.49°C
BED STANDARD DEVIATION	0.08–0.76°C
MEAN ABSOLUTE ERROR (MAE)	0.07–0.37°C
OVERSHOOT	0.36–4.15°C
SETTLING TIME	72–181 sec
SELECTED SAMPLE SIZE	12 Samples
SUCCESS RATE	100%
OVERALL RELIABILITY	89.38%

The combined evaluation of these indicators confirms that the developed AI-based monitoring system satisfies all predefined performance requirements. The system achieved high accuracy, stable thermal regulation, acceptable transient response, efficient sampling behavior, and strong reliability across repeated printing experiments. Consequently, the proposed framework can be considered a robust and dependable solution for intelligent thermal monitoring and control in additive manufacturing applications.

CHAPTER 5
CONCLUSION AND RECOMMENDATIONS

5.1CONCLUSION

This book presents a comprehensive, intelligent framework designed to advance additive manufacturing through artificial intelligence augmentation, focusing heavily on optimization, material classification, and real-time process monitoring. The proposed system effectively bridges the gap between conventional static manufacturing protocols and dynamic, expert-driven automation.

A foundational element of this work is the AI-Augmented Material Selection System detailed in Chapter IV. This subsystem significantly optimizes the pre-production workflow by evaluating several key engineering properties simultaneously: yield strength, elastic modulus, damping ratio, density, heat resistance, ease of printing, and production cost. By transitioning away from tedious manual reviews of physical datasheets, the system utilizes weighted distance calculations and similarity analysis to provide instant, multi-criteria material recommendations customized to user- controlled prioritization. Furthermore, its ability to classify materials across diverse manufacturing technologies—including FDM, SLA, SLS, SLM, Ceramic, Bio, and Food printing—ensures that mechanical requirements align seamlessly with process capabilities, mitigating risks of incompatible material-technology combinations.

The ultimate validation of this research is demonstrated through the implementation and empirical analysis of the AI-Based Thermal Monitoring and Control System (the core focus of Chapter VII). Experimental evaluations conducted across a sample size of 12 distinct printed datasets yielded a 100% success rate in satisfying predefined engineering acceptance criteria. The system demonstrated robust steady-state accuracy and tight thermal regulation, maintaining a mean nozzle temperature of approximately 200°C and a mean bed temperature of approximately 50°C.

The transient and steady-state performance indicators highlight exceptional precision, with a Mean Absolute Error (MAE) restricted to 0.07–0.37°C and remarkably low standard deviations for both the nozzle (0.11–0.49°C) and the heated bed (0.08–0.76°C). Thermal overshoots were well-managed within a tight band of 0.36–4.15°C, while the system achieved stable settling times ranging between 72 and 181 seconds. Culminating in an overall operational reliability of 89.38%, the experimental results confirm that integrating intelligent monitoring frameworks provides a highly dependable, stable, and accurate solution for thermal regulation and quality control in modern additive manufacturing applications.

5.2RECOMMENDATIONS

To address the practical constraints encountered across the various phases of this research and to optimize the deployment of the intelligent platform, the following engineering recommendations are proposed to address individual chapter limitations neatly and briefly:

System Architecture & Connectivity: It is highly recommended to standardize asynchronous, lightweight communication protocols (such as edge-optimized WebSockets or MQTT) between the manufacturing hardware and the cloud/edge AI server. This minimizes latency bottlenecks and safeguards real-time processing threads against data packet drops during heavy telemetry transmission.

Knowledge-Base and Material Sourcing: Rather than relying on localized SQL databases which suffer from data staleness, future implementations should transition to live, cloud-hosted API integration with international material manufacturers. Additionally, embedding dynamic imputation algorithms is recommended to handle missing or non-standard mechanical attributes within custom polymer and composite datasets.

Slicing Optimization & Process Planning: Slicing profiles should move away from static G-code generation. It is recommended to implement an inline preprocessing module that dynamically modifies extrusion widths and volumetric speed limits based on physical filament constraints (such as measured diameter fluctuations and batch-specific thermal characteristics).

Sensor Telemetry & Thermal Regulation: To overcome the 10.62% deviation from absolute reliability caused by industrial electrical noise and sensor drift, hardware configurations must incorporate high-grade electromagnetic interference (EMI) shielding for thermocouple/thermistor lines. Furthermore, implementing software-level Kalman filtering alongside adaptive PID co- regulation will suppress transient overshoots and reduce settling times when operating under high thermal mass conditions or varied ambient environments.

5.3. PILOT CLOUD DEPLOYMENT AND LIVE BOT INTEGRATION

Rather than leaving the proposed architecture as a theoretical concept, Phase 1 of the deployment roadmap has been actively initiated and implemented. A fully operational cloud-based prototype has been established, leveraging a dedicated Cloud Server (Virtual Private Server - VPS) environment to host the system's core intelligence.

The platform currently utilizes an advanced, agile Telegram Bot framework, deployed under the active username **@ALXFFFBot**, serving as its live Conversational **Human-Machine Interface** (Conversational **HMI**).

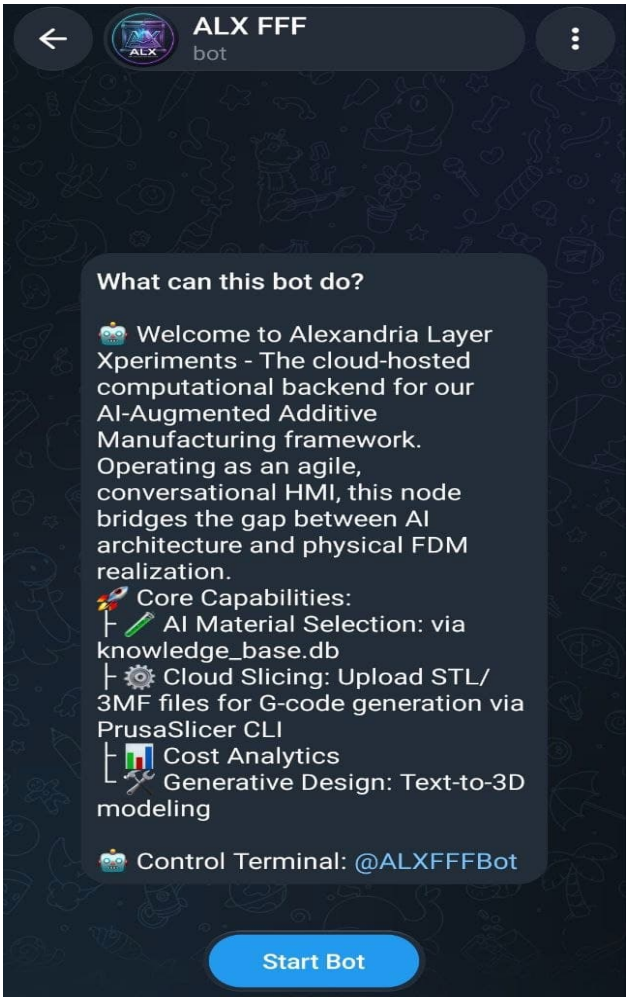


Figure 0.1 The live user interface and welcome layout of the @ALXFFFBot Conversational HMI on the cloud server.

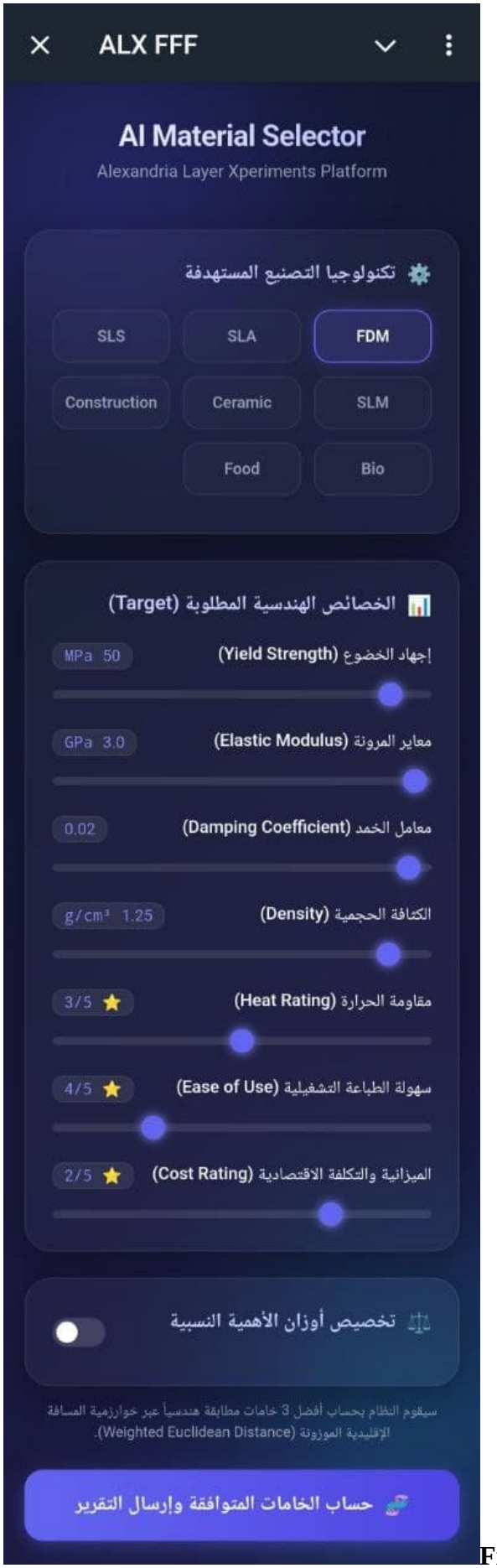


Figure 0.2 The AI Material Selector interface.

This strategic implementation has successfully migrated several key future work objectives into the active production phase, demonstrating a highly responsive, end-to-end automated manufacturing workflow:

Active Cloud Slicing Engine: The server successfully orchestrates background execution of PrusaSlicer CLI. Users can upload raw design files (e.g., .STL or .3MF) directly through the **@ALXFFFBot** interface and receive dynamically sliced, machine-ready G-codes generated autonomously on the cloud server.



Figure 0.3 System snippet showing a successful background execution of the PrusaSlicer CLI engine and G-code generation triggered by user input.

Live Automated Generative Design: The backend successfully handles parametric JSON outputs generated by the LLM core. These parameters are directly piped into the geometry engine running on the cloud server, generating valid, watertight 3D CAD components on demand without human intervention.



Figure 0.4 User prompt preview demonstrating text-to-3D generation utilizing the geometry engine via the bot interface.

Dynamic Cost & Database Calculation: The bot is actively tied to a live relational SQLite database (knowledge_base.db). Before initiating any slicing or manufacturing commands, the system executes real-time material cost profiling, density verification, and localized economic estimations based on dynamically updated filament metrics.



Figure 0.5 The Cost Calculator interface

5.4. LONG-TERM INDUSTRIAL ROADMAP AND FUTURE WORK

Building upon the successful pilot deployment of the current cloud-connected bot framework, the future development roadmap focuses on scaling the system into a robust commercial standard via six critical, high-impact technical vectors:

Transition to Dedicated Web Platform (Website Deployment): Migrate the current conversational HMI from the Telegram bot interface into a centralized, full-scale standalone Web Application. This future website will feature an enterprise dashboard, utilizing Three.js WebApps for interactive, client-side 3D model visualization and multi-user profile management.

Expand Material Database: Broaden application coverage by incorporating an extensive matrix of advanced engineering polymers, high-performance composites, and metal-infused filaments into the intelligent selection core.

Closed-Loop Firmware Control: Migrate the AI control loop from external execution blocks directly into open-source 3D printer firmware architectures (e.g., Klipper or Marlin). This will enable real-time, step-by-step firmware adjustments of acceleration, jerk, and thermal parameters without external server reliance.

Enhanced Generative Design: Advance the geometric engine by integrating structural topology optimization and variable-density lattice structures to manufacture ultra-lightweight, high-strength functional components.

Multi-Printer Fleet Management: Scale the cloud architecture to support centralized fleet management, allowing automated print scheduling, load balancing, and cross-machine quality synchronization across multiple printing units in a smart factory setup.

ML Model Training: Continuously train deep learning architectures on vast historical print data logs to elevate the accuracy of predictive quality assurance and early-stage failure prevention models.

GLOSSARY

CORE ADDITIVE MANUFACTURING TERMS

- Additive Manufacturing (AM)

The process of creating a three-dimensional object by building it up layer by layer from digital models using computer-controlled equipment.

- Fused Deposition Modeling FDM / Fused Filament Fabrication FFF

A filament-based AM process in which thermoplastic filament is melted and extruded through a nozzle to deposit successive layers.

- Stereolithography SLA

A vat-polymerization AM process that cures liquid photopolymer resin with a light source to form high-resolution parts.

- Selective Laser Sintering SLS / Selective Laser Melting SLM

Powder-bed AM processes that fuse powder particles using a laser; SLS typically sinters polymers, SLM fully melts metal powders.

- Build Volume

The maximum physical envelope (X × Y × Z) that a printer can fabricate in a single job.

- Layer Height

The vertical thickness of each deposited or cured layer; a primary determinant of surface resolution and print time.

- Extruder

The mechanism that feeds, melts, and pushes filament toward the nozzle in FDM printers.

- Nozzle

The orifice through which melted filament is extruded; nozzle diameter affects feature resolution and extrusion flow.

MATERIALS AND MATERIAL PROPERTIES

- PLA

Polylactic acid, a common, easy-to-print thermoplastic used for prototyping and educational FDM printing.

- PETG

A thermoplastic combining toughness and printability; often used for functional FDM parts.

- TPU 95A

A shore-hardness designation for a flexible thermoplastic polyurethane used to add compliant, damping regions in multi-material prints.

- Thermoplastics, Photopolymers, Elastomers, Composites

Broad material categories used in AM, each with distinct mechanical, thermal, and processing characteristics.

- Yield Strength

The stress at which a material begins to deform plastically; used to assess load capacity.

- Elastic Modulus

A measure of material stiffness; ratio of stress to elastic strain in the linear region.

- Damping Ratio

A measure of how quickly vibrations decay in a material or structure; relevant for ergonomic and dynamic performance.

- Density

Mass per unit volume; affects weight, inertia, and material selection tradeoffs.

- Heat Resistance and Printability

Qualitative or quantitative measures of a material's thermal stability and ease of processing on a given AM platform.

GEOMETRY, FILES, AND MODELING

- STL file

A tessellated surface representation that encodes only geometry as a mesh of triangles; lacks color, material, or parametric data.

- Point Cloud

A set of 3D points captured from sensors or photogrammetry representing the object surface prior to meshing.

- Mesh

A connected network of polygons (typically triangles) representing a surface; used for visualization, editing, and slicing.

- Mesh Validation

Automated or manual checks that ensure a mesh is watertight, non-degenerate, and printable (no inverted normals, holes, or disconnected shells).

- Parametric CAD Model

A geometry representation defined by parameters and constraints that can be edited and re-evaluated without remodelling.

- CadQuery

(Project context) A programmatic CAD toolkit used to generate parametric geometry via code.

REVERSE ENGINEERING AND PHOTOGRAMMETRY

- Reverse Engineering RE

The process of extracting design information from an existing physical object and reconstructing a usable digital model.

- Photogrammetry

A non-contact method for reconstructing 3D geometry from multiple overlapping photographs using structure-from-motion and bundle adjustment.

- Structure-from-Motion SfM

A photogrammetric technique that simultaneously estimates camera poses and 3D point positions from image sets.

- Bundle Adjustment

An optimization that refines camera parameters and 3D point positions to minimize reprojection error across all images.

- Reprojection Error

The difference between observed image points and the projection of reconstructed 3D points; used to assess photogrammetry accuracy.

GENERATIVE DESIGN AND AI CONCEPTS

- Generative Design

An algorithmic workflow that explores design alternatives from goals, constraints, and manufacturing rules to produce feasible geometries.

- Topology Optimization TO

A physics-based mathematical method that optimizes material distribution within a domain to meet performance objectives under given loads and constraints.

- Large Language Model LLM

A neural network trained on large text corpora used here for intent parsing and prompt understanding to convert natural language into structured design parameters.

- Family Classification

The process of mapping a user prompt to a predefined design family (e.g., spur gear, phone stand) to route generation to the appropriate generator.

- Parameter Extraction

The step that converts a classified prompt into explicit numeric or categorical parameters (e.g., tooth count, diameter) used by generators.

- Programmatic Generation

Deterministic geometry creation using scripted rules and parametric code; precise and controllable for known families.

- Model-Based 3D Generation

Using trained 3D models or single-image reconstruction networks to infer geometry from examples or images.

- Hybrid Architecture

A combined approach that uses prompt understanding, family routing, programmatic generators, and trained models to balance control and generality.

MONITORING, CONTROL, AND CLOSED-LOOP SYSTEMS

- Real-Time Monitoring

Continuous acquisition of process telemetry (temperatures, printer state) and visual data during printing to detect anomalies.

- Closed-Loop System

A control architecture that uses sensor feedback and decision logic (including AI) to automatically adjust process parameters during printing to maintain target performance.

- OctoPrint

(Project context) A server platform that interfaces with FDM printers to provide remote control, telemetry access, and plugin integration.

- Obico

(Project context) A commercial platform used for AI-based visual failure detection from webcam feeds.

- In-Situ Monitoring

The practice of observing and measuring the process while it runs (e.g., webcam, thermistors, profilometry) to enable immediate corrective actions.

- Failure Detection

AI or rule-based identification of common print faults (spaghetti, layer shift, bed detachment) from visual and telemetry cues.

- Automated Mitigation

System responses such as pausing the print, adjusting parameters, or alerting operators when a failure is detected.

EXPERIMENTAL METRICS AND STATISTICAL TERMS

- Calibration Cube

A standard 20 × 20 × 20 mm test artifact used to evaluate dimensional accuracy and print quality.

- Mean Absolute Error MAE

The average absolute difference between measured values and a reference; used to quantify temperature stability or dimensional error.

- Overshoot and Settling Time

Control metrics: overshoot measures peak deviation beyond a setpoint; settling time is the time required for a signal to remain within a tolerance band around the setpoint.

- Sampling Interval and Sample Size

The temporal spacing of measurements and the number of samples collected; both affect statistical representativeness and computational load.

- Repeatability and Reliability

Repeatability measures the consistency of results under identical conditions; reliability assesses the system’s robustness across runs and conditions.

- Von Mises Stress

A scalar stress measure used in FEA to predict yielding under complex loading; commonly used for structural safety assessment.

- Factor of Safety FOS

The ratio of material strength to applied stress; indicates how much stronger a design is than required for expected loads.

- Sweet Spot Impact Load

In racket testing, a representative concentrated load applied to the string bed to simulate ball impact at the optimal contact region.

PROCESS PARAMETERS AND PRINTING SETTINGS

- Nozzle Temperature

The setpoint for the extruder heater; affects melt viscosity, layer adhesion, and surface finish.

- Bed Temperature

The heated build platform setpoint; influences first-layer adhesion and warping.

- Print Speed

The linear velocity at which the nozzle moves; higher speeds reduce print time but can degrade quality.

- Flow Rate (Extrusion Multiplier)

The volumetric rate of filament extrusion relative to nominal; controls material deposition consistency.

- Empirical Engineering Metrics

Derived indicators (predicted roughness, strain index) computed from telemetry using empirical formulas; useful for monitoring but require calibration for quantitative accuracy.

- Cooling Fan Speed

The percentage of part-cooling airflow; influences layer solidification, bridging performance, and overhang quality..

- Infill Density and Pattern

Internal fill percentage and geometry (grid, honeycomb, gyroid) that determine part stiffness, weight, and print time.

- Shell/Wall Thickness

Number of outer perimeters or wall thickness that control surface strength, sealing, and dimensional accuracy.

- Acceleration and Jerk (Motion Control)

Motion controller limits that affect print smoothness and dimensional fidelity; lower values reduce ringing but increase time.

- Z-Hop / Lift on Retract

Vertical lift during travel moves to avoid collisions with printed features; helps prevent surface scarring.

- Support Settings

Support type, density, and interface layers that enable overhangs but affect surface finish and post-processing effort.

- Bed Adhesion Method

Choice of adhesion aid (glue, tape, PEI, brim, raft) to improve first-layer bonding and reduce warping.

MULTI-MATERIAL AND MANUFACTURING CONCEPTS

- Multi-Material Printing

The deliberate co-location of materials with different mechanical properties (e.g., PETG + TPU) within a single part to achieve combined stiffness, damping, or functional gradients.

- Bridge Manufacturing

A transitional production phase using flexible, low-volume technologies (AM, CNC) to produce near-final parts while tooling for mass production is prepared.

- Rapid Prototyping RP

Fast fabrication of prototypes from CAD data to validate form, fit, and function early in development.

- Co-Extrusion and Tool-Changing

Methods for depositing multiple materials: simultaneous co-extrusion or sequential tool-change strategies in multi-head printers.

- Soluble and Sacrificial Supports

Use of dissolvable materials (PVA, HIPS) as supports to enable complex internal geometries and easier post-processing.

- Material Interface Design

Geometric and surface strategies (interlocks, fillets, dovetails) to improve adhesion and load transfer between dissimilar materials.

- Functionally Graded Materials (FGM)

Gradual variation of material composition or properties across a part to tailor local performance without discrete joints.

- Material Compatibility Testing

Small-scale prints and adhesion tests to verify bonding, thermal compatibility, and printability before full production.

- Embedded Components and Inserts

Techniques for integrating nuts, sensors, or electronics during printing to create ready-to-use assemblies.

- Slicer and Toolpath Configuration

Multi-material slicing strategies, purge towers, and transition paths that minimize contamination and ensure clean material changes.

REFERENCES

1] https://www.jsadditive.com/ar/news/integrating-ai-and-big-data-in-3d-printing/

2] https://sungplastic.com/ar/how-ai-affects-3d-printing/

3] https://tinyurl.com/5ezddjrj

4] Farag, M. M., "Materials and Process Selection for Engineering Design", 4th ed., CRC Press, Boca Raton, FL, 2021.

5] Gibson, I., Rosen, D. W., & Stucker, B. Additive Manufacturing Technologies: 3D Printing, Rapid Prototyping, and Direct Digital Manufacturing. Springer, 2nd Edition, 2015.

6] Montgomery, D. C. Design and Analysis of Experiments. Wiley, 9th Edition, 2017.

7] Goodfellow, I., Bengio, Y., & Courville, A. Deep Learning. MIT Press, 2016.

8] Redmon, J., & Farhadi, A. YOLOv3: An Incremental Improvement. arXiv preprint arXiv:1804.02767, 2018.

9] Bishop, C. M. Pattern Recognition and Machine Learning. Springer, 2006.

10] DebRoy, T., Wei, H. L., Zuback, J. S., Mukherjee, T., Elmer, J. W., Milewski, J. O., ... & Zhang, W. Additive Manufacturing of Metallic Components – Process, Structure and Properties. Progress in Materials Science, 92, 112–224, 2018.

11] Ngo, T. D., Kashani, A., Imbalzano, G., Nguyen, T. Q., & Hui, D. Additive Manufacturing (3D Printing): A Review of Materials, Methods, Applications and Challenges. Composites Part B: Engineering, 143, 172–196, 2018.

12] Zhang, Y., Bernard, A., Gupta, R. K., & Harik, R. A Framework for Design for Additive Manufacturing. CIRP Annals, 65(1), 201–204, 2016.

13] Szeliski, R. Computer Vision: Algorithms and Applications. Springer, 2nd Edition, 2022.

14] Kalpakjian, S., & Schmid, S. R. Manufacturing Engineering and Technology. Pearson, 7th Edition, 2014.

15] Ben Said L, Ayadi B, Alharbi S, Dammak F. Recent Advances in Additive Manufacturing: A Review of Current Developments and Future Directions. *Machines*. 2025; 13(9):813. https://doi.org/10.3390/machines13090813

16] Jagriti Srivastava, Hiroshi Kawakami, Systematic Review of Difference Between Topology Optimization and Generative Design, IFAC-Papers Online, Volume 56, Issue 2, 2023, Pages 6561-6568, ISSN 2405-8963, https://doi.org/10.1016/j.ifacol.2023.10.307.

17] Kiran, MB "Application of Artificial Intelligence in Additive Manufacturing- A Review." *11th Annual International Conference on Industrial Engineering and Operations Management*. 2021, https://www.ieomsociety.org/singapore2021/papers/476.pdf.

18] Bradley, Craig. "Additive Manufacturing Materials: The Future of 3D Printing." Lab Manager, Sep 18, 2025, https://www.labmanager.com/additive-manufacturing-materials-the-future-of-3d-printing-34341.

19] Ashby, M. F., Materials Selection in Mechanical Design, 4th ed., Butterworth-Heinemann, Oxford, 2011.

20] Zomer, Thayla & Scabora, Rachel & Durão, Luiz & Rein, Justus & Zancul, Eduardo & Schützer, Klaus & Schleich, Benjamin. (2025). Artificial Intelligence in Additive Manufacturing: A Systematic Review Across the Digital-to-Physical Process Chain. 10.1007/978-3-032-09700-2_21.

21] Saimon, S. R., et al. (2026). Deep learning in additive manufacturing: Progress and future directions. Journal of Manufacturing Systems. https://doi.org/10.1016/j.jmsy.2026.01.002

22] Zaman, S., et al. (2026). Multi-material additive manufacturing of ultra-high temperature ceramics. Ceramics International, 52(1), 2345–2356. https://doi.org/10.1016/j.ceramint.2025.09.012

23] Shangguan, H., et al. (2025). AI-driven material development for additive manufacturing: A critical review. Materials & Design, 256, 113456. https://doi.org/10.1016/j.matdes.2025.113456

24] Inayathullah, M., & Buddala, S. K. (2025). Applications of machine learning in additive manufacturing: A review. Journal of Manufacturing Processes, 110, 456–478. https://doi.org/10.1016/j.jmapro.2025.02.015

25] Sousa, M., et al. (2025). Systematic review of AI in laser-based additive manufacturing process control. Optics & Laser Technology, 178, 111234. https://doi.org/10.1016/j.optlastec.2025.111234

26] Yi, X., et al. (2025). A new era towards autonomous additive manufacturing. Progress in Materials Science, 145, 101234. https://doi.org/10.1016/j.pmatsci.2025.101234

27] Bordekar, S., et al. (2025). Explainable AI for automated defect detection in additive manufacturing using CT scan analysis. NDT & E International, 145, 103456. https://doi.org/10.1016/j.ndteint.2025.103456

28] Al-Zuriqat, A., et al. (2025). Defect detection in fused filament fabrication using deep learning and computer vision. Materials, 18(3), 567. https://doi.org/10.3390/ma18030567

29] Mahdi, A., et al. (2025). Federated learning for anomaly detection in wire arc additive manufacturing. Journal of Manufacturing Processes, 115, 456–468. https://doi.org/10.1016/j.jmapro.2025.01.034

30] Utzeri, G., et al. (2025). Autonomous sensing architected materials. Nature, 635, 345–351. https://doi.org/10.1038/s41586-025-08234-5

ملخص المشروع

المقدمة

يهدف هذا المشروع إلى تطوير منظومة ذكية للتصنيع بالإضافة تعتمد على دمج تقنيات الذكاء الاصطناعي مع الطباعة ثلاثية الأبعاد لتحسين كفاءة عمليات التصميم والتصنيع ومراقبة الجودة. ويعالج المشروع التحديات التي تواجه الطباعة ثلاثية الأبعاد، مثل اختيار المواد المناسبة، وظهور العيوب أثناء الطباعة، وعدم استقرار جودة المنتج، من خلال توفير إطار عمل متكامل يعتمد على اتخاذ القرار الذكي والمراقبة اللحظية.

أهداف المشروع

يسعى المشروع إلى بناء منظومة متكاملة تشمل اختيار المادة المناسبة باستخدام الذكاء الاصطناعي، والتصميم التوليدي للنماذج ثلاثية الأبعاد، والمراقبة اللحظية لعملية الطباعة للكشف المبكر عن العيوب، بالإضافة إلى تحسين معاملات الطباعة، ورفع دقة وجودة المنتجات المطبوعة، وتقليل الهدر وزيادة موثوقية عملية التصنيع.

مكونات المشروع

يتكون المشروع من عدة أجزاء مترابطة، تشمل دراسة نظرية حول التصنيع بالإضافة والذكاء الاصطناعي، ونظامًا ذكيًا لاختيار المواد، والتصميم التوليدي للنماذج الهندسية، ودراسة تطبيقية للهندسة العكسية لمضرب تنس، ونظام مراقبة لحظية يعتمد على الرؤية الحاسوبية والذكاء الاصطناعي، إلى جانب التحليل الإحصائي لتقييم أداء النظام وقياس الموثوقية.

النتائج المتوقعة

من المتوقع أن يحقق النظام تحسينًا في جودة الطباعة ودقتها، وتقليل معدلات فشل الطباعة واستهلاك المواد، وزيادة استقرار العملية التصنيعية، مع توفير توصيات ذكية لاختيار المواد ومعلمات التشغيل، والوصول إلى منظومة أكثر كفاءة وموثوقية في بيئات التصنيع بالإضافة.

التحديات والاعتبارات

يواجه المشروع عددًا من التحديات، من أهمها الحاجة إلى بيانات تدريب عالية الجودة، واختلاف خصائص الطابعات والمواد، ومتطلبات المعالجة الفورية للبيانات، بالإضافة إلى ضرورة تحقيق التوازن بين دقة نماذج الذكاء الاصطناعي وسرعة الاستجابة، مع مراعاة إمكانية تطبيق النظام على نطاق صناعي.

التطبيقات والآفاق المستقبلية

يمكن تطبيق النظام في العديد من المجالات مثل الصناعات الطبية، وصناعة الطيران، والسيارات، والتعليم، وإنتاج النماذج الأولية والمنتجات المخصصة. كما يمكن مستقبلاً تطويره من خلال دمجه مع تقنيات التوأم الرقمي، والحوسبة السحابية، وإنترنت الأشياء، وأنظمة التحكم المغلقة، بما يدعم إنشاء مصانع ذكية تعتمد على التصنيع المستقل.

الخلاصة

يوضح المشروع دور الذكاء الاصطناعي في تحسين كفاءة التصنيع بالإضافة من خلال دعم اختيار المواد، والتصميم، والمراقبة اللحظية لعمليات الطباعة ثلاثية الأبعاد، بما يسهم في تحسين جودة المنتجات وتقليل العيوب والهدر.